Host-specific innate and adaptive immune responses in therapy-naïve human immunodeficiency virus 1 infected patients

Inaugural-Dissertation

zur

Erlangung des Doktorgrades

der Mathematisch-Naturwissenschaftlichen Fakultät

der Universität zu Köln

vorgelegt von

Finja Schweitzer

aus Langenfeld

Köln, 2014

Berichterstatter:	Prof. Dr. med. Walter Doerfler
	Prof. Dr. rer. nat. Kay Hofmann
Vorsitzender:	Prof. Dr. rer. nat. Siegfried Roth
Beisitzer:	Dr. rer. nat. Matthias Cramer

Tag der Disputation: 6. Dezember 2013

1. Introduction

1.1 The human immunodeficiency virus type 1 (HIV-1)

In 1983, the human immunodeficiency virus type 1 (HIV-1) was identified to be the causative agent of the acquired immunodeficiency syndrome (AIDS) by scientists of the Pasteur Institute in Paris, France and the National Institute of Health in Bethesda, USA [1, 2].

HIV-1 belongs to the family of retroviridae defined to have a single-stranded (ss) RNA genome in positive-sense orientation and characterized by the possession of the enzyme reverse transcriptase (RT) [3]. This particular retrovirus belongs to the genus lentivirus (lat. lentus for slow), which is defined to have a long period of incubation and an extensive duration of illness [4]. Due to differences in the HIV genome, the virus is classified into three major groups of HIV-1 M (main phylogenetic group), N (non-M / non-O) and O (outliner), in which M is the most prominent. Group M is further subdivided into different subtypes (A – I); these are genetically and geographically distinct [5-7]. Most commonly found in Western Europe and North America is subtype B [8, 9].

Structure and genome

The fully developed spherically structured HIV-1 particle has a diameter of about 100-120 nm [10] (figure 1.1 (A)). It contains two copies of the genomic, ss approximately 9.2 kilo bases (kb) RNA molecules encoding for its nine genes [3, 11]. There are three structural genes, namely gag, pol and env, as well as six non-structural genes, explicitly tat, rev, nef, vif, vpr and vpu, which are responsible for the infection of cells and the production of viral particles [3] (figure 1.1 (B)). RNA molecules and, in addition, the virus specific enzymes RT, protease (PR) and integrase (IN) are enclosed by a conical nucleocapsid made up of the p24 viral protein [12]. The RT is a heterodimer comprised of two structurally distinct subunits (p51 and p66). Its catalytic activity includes a RNA-dependent DNA polymerase as well as RNase H which are required to transcribe the ss viral RNA genome into double-stranded (ds) DNA after the host cell has been entered [4]. The p66 subunit contains both DNA polymerase and RNase H activity, while the p51 subunit lacks the domain responsible for RNase H activity [13-15]. The PR is essential for the maturation of the virus particle by cleaving non-functional polyproteins into functional proteins [16]. It is a small aspartyl protease and active as a symmetric homodimer, each 99 amino acids (aa) in length.

Each monomer contributes one critical aspartic acid forming the active enzyme [17]. The IN incorporates the ds proviral DNA into the chromosomal DNA of the host cell. It has a restriction and ligation activity [18], by (a) 3'-processing of ds proviral DNA ends, followed by (b) integration of the processed ends into chromosomal DNA of the host [19]. The capsid in turn is surrounded by a matrix, ensuring integrity of viral particles and enclosed by a lipid-bilayer membrane. The surface of the viral envelope holds 70 spikes, which are composed of three heterodimers of the viral glycoproteins gp120 and gp41 [20].

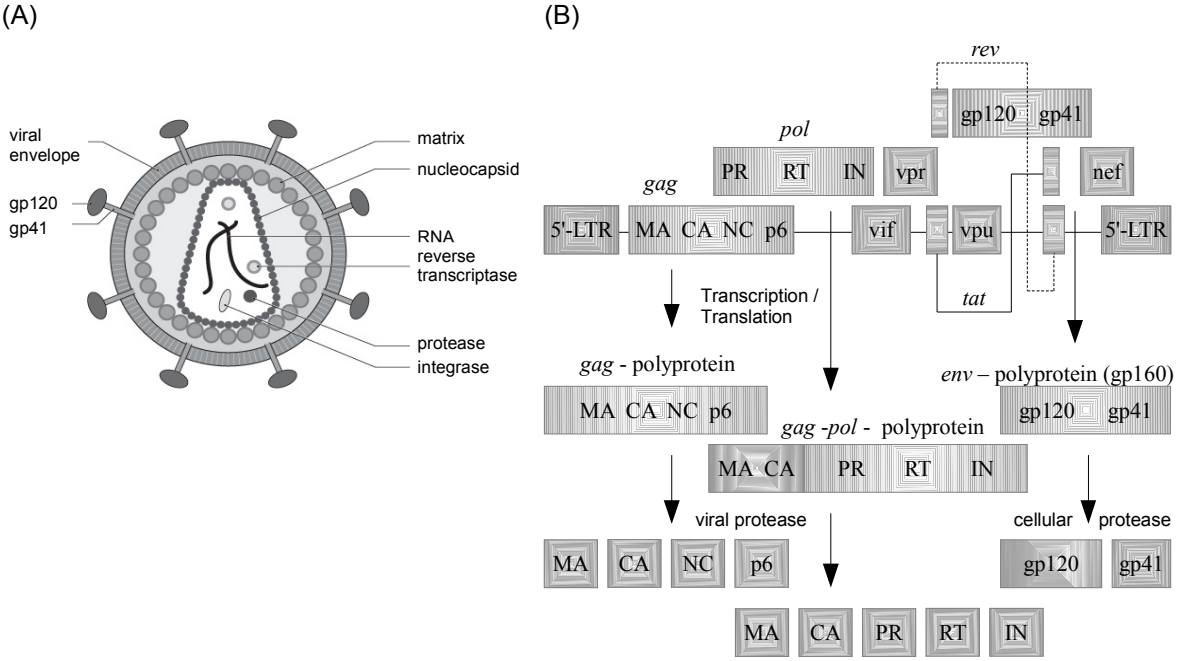

Figure 1.1 The human immunodeficiency virus type 1. (A) Diagram of HIV-1 particle. The HIV-1 envelope is composed of a lipid-bilayer membrane, holding receptors, composed of heterodimers of the glycoproteins gp120 and gp41. The integrity of viral RNA and proteins (protease, reverse transcriptase and integrase) is ensured by the matrix and a conical nucleocapsid (adapted from [21]). (B) Organization of the HIV-1 genome. HIV-1 is composed of three structural genes, gag, pol and env, as well as six non-structural genes, tat, rev, nef, vif, vpr and vpu. Transcription, translation and the cleavage by a cellular and the viral protease results in functional viral proteins (adapted from [22]).

Replication cycle

Once virus particles are adsorbed onto the host cell, they fuse to the membrane (figure 1.2 (1)). Viral gp120 is comprised of binding domains for the cellular CD4-receptor and a second, so called co-receptor, which is a chemokine receptor [23, 24]. This co-receptor can either be the C-C chemokine receptor type 5 (CCR5), which is present on macrophages (MΦ) and T cells [25] or the C-X-C chemokine receptor type 4 (CXCR4), which is only expressed by T cells [26]. A conformational change is provoked when gp120 attaches to the cellular CD4-receptor, enabling the interaction with the co-receptor. At the same time the viral transmembrane protein gp41 is allowed to get in contact with the fusion domain of the cell membrane, leading to a melting of the membranes. The capsid, with its content, is released into the cytoplasm of the cell [27] and after it dissolves, a reverse transcription complex is build (figure 1.2 (2)). The ss viral RNA is transcribed by the RT into a ds complementary DNA (cDNA) [28] (figure 1.2 (3)). This cDNA viral genome together with its protein complexes are transported into the nucleus, where the viral cDNA is integrated into the hosts' genome due to catalysation of the IN [19, 29] (figure 1.2 (4)). The integrated provirus can now enter genetic latency or continue with its replication. Transcription occurs with the help of the cellular RNA-polymerase II. The generated mRNA, encoding viral proteins, is subsequently spliced and transported into the cytoplasm in order to be translated [30] (figure 1.2 (5)). At this stage, structural proteins as well as full-length viral RNAs are produced. While structural proteins are giving the virus its shape, full-length viral RNAs hold the HIV-1 genome [3] (figure 1.2 (6)). Env-proteins are synthesized and glycosylated within the endoplasmatic reticulum (ER) and transported to the cell surface facilitated by the Golgi complex. After the assembly of viral proteins, protein precursor and RNA molecules bud from the host cell forming immature non infectious viral particles (figure 1.2 (7)). Maturation occurs in the forming bud or in the immature virion after budding. This process is initiated by proteases, which cleave polyproteins into individual functional HIV-1 proteins [16, 31] (figure 1.2 (8)). Figure 1.2 shows a schematic overview of the HIV-1 replication cycle.

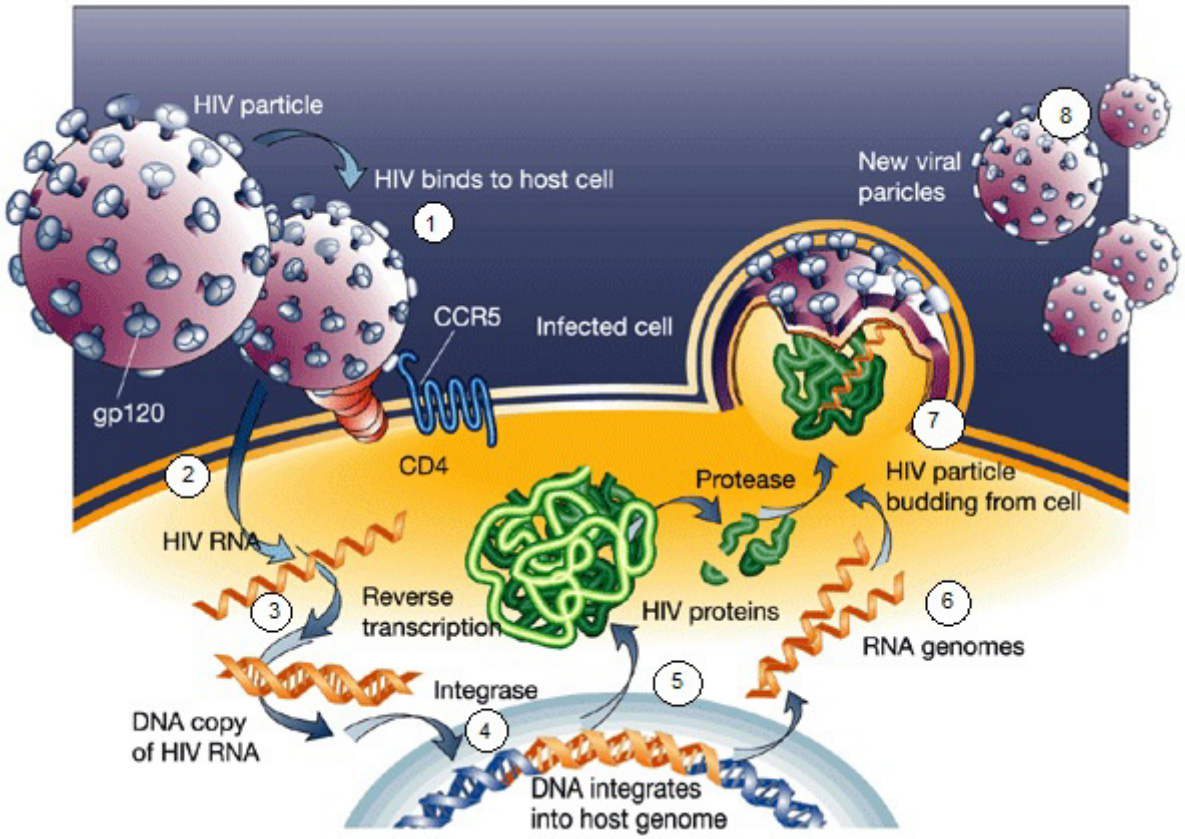

Figure 1.2 HIV-1 Replication cycle. Virus particles are adsorbed onto the host cell and fuse to the membrane (1). Viral gp120 binds cellular CD4-receptor and a co-receptor. After the fusion of the cell membranes, the capsid, with its content, is released into the cytoplasm of the cell (2). The ss viral RNA is transcribed by the RT into a ds cDNA (3) and transported into the nucleus, where the viral cDNA is integrated into the hosts' genome (4). Generated mRNA, encoding viral proteins, is spliced and transported into the cytoplasm in order to be translated (5). While the structural proteins are giving the virus its shape, full-length viral RNA holds the HIV-1 genome (6). After the assembly of viral proteins, protein precursor and RNA molecules bud from the host cell forming immature, non-infectious viral particles (7). Maturation occurs in the forming bud or in the immature virion after budding by cleavage of polyproteins into individual functional HIV-1 proteins (8) (adapted from [32]).

Course of infection and immune response

An HIV-1 infected person transmits viral particles via body fluids during direct contact. This can either occur by blood transfer or by other body fluids (e.g. seminal fluid, vaginal fluid and mother's milk) via injured mucosa [33-35]. Viral particles have not only been isolated from body fluids but are also present in infected $CD4^+$ T cells, MΦ and dendritic cells (DCs) [36-38]. MΦ and DCs of the skin (Langerhans cells, LCs) are most probable the first targets addressed by virus particles. After infection with HIV-1, these cells migrate through lymphatic vessels to the nearest lymph node,

which become virus reservoirs. A huge number of cells, including monocytes, MΦ and naive T cells are present, creating ideal replication conditions for HIV-1 [39-41].
The first phase of infection, the so called primary infection (figure 1.3 (1)), proceeds predominantly asymptomatic. In a few cases, flu-like symptoms are described within the first two weeks. As a result of the rapid virus replication a high virus titer of up to 10^8 particles mL^{-1} can be detected in peripheral blood [42]. Temporarily the number of $CD4^+$ T cells is significantly low. This acute viremia is in all patients associated with an activation of $CD8^+$ T cells, which are then referred to as cytotoxic T cells (CTLs). These are able to induce cell death of HIV-1 infected cells [43, 44]. After several weeks, the adaptive immune response is fully initiated and HIV-1-specific antibodies (seroconversion) are generated. This leads to a noticeable decrease in the amount of virus in the peripheral blood followed by a phase of clinical latency [45, 46]. Most infected individuals do not show symptoms in this stage of disease (figure 1.3 (2)). Within this period an active virus replication occurs with a de novo synthesis resulting in up to 10^9 infectious particles per day [47]. At this point, virus particles are trapped and eliminated by the fully functioning immune system. The transition towards a symptomatic period is initiated by the breakdown of the equilibrium between virus replication and immune defense. As a consequence of the progressive virus replication, the amount of $CD4^+$ T cells decrease slowly and the viral load increases [48]. The virus replicates explosively in lymphatic tissues and infected cells are destroyed by CTLs in that course. An ever increasing number of $CD4^+$ T cells is destroyed and cannot be replaced. Thus the immune system is less capable of controlling HIV-1-propagation and becomes susceptible to opportunistic infections leading to the progression to AIDS (figure 1.3 (3)) [49]. Figure 1.3 shows the course of infection and immune response over time.

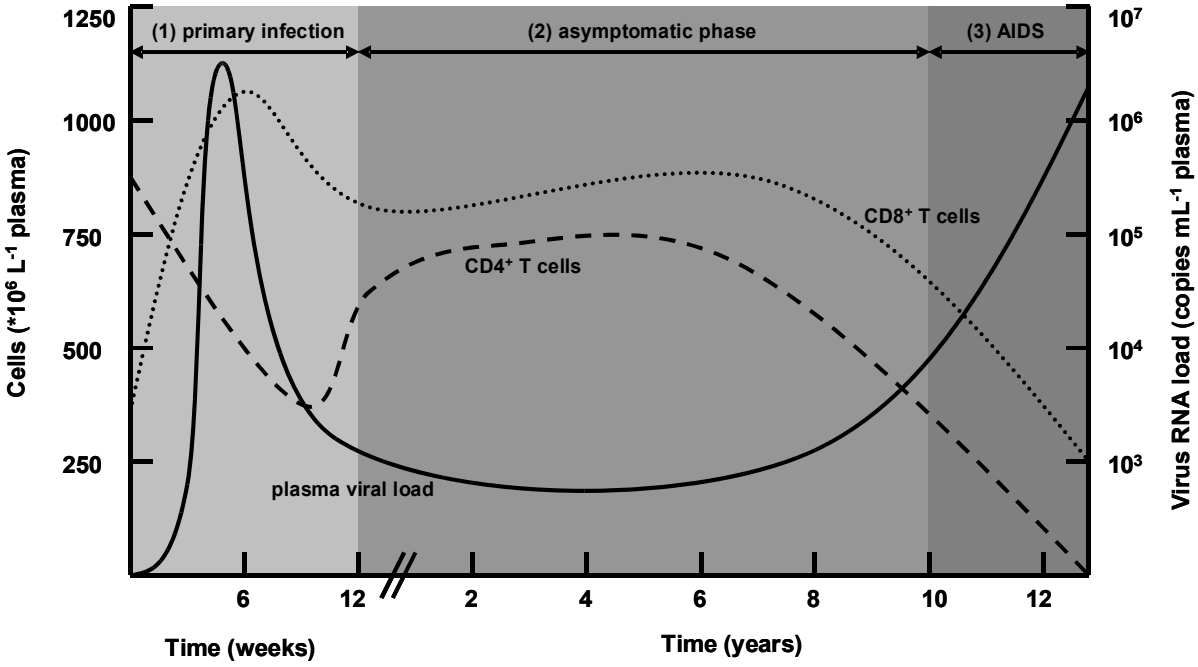

Figure 1.3 Course of infection and immune response. The phase of the primary infection (1) is defined by a rapid virus replication resulting in a high virus titer and a temporarily low number of $CD4^+$ T cells. $CD8^+$ T cells become activated, inducing the cell death of HIV-1 infected cells. Seroconversion and the full initiation of the adaptive immune response lead to a decrease in the amount of virus. Most infected individuals do not show symptoms in this stage of disease (2). The transition towards a symptomatic period is initiated by the breakdown of the equilibrium between virus replication and immune defense. As a consequence of the progressive virus replication, the amount of $CD4^+$ T cells decreases slowly and the viral load increases. The immune system is less capable of controlling HIV-1-propagation leading to the progression to AIDS (3) (adapted from [50]).

1.2 Innate immune response

Innate immune responses are immediately activated upon infection non-specifically by pathogen-associated molecular patterns (PAMPs). PAMPs are small molecular motifs conserved by pathogens (e.g. lipopolysaccharides of gram-negative bacteria (LPS), dsRNA of certain viruses) and recognized by toll-like receptors (TLRs) of specific immune cells [51, 52]. These are located on epithelial surfaces of skin and within the gut and reproductive tract. The entering of pathogens is facilitated by lesions leading to the activation of immune cells placed in underlying tissues. MΦ and DCs play an important role, but also contribute to immune defenses throughout the course of infection [38, 49]. Additionally, natural killer cells (NK cells) are specialized cytotoxic cells of the innate immune system, recognizing infected cells to induce their lysis [53, 54]. However, HIV-1 is able to circumvent presentation and recognition by these innate immune cells. Furthermore, monocytes, MΦ and DCs provide major virus reservoirs [40, 41] producing high-grade infectious virus [55]. To recruit more immune cells such as $CD4^+$ T cells, monocytes, MΦ and DCs secrete several cytokines and chemokines. The close contact of infected reservoirs and non-infected $CD4^+$ T cells facilitates the transmission of viral particles. In addition, adaptive immune responses are activated [36, 38].

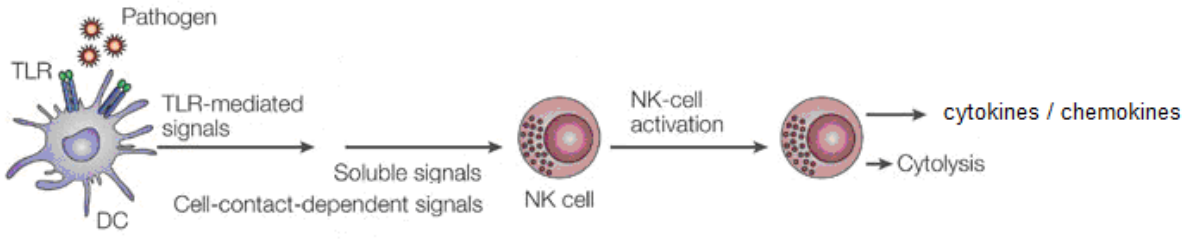

Figure 1.4 Activation of innate immunity by unspecific pathogen stimulation. Unspecific pathogen stimuli trigger the maturation of DCs, which in turn activate NK cells, resulting in the secretion of cytokines and chemokines and the cytolysis of infected cells (adapted from [56]).

Antigen presenting cells (APCs)

The most important APCs with a broad range of antigen presentation are DCs. They derive from the bone marrow, are positioned at epithelial surfaces and circulate in blood and lymphoid tissues in an immature state, to interact with pathogens, including HIV-1 [57, 58]. DCs present both self and non-self antigens on human

leukocyte antigen (HLA) complexes on their cell surfaces. These are in turn recognized by T cells in particular by their T cell receptors (TCRs) [59].
To present non-self antigens, DCs phagocytose pathogens, which are enzymatically digested into smaller pieces containing epitopes. Only immunodominant epitopes of a pathogen are presented [60]. After phagocytosis, DCs migrate attracted by chemokines through the network of lymph vessels to lymph nodes to interact with naïve T cells. While migrating DCs undergo maturation, they lose the ability to phagocytose further pathogens and increase their ability to communicate with naïve T cells [38]. Only a strong binding affinity of HLA:epitope complexes allows the recognition by T cells leading to adaptive immune responses [61].

Natural killer cells (NK cells)
Cytotoxic NK cells are specific cells of the innate immune system expressing CD16 and CD56 on their surface. NK cells derive from the common lymphoid progenitor cell and differentiate and mature in bone marrow, lymph nodes, the spleen, tonsils and thymus before starting to circulate in the blood [62]. NK cells have characteristic cytoplasmic granules. These granules can be released onto the surface of the bound target cell, whereupon effector proteins like perforin and proteases enter the cell to induce cell death [63]. Activated NK cells also secrete cytokines to regulate down-stream immune responses in reaction to pathogens [64].
NK cell cytotoxic activity is regulated by a balance of activating and inhibitory receptors. In the case of a predominant activating signal, NK cells are activated, likewise if inhibitory signals overbalance, activity is inhibited [65]. In addition, cytokines are involved in NK cell activation [64, 66].

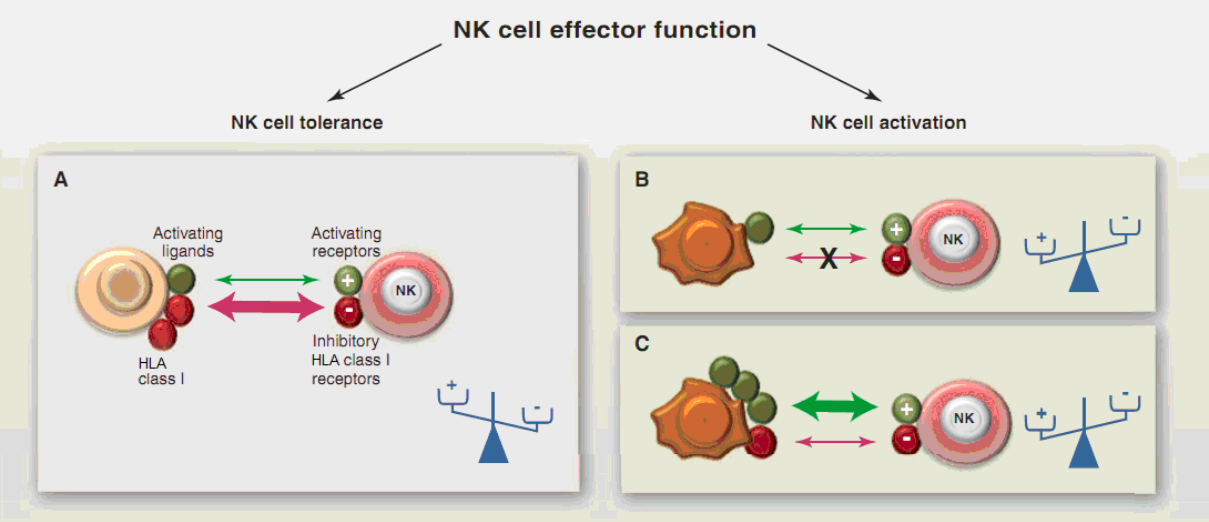

Figure 1.5 Regulation of NK cell cytotoxic activity by a balance of activating and inhibitory receptors. NK cells tolerate cells, displaying self molecules (red) and only small amounts of stress-induced self-molecules (green) (A). They become activated and selectively kill infected cells with down-regulated HLA class I molecules (B) or up-regulated stress-induced self-molecules (C) (adapted from [67]).

Activating receptors directly induce cell death after binding to ligands which indicate infection of a cell, inhibitory receptors recognize HLA class I alleles, preventing the killing of healthy cells [65]. HIV-1 viral particles are able to alter the expression of HLA class I molecules. A down-regulation of these molecules leads to an interference with the activation of NK cells [68, 69].

Cytokines and chemokines

Cytokines are small signaling proteins (~25kDa) mediating immune and inflammatory responses and are released by various cells (e.g. NK cells, APCs, CTLs) [70-73]. The binding to specific cell surface receptors provokes the activation of intracellular pathways, leading to an up- or down-regulation of several genes and their transcription factors [74]. The granulocyte macrophage colony-stimulating factor (GM-CSF) is a hematopoietic regulator of both granulocytes and MΦ, but it can also potentiate their function in inflammation [75]. Interferons (IFNs) possess antiviral activity and can inhibit viral replication. Type I IFN-α and -β are directly induced by infection, while type II IFN-γ, also known as an immune IFN, is induced by mitogenic or antigenic stimuli [76]. Interleukins (ILs) are a large group of immunomodulatory proteins activating specific signalling cascades after binding to cells, thereby interfering with the growth, differentiation and activation of immune cells [77]. The

tumor necrosis factor (TNF) is a key regulator of inflammatory responses, causing a variety of cellular responses, including cell death, survival, differentiation, proliferation and migration [78].

Chemokines are a subgroup of cytokines, which are relatively smaller in size (8-10kDa) [79]. Their major role is to act as a chemoattractant to guide migration of cells, such as DCs to lymph nodes [80]. Eotaxin (CCL11) is an important eosinophil attractant [81]. IFN-γ induced protein 10 (IP-10, CCL10) specifically attracts activated T cells, monocytes and NK cells to sites of infection [82]. The monocyte chemotactic protein-1 (MCP-1, CCL2) is one of the key chemokines regulating migration and infiltration of monocytes and MΦ in diseased tissue [83]. Monocyte interferon gamma inducing factor (MIG, CXCL9) is an IFN-γ inducible chemokine, produced mainly by DCs, B cells and MΦ, predominantly attracting memory and effector T cells [84]. MΦ inflammatory protein (MIP-1α, CCL3 / MIP-1β, CCL4) enhances granulocyte-macrophage colony formation and can cause localized inflammatory reactions, characterized by a rapid influx of polymorphonuclear cells [85]. The chemokine called regulated upon activation normal T cell expressed and presumably secreted (RANTES, CCL5) plays an important role in homing and migration of effector and memory T cells during acute infection, but can also chemoattract a variety of additional cells, such as monocytes, NK cells and DCs [86].

1.3 Adaptive immune response

The adaptive immunity is initiated when an infection overpowers innate immune responses [87]. It becomes effective after several days, requiring antigen specific T cells (and B cells) to encounter their specific foreign antigen, delivered and presented on HLA molecules by DCs, to proliferate and to differentiate into effector cells (figure 1.6) [88, 89].

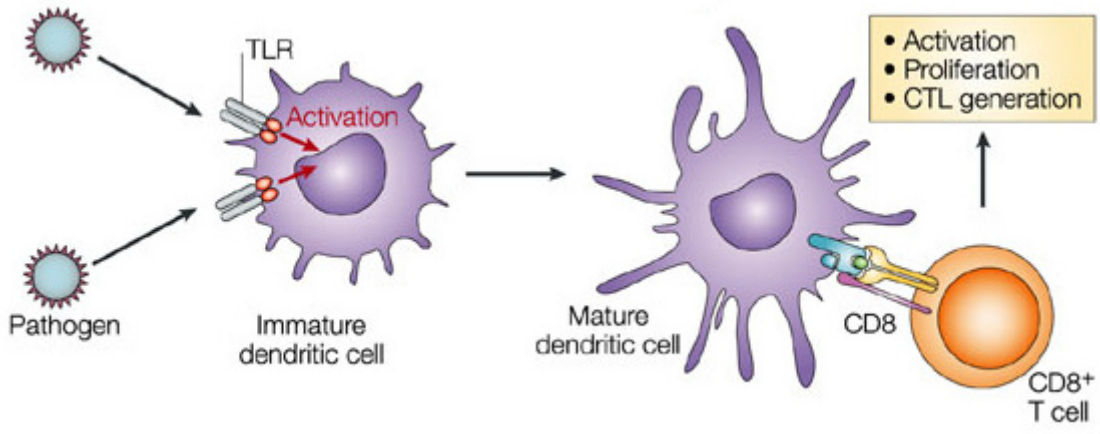

Figure 1.6 Initiation of the adaptive immune response. The maturation of immature DCs is triggered by the stimulation with pathogens. Mature DCs display fragmented pieces of pathogens on HLA class I molecules on their cell surface to activate $CD8^+$ T cells, leading to proliferation and CTL generation (adapted from [90]).

Human leucocyte antigen (HLA) complex

Genes encoding for the HLA complex are located on the short arm of chromosome 6. 140 genes have been described, of which about half have a known immunological function [91, 92]. The HLA region is the most polymorphic of the entire human genome to ensure a broad range of antigen presentation [93].

HLA complexes act as indicators that display fragmented pieces of antigens on cell surfaces. Those antigens can be self or non-self. Self antigens are present on generally every nucleated cell and are unique to that person [59]. Non-self antigens can be acquired in two different ways: Fragments, which are later displayed on HLA class II molecules, originate from particles engulfed by e.g. MΦ and digested by lysozymes [94]. If a virus is infecting a cell, cleaved peptides are displayed on the surface of HLA class I [95].

HLA-A, -B and -C belong to the HLA class I [96, 97]. Regarding the nomenclature, HLA is registered with a letter and a number, designating a specific allele (number) to

a given HLA locus (letter). The first two digits correspond to a group of alleles encoding a specific antigen. The third and fourth digits can be used to describe a certain subtype [98].

HLA molecules are heterodimers that are anchored in the cell membrane and consist of a single transmembrane polypeptide α-chain and a β_2-microglobulin. The α-chain has two polymorphic domains, α_1 and α_2, which are able to bind peptides (figure 1.7 (A)) [99]. These derive from cytosolic proteins generated by proteasomes, degrading intracellular proteins into peptides of usually 8-10 amino acids (aa) (figure 1.7 (B.1)) [100]. Peptides have to be translocated from the cytosol into the ER to get in contact with HLA class I molecules. The transporter associated with this process (TAP) is able to bind peptides to translocate them ATP-dependent into the ER (figure 1.7 (B.2)). Subsequently, several molecules e.g. tapasin, calreticulin and calnexin are necessary for loading the peptide onto the HLA class I molecule, which then leave through the secretory pathway to the cell surface (figure 1.7. (B.3/4/5)) [101]. HLA class I molecules on DCs generally interact with CTLs, which can initiate the cell death of a virus-infected cell [44].

Unfortunately, HIV-1 found several ways to circumvent the presentation of its antigens. This can either result in the down-regulation of HLA molecules at the surface, and / or prevents the HLA molecule to reach the cell surface. In addition, proteasomal cleavage can be interfered; all leading to a progression of disease [102-105].

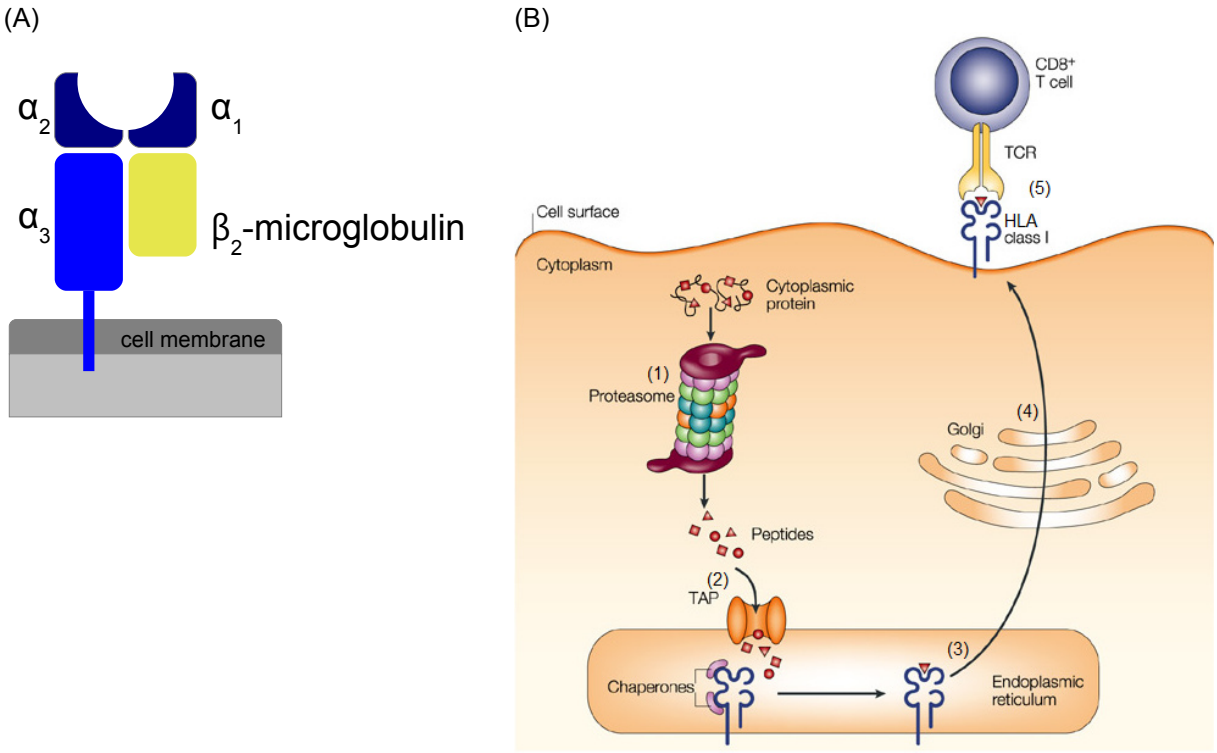

Figure 1.7 The Human leucocyte antigen (HLA) complex (A) Structure of an HLA class I molecule. HLA class I molecules are anchored in the cell membrane by the transmembrane α-chain. Its polymorphic domains α_1 and α_2 are able to bind peptides. In addition it consists of the single polypeptide β_2-microglobulin (adapted from [99]). (B) Schematic overview of peptide processing and presentation on a HLA class I molecule. Viral peptides cleaved by the cellular proteasome (1) are translocated into the ER (2), loaded onto the HLA class I molecule (3) and transported to the cell surface (4/5) [106].

Cytotoxic T cells (CTLs)

$CD8^+$ T cells originating in the bone marrow migrate as precursor $CD8^+$ T cells to the thymus to undergo maturation. Mature naïve $CD8^+$ T cells enter the bloodstream to continually circulate through lymphoid organs and tissues [107].

Within lymphoid organs, mature DCs (mDCs) display antigens to naïve $CD8^+$ T cells allowing naïve $CD8^+$ T cells to screen HLA class I complexes. Displayed self-antigens support the selection of T cell receptors (TCRs) which are able to interact with the specific HLA:self-antigen complex. In this way a repertoire of mature $CD8^+$ T cells that can be activated by non-self antigen bound to the same HLA molecule is assured [88, 89]. In addition to the initial activation by HLA:non-self-antigen (DCs) and TCR (CTL), a supportive T cell activation mediated by co-stimulatory molecules such as CD80 and CD86 expressed by APCs and CD28 on CTL starts [108, 109].

Most TCRs are membrane-anchored heterodimers and are composed of an α- and a β-chain, a few of a γ- and a δ-chain. Chains are discriminated in a variable and a

constant region. While the constant region is responsible for the anchoring in the cell membrane, the variable region binds to the HLA:antigen complex [110]. Recognition of an HLA:antigen complex by a specific TCR leads to the differentiation and proliferation of naïve $CD8^+$ T cells to effector CTLs. CTLs leave the lymphoid organ and enter the bloodstream to migrate to sites of infection, attracted by chemokines [80]. When encountering infected cells, CTLs release the cytotoxins perforin, granulysin and granzymes. Perforin and granulysin form pores in the membrane of infected cells allowing granzymes to enter the target cell inducing cell death [111]. However, mutated HIV-1 antigens are altering the recognition by CTLs, resulting in non-recognition thus in immune escape [112, 113].

1.4 Antiretroviral therapy and development of resistances

Highly active antiretroviral therapy (HAART)

The introduction of the highly active antiretroviral therapy (HAART) in 1996 allows a successful treatment of HIV-1 infected patients over a long period of time [114-116]. The treatment's goal is a permanent suppression of virus replication to reduce plasma viral load below the currently existing limit of detection of 40 copies mL^{-1} plasma [117].

HAART includes agents of at least two distinct classes of antiretrovirals: inhibitors of the RT (nucleoside/nucleotide, NRTI, and non-nucleoside, NNRTI), PR inhibitors (PI), a fusion inhibitor, a co-receptor antagonist and IN inhibitors, targeting all steps in the viral replication cycle [118, 119]. The three major groups of drugs being used in the clinical practice are inhibitors of the RT (NRTI and NNRTI) and the PR (PI). NRTIs are analogues of the nucleobases cytosine, guanidine, adenosine and thymidine, which in contrast do not posses the hydroxyl group at the 3'-position of the desoxyribose, hampering the elongation of the strand in the process of DNA-synthesis [120]. NNRTIs bind to the hydrophobic domain of the p66-subunit of the RT nearby the active center, interfering with the assembly of dNTPs [121]. PIs block the proteolytic cleavage of protein precursors, thereby inhibiting maturation of viral particles [122].

Development of resistance and therapy failure

The major cause of therapy failure is the development of drug resistance associated mutations (RAMs) [119]. RAMs may evolve quite fast in virus replication in the presence of drugs as a consequence of low drug pressure and the high mutation rate of HIV-1 [123].

RAMs are well characterized and localized to specific positions within the targeted proteins [124-126]. Once detected, therapy can be optimized according to resistance profile of the dominant viral strain [126]. However, in about 10% of therapy-naïve patients of the RESINA cohort (primary drug RESIstance in treatment-NAïve HIV-1 infected patients), RAMs can be detected, although those patients never received any therapy [127, 128]. Those RAM-containing viral stains were transmitted from one patient to the other and persist over time [129]. The RESINA study is a multicentre study conducted in North Rhine-Westphalia, Germany. With about 18 million inhabitants, the state accounts for approximately 21% of documented HIV-1 cases in

Germany. Clinical data is collected and a genotypic resistance testing is performed in therapy-naïve HIV-1 infected individuals prior to the start of antiretroviral treatment [127, 128].

1.5 Aim

RAMs localize to particular genomic sites in targeted proteins and are associated with specific amino acid changes [124-126]. When located within HLA class I restricted epitopes, they can negatively influence immunogenicity by hampering the binding of viral peptides to the restricting HLA class I allele, changing T cell recognition sites or altering peptide processing by the cellular proteasome [130-140].

In this study, the persistence of transmitted RAMs (tRAMs) in therapy-naïve patients is explained by the mechanism of immune selection: in the background of specific HLA class I alleles, some tRAMs might be concomitant mutations evading the recognition by the immune system, thereby conferring the survival advantage of the mutated viral strain.

A standard antiretroviral therapy without the consideration of HLA-allele mediated immune selection could include antiretroviral drugs that would promote a therapy failure by providing a selective pressure for tRAMs conferring not only resistance to the drug but also immune escape. The host immune response is therefore especially important to consider in the treatment of therapy-naïve patients already harbouring tRAMs. Their treatment, therefore, should be optimized using all available information regarding virus and host in order to facilitate a long lasting and successful therapy. Processing and presentation of viral peptides is influenced by a variety of factors. HLA class I restricted epitopes are presented by a huge variety of HLA-molecules ensuring broad epitope recognition. Therefore, it is necessary to establish a model system that allows studying immune function in the context of the whole viral particle and defined HLA alleles, independent of patient samples, but still close to the in vivo environment.

The assessment of significant associations between HLA class I alleles and HIV-1 tRAMs allowed for the identification of possible immune escape mutants among tRAMs. These in silico obtained results were verified, establishing a suitable cell culture model: HLA alleles of interest were over expressed on monocyte-derived DCs (moDCs). A VSV-G-pseudotyped lentiviral vector system was chosen to ensure (1) the delivery of the gene of interest independent of receptor interaction and (2) a stable integration and expression of the gene of interest in these non-dividing cells. Pseudotyping with VSV-G allows the transduction of monocytes via endocytosis. Lentiviral vectors were generated, carrying two HLA open reading frames (ORF) (HLA-A*02:01 and HLA-B*44:03) of interest aiming to deliver those HLA ORF into

moDCs to generate the so called recombinant DCs. These recombinant DCs, over-expressing the HLAs of interest, were infected with HIV-1 carrying tRAMs in PR and RT to determine changes in immunogenicity. Differences in cytokine and chemokine release in the co-cultures of either $CD16^+CD56^+$ NK cells or $CD8^+$ T cells and recombinant moDCs infected with HIV-1 ADA carrying different tRAMs (V82A (PR) and L210F (RT)), indicate cell to cell interactions leading to immune escape. Two possible models of cytokine and chemokine release upon infection with either HIV-1 ADA_V82A or ADA_L210F by moDCs in the background of HLA-A*02:01 and HLA-B*44:03 could be feasible. One is based on an increase of cytokines and chemokines, while the second is based on a decrease.

Figure 1.8 shows schematically how cytokine and chemokine release can be interpreted according to the assumptions made of V82A (PR) being an immune escape mutation in the background of HLA-A*02:01 and L210F (RT) in HLA-B*44:03. In HLA-A*02:01 positive donors a higher release of cytokines and chemokines is, according to model A1, expected after infection with HIV-1 ADA_L210F than after infection with ADA_V82A (ratio ADA_L210F : ADA_V82A > 1). In contrast, the introduction of HLA-B*44:03 would result in a decrease of release when infected with ADA_L210F (ratio ADA_L210F : ADA_V82A $\leq$ 1) (figure 1.8 (A1)). Model A2 relies on model A1, but is based on a decrease of cytokines and chemokines (ratio ADA_L210F : ADA_V82A < 1 / ratio ADA_L210F : ADA_V82A $\geq$ 1) (figure 1.8 (A2)). For HLA-B*44:03 positive donors, a higher release of cytokines and chemokines is, according to model B1, expected after infection with HIV-1 ADA_V82A than after infection with ADA_L210F (ratio ADA_V82A : ADA_L210F > 1). In contrast, the introduction of HLA-A*02:01 would result in a decrease of release when infected with ADA_V82A (ratio ADA_V82A : ADA_L210F $\leq$ 1) (figure 1.8 (B1)). Model B2 relies on model B1, but is based on a decrease of cytokines and chemokines (ratio ADA_V82A : ADA_L210F < 1 / ratio ADA_V82A : ADA_L210F $\geq$ 1) (figure 1.8 (B2)).

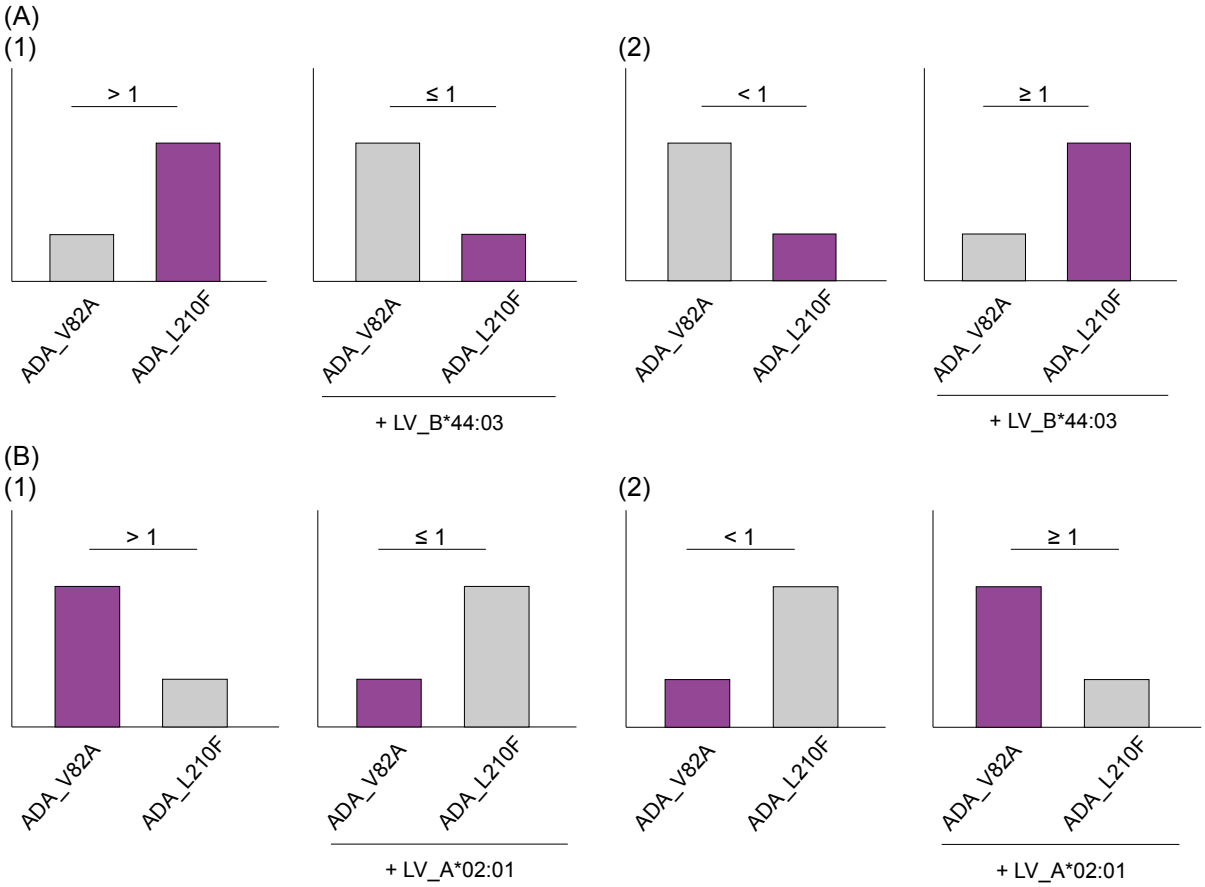

Figure 1.8 Interpretation models of cytokine and chemokine release in co-cultures containing moDCs deriving from (A) HLA-A*02:01 and (B) HLA-B*44:03 positive donors. The influence of two different mutations (V82A (PR) and L210F (RT)) are evaluated in the HLA background of the donor and in the LV-introduced HLA-background. Grey bars represent cytokine and chemokine release upon encountering HIV-1 ADA including the respective possible immune escape mutation, purple bars the "wild type". Differences between cytokine and chemokine release upon encountering the two viral strains were calculated, dividing wild type by immune escape mutation. A value above 1 represents an increased release in cytokines and chemokines upon infection with wild type viral strain and a value below 1, an increased release upon infection with viral strains containing the possible escape mutation. (1) represents an increase of cytokine and chemokine release caused by immune escape (2) a decrease in cytokine and chemokine levels.

2. Materials

2.1 Prokaryotes

Bacterial strains

Escherichia coli (E.coli) strain JM109 (table 2.1) were made competent for transformation purposes, while purchased One Shot®Top10 Competent Cells (Top10) (table 2.1) were made competent by the manufacturer. Both were stored until further use at -80°C.

Table 2.1 Overview and description of bacterial strains used for transformation purposes

Bacterial strain	Genotype	Manufacturer
One Shot®Top10 Competent Cells	F- *mcr*A Δ(*mrr-hsd*RMS-*mcr*BC) φ80*lacZ*ΔM15 Δ*lac*X74 *rec*A1 *ara*D139 Δ(*araleu*); 7697 *gal*U *gal*K *rps*L (StrR) *end*A1 *nup*G	Invitrogen, Darmstadt, Germany
E. coli JM109	*e14-(McrA-) recA1 endA1 gyrA96 thi-1; hsdR17(rK- mK+) supE44 relA1 Δ(lac-proAB); [F' traD36 proAB lacIqZΔM15]*	Promega, Mannheim, Germany

2.2 Eukaryotes

Cell lines

Cell lines, listed in table 2.2, were used for different transfection and stimulation assays. They were cultured in appropriate cell culture media (table 2.11) at 37 °C with 5 % of CO_2.

Table 2.2 Overview and description of cell lines used for transfection and stimulation assays

Cell name	Description	Obtained from
293T/17 SF (ATCC® No.: CRL-11268)	*Homo sapiens* (human), embryonic kidney cell line, stably transfected with large T-antigen of simian virus 40 (SV40)	kindly provided by H. Walter
CEMx174-M7R5-EGFP-Luc [141]	eGFP, Luc and CCR5 stably transfected CEMx174, human $CD4^+$ T cell / B cell hybrid	kindly provided by S.Pöhlmann
PM-1 [142]	Human T cell line, derived from HUT-78, expressing CXCR4 and CCR5 receptor	kindly provided by P.Lusso and R.Gallo

Primary cells

$CD8^+$ T cells, $CD14^+$ monocytes, $CD16^+CD56^+$ NK cells were selected from PBMCs of healthy donors using CD8 / CD14 MicroBeads and the $CD56^+CD16^+$ NK Cell Isolation Kit according to the manufacturers' protocol. HLA-A, –B and –C alleles are given in table 2.3. Cells were cultured in the appropriate cell culture media (table 2.11) at 37 °C with 5 % of CO_2.

Table 2.3 Overview of HLA-A, -B and –C alleles of healthy donors

Healthy donor	HLA-A alleles	HLA-B alleles	HLA-C alleles
1	**0201, 0201**	1501, 5101	0702, 1502
2	**0201, 0201**	3901, 5101	1203, 1502
3	0301, 2402	0702, **4403**	0702, 1601
4	2301, 2601	5101, **4403**	0401, 1203

2.3 Nucleic acids

Oligonucleotides

Oligonucleotide primer for polymerase chain reaction (PCR) were obtained from Eurofins MWG, Ebersberg, Germany and real-time PCR oligonucleotide primer and probes from TIB MOLBIOL, Berlin, Germany. The Oligo(dT)18 primer was purchased from Thermo Fisher Scientific, Schwerte, Germany. Sequences (5'→3') of oligonucleotide primer are listed in table 2.4.

Table 2.4 Overview and sequence of oligonucleotide primer and probes

Oligonucleotide name	Sequence 5'→ 3'
(a) Used for the amplification of HLA-ORF from cDNA [143]	
HLA-A_5'-Bam	TATAGGATCCGATTCTCCCCAGACGCCGAGG
HLA-A_3'-Nsi-6His	GGGGTCATGCATTCAATGATGATGATGATGATGCACTTTACAAGCTGTGAGAGACAC
HLA-B_5'-Bam	TATAGGATCCCACCCGGACTCAGAATCTCCT
HLA-B_3'-Nsi-6his	GGGCGCATGCATTCAATGATGATGATGATGATGAGCTGTGAGAGACACATCAGAGCC
HLA-C_5'-Bam	TATAGGATCCTTCTCCCCAGACGCCGAGA
HLA-C_3'-Nsi-6His	GGGGTCATGCATTCAATGATGATGATGATGATGGGCTTTACAAGCGATGAGAGACTC
(b) used for the amplification of HIV-1 pol, HLA-ORF in pHR'SIN-cPPT-SEW and amplification and sequencing of ligation products in pCR2.1®-TOPO®TA	
HIV-pol-5'	GAAGAAATGATGACAGCATGTCAGGG
HIV-pol-3'	TAATTTATCTACTTGTTCATTTCCTCCAAT
SEW-5'-HLA-ORF	TATTTGAATTAACCAATCAG
SEW-3'-HLA-ORF	TGATACAAAGGCATTAAAGC
TOPO-5'	GTAAAACGACGGCCAG
TOPO-3'	CAGGAAACAGCTATGAC
(c) Used for site directed mutagenesis (SDM)	
PR_V82A-5'	TATTAGTAGGACCTACACCTGCCAACATAATTGGAAGAAATCTG
PR_V82A-3'	CAGATTTCTTCCAATTATGTTGGCAGGTGTAGGTCCTACTAATA
RT_L210F-5'	AGGAACTGAGACAACATCTGTTCAGGTGGGGATTT
RT_L210F-3'	AAATCCCCACCTGAACAGATGTTGTCTCAGTTCCT
(d) Used for Real-time PCR [144]	
Albumin-5'	TGAAACATACGTTCCCAAAGAGTTT
Albumin-3'	CTCTCCTTCTCAGAAAGTGTGCATAT
Albumin-Probe	6FAM-TGCTGAAACATTCACCTTCCATGCAGA-BBQ
β-Actin-5'	GCGAGAAGATGACCCAGATC
β-Actin-3'	CCAGTGGTACGGCCAGAGG
β-Actin-Probe	6FAM-CCAGCCATGTACGTTGCTATCCAGGC-BBQ
WPRE-5'	CCGTTGTCAGGCAACGTG
WPRE-3'	AGCTGACAGGTGGTGGCAAT
WPRE-Probe	6FAM-TGCTGACGCAACCCCCACTGGT-BBQ

Plasmids

The cloning plasmid pCR2.1®-TOPO®TA was part of the TOPO®TA Cloning® Kit obtained from Invitrogen, Darmstadt, Germany. Plasmids to generate lentiviral vectors were kindly provided by Dr. U. Dietrich and Prof. Dr. C. Münck. The plasmid used for the generation of recombinant HIV-1 was kindly provided by Prof. Dr. M. Stevenson. All plasmids were transformed in E.coli JM109 for storage as well as for duplication purposes. Table 2.5 gives an overview and short description of the plasmids used.

Table 2.5 Overview, specifications and maps of plasmids

Plasmid	Specifications	Obtained from
pHR'SINcPPT-SEW (9659bp) [145]	Lentiviral expression vector; Amp^R SFFV promoter in front of reporter gene eGFP, ψ-Signal, HIV-1-5'-LTR und 3'-SIN-LTR	kindly provided by Dr. U. Dietrich, GSH Frankfurt, Germany

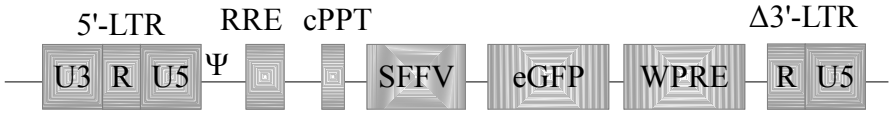

pCMVΔR8.91 (12150bp) [146]	Lentiviral expression vector, Amp^R coding for HIV-1 proteins (*gag, pol, rev, tat*); CMV-IE promoter	kindly provided by Dr. U. Dietrich, GSH Frankfurt, Germany

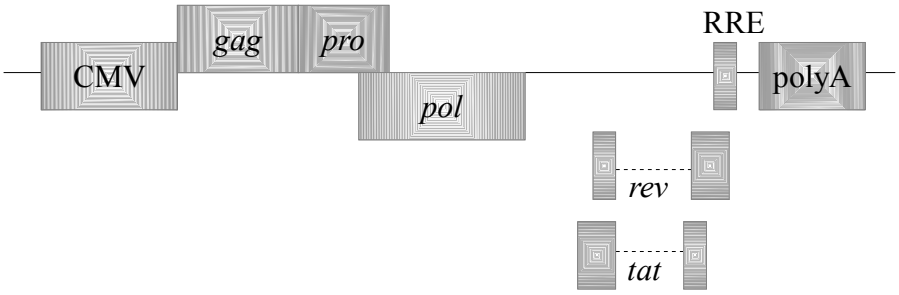

pM.DG (6363bp) [147]	expression vector coding for VSV-G (Vesicular stomatitis virus G glycoprotein), Amp^R	kindly provided by Prof. Dr. C. Münck, Heinrich-Heine University, Düsseldorf, Germany

pADA (14834bp) [148]	full-length HIV-1 clone, Amp^R	Kindly provided by Prof. Dr. M. Stevenson, Center for AIDS research, MA, USA

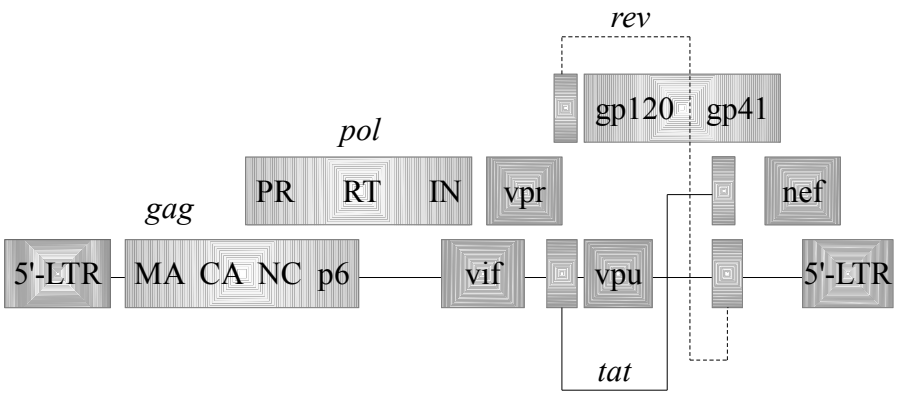

Molecular weight size marker

GeneRuler™ 1 kb Ladder (Fermentas, St.Leon, Germany) was used in agarose gel electrophoresis to estimate the size of DNA fragments.

2.4 Enzymes

Specific-buffers for each restriction enzyme used as well as bovine serum albumin (BSA) were provided with the restriction enzymes by the manufacturer. Table 2.6 shows the enzymes and their manufacturer.

Table 2.6 Overview of restriction enzymes and other enzymes used for work with nucleic acids

Enzyme	Manufacturer
BamHI-HF	New England Biolabs, Frankfurt a.M., Germany
DpnI	
EcoRI	
NsiI	
SbfI-HF	
shrimp alkaline phosphatase (SAP)	Fermentas, St. Leon, Germany
SpeI	New England Biolabs, Frankfurt a.M., Germany

2.5 Antibodies and isotype controls

Monoclonal antibodies were used in flow cytometry to characterize eukaryotic cells. Table 2.7 lists these antibodies and antibody specific information.

Table 2.7 Overview of (a) antibodies and (b) isotype controls used for flow cytometry

Antigen	Clone	Isotype (mouse)	Conjugated dye	Used Dilution	Manufacturer
(a) Antibodies					
HLA-ABC	G46-2.6	IgG1, κ	PE	1:50	BD Biosciences, Heidelberg, Germany
HLA-DR	TU36	IgG2b, κ	FITC	1:50	
CD3	BW264/56	IgG2a, κ	VioBlue	1:50	Miltenyi Biotec, Bergisch Gladbach, Germany
CD4	RPA-T4	IgG1, κ	APC	1:50	BD Biosciences, Heidelberg, Germany
CD8	SK1	IgG1, κ	PerCP	1:50	
CD14	TÜK4	IgG2a, κ	PE	1:50	Miltenyi Biotec, Bergisch Gladbach, Germany
CD16	VEP13	IgM	FITC	1:50	
CD25	M-A251	IgG1, κ	PE	1:50	BD Biosciences, Heidelberg, Germany
CD56	AF12-7H3	IgG1, κ	PE	1:50	Miltenyi Biotec, Bergisch Gladbach, Germany
CD80	B7-1	IgG1, κ	PE	1:50	BD Biosciences, Heidelberg, Germany
CD83	HB15e	IgG1, κ	PE	1:50	
CD86	2331 (FUN-1)	IgG1, κ	PE	1:50	
6xHis	GG11-8F3.5.1	IgG2b, κ	FITC	1:200	Miltenyi Biotec, Bergisch Gladbach, Germany
(b) Isotype controls					
KLH (keyhole limpet hemocyanin)	G155-178	IgG2a, κ	Biotin	1:50	BD Biosciences, Heidelberg, Germany
	27-35	IgG2b, κ	FITC		
	MOPC-21	IgG1, κ	APC		
			PE		
	IS5-20C4	IgM	FITC		Miltenyi Biotec, Bergisch Gladbach, Germany
Streptavidin-Phycoerythrin (SAv-PE)			PE	1:100	BD Biosciences, Heidelberg, Germany

2.6 Reagent kits

Reagent kits were applied to perform some experiments or preparation procedures. These kits are listed in table 2.8.

Table 2.8 Overview of reagent kits

Reagent Kit	Manufacturer
(a) Used for the purification of nucleic acids	
NucleoBond®Xtra Maxi	Macherey-Nagel, Düren, Germany
NucleoSpin®Tissue	
NucleoSpin®Gel and PCR Clean-up	
NucleoSpin®Plasmid	
NucleoSpin®RNA Blood	
AllPrep DNA/RNA Mini Kit	Qiagen, Hilden, Germany
(b) Used for different PCR based techniques	
HotStarTaq DNA Polymerase	Qiagen, Hilden, Germany
High Capacity cDNA Reverse Transcription Kit	Applied Biosystems, Darmstadt,Germany
Maxima® Reverse Transcripase	Fermentas, St. Leon, Germany
QuikChange®Site-Directed Mutagenesis Kit	Stratagene, Waldbronn, Germany
Light Cycler® 480 Probes Master	Roche Applied Science, Mannheim, Germany
Protector RNase Inhibitor	Roche Applied Science, Mannheim, Germany
(c) Used for nucleic acid sequencing	
ViroSeq® HIV-1 Genotyping System	Abbott Molecular, Wiesbaden, Germany
BigDye® Terminator v3.1	Invitrogen, Darmstadt, Germany
(d) Used for cloning purposes	
TOPO®TA Cloning® Kit, including pCR2.1®-TOPO®TA and One Shot®Top10 Competent Cells	Invitrogen, Darmstadt, Germany
Quick Ligation™ Kit	New England Biolabs, Frankfurt a.M., Germany
(e) Used for protein detection	
Bradford Protein Assay	Biorad, München, Germany
Cytokine Human 25-Plex Panel	Invitrogen, Darmstadt, Germany
(f) Used for the isolation of specific cell types	
$CD56^+CD16^+$ NK Cell Isolation Kit	Miltenyi Biotec, Bergisch Gladbach, Germany
CD8 MicroBeads, human	
CD14 MicroBeads, human	
(g) Used for the transfection of cells	
FuGENE® HD Transfection Reagent	Promega, Mannheim, Germany
(h) Used for the detection and quantification of HIV	
Architect HIV Ag/Ab Combo	Abbott Diagnostics, Wiesbaden, Germany
RealTime HIV-1 Assay	

2.7 Chemical products and reagents

For the preparation of certain solutions described inhere chemical products and other reagents were used. Table 2.9 shows the chemical product or reagent and its manufacturer.

Table 2.9 Overview of chemical products and reagents

Chemical product / reagent	Manufacturer
6x DNA Loading Dye	Fermentas, St. Leon, Germany
Ampicillin	Sigma-Aldrich, Taufkirchen, Germany
Ampuwa, *aqua ad injectabilia*	DelterSelect, Pfullingen, Germany
BD Cytofix / Cytoperm™ –buffer	Becton Dickinson, Heidelberg, Germany
BD Perm / Wash™ –buffer	
β-Mercaptoethanol	AppliChem, Darmstadt, Germany
Deoxyribonucleic acid, low molecular weight from salmon sperm	Sigma-Aldrich, Taufkirchen, Germany
Dimethyl sulfoxide (DMSO)	AppliChem, Darmstadt, Germany
Dulbecco's Phoshate-buffered Saline (1x) (D-PBS)	Invitrogen, Darmstadt, Germany
Empigen® BB detergent	Sigma-Aldrich, Taufkirchen, Germany
Ethanol	Roth, Karlsruhe, Germany
Ethidiumbromid	Roth, Karlsruhe, Germany
Ethylenediaminetetraacetic acid (EDTA)	AppliChem, Darmstadt, Germany
Fetal Bovine Serum (FBS)	Invitrogen, Darmstadt, Germany
Ficoll-Paque™ PLUS	GE Healthcare, Freiburg, Germany
Gibco® Dulbecco's Modified Eagle Medium (D-MEM) GlutaMAX™	Invitrogen, Darmstadt, Germany
Gibco® RPMI 1640 GlutaMAX™	
Glucose	AppliChem, Darmstadt, Germany
Glycerol	Calbiochem, Schwalbach, Germany
GM-CSF, human	Miltenyi Biotec, Bergisch Gladbach, Germany
Hi-Di™ Formamide	Invitrogen, Darmstadt, Germany
Human serum	Sigma-Aldrich, Taufkirchen, Germany
Hydrogen chloride (HCl)	Roth, Karlsruhe, Germany
IL-2, human	Roche Applied Science, Mannheim, Germany
IL-4, human	Miltenyi Biotec, Bergisch Gladbach, Germany
Isopropanol	Sigma-Aldrich, Taufkirchen, Germany
LB-Agar – Powder according to Lennox	AppliChem, Darmstadt, Germany
LB-Media – Powder according to Miller	
LE Agarose	Biozym, Hessisch Oldendorf, Germany
Lectin (Phytohemagglutinin PHA-M) from *Phaseolus vulgaris* (red kidney bean)	Sigma-Aldrich, Taufkirchen, Germany
MACSQuant Bleach Solution	Miltenyi Biotec, Bergisch Gladbach, Germany
MACSQuant Running –buffer	
MACSQuant Storage Solution	
MACSQuant Washing Solution	
Magnesium chloride ($MgCl_2$)	Merck, Darmstadt, Germany
Magnesium sulfate ($MgSO_4$)	Merck, Darmstadt, Germany
H_2O for analysis	Merck, Darmstadt, Germany
Paraformaldehyd (PFA)	Electron, München, Germany
Penicillin / Streptavidin	Invitrogen, Darmstadt, Germany
Polyethylene glycol (PEG)	ICN Biomedicals, Inc., Aurola, OH, USA
Puromycin dihydrochloride	Sigma-Aldrich, Taufkirchen, Germany
Sephadex™ G-50 Superfine	Merck, Darmstadt, Germany
S.O.C. Medium	Invitrogen, Darmstadt, Germany
Sodium azide (NaN_3)	AppliChem, Darmstadt, Germany
TAE -buffer (50x)	5 Prime, Hamburg, Germany
Tris base	Merck, Darmstadt, Germany
0.25 % Trypsin-EDTA (1x), Phenol Red	Invitrogen, Darmstadt, Germany

2.8 Buffers and Solutions

Certain solutions and buffers were prepared with the ingredients and concentration listed in table 2.10.

Table 2.10 Overview of buffer and solutions

Buffer / Solution	Components	Concentration
Transformation and storage-buffer (TSB)	PEG	30 mM
	DMSO	5 % (w/v)
	$MgCl_2$	10 mM
	$MgSO_4$	10 mM
Tris-EDTA (TE) buffer	Tris pH 8.0	10 mM
	EDTA	1 mM
FACS wash in D-PBS	FBS	4 % (v/v)
	NaN_3	0.1 % (w/v)
MACS buffer	D-PBS	500 mL
	EDTA	1 mM
	human serum	1 % (v/v)

2.9 Media

Media for bacterial culture

Transformed bacteria were plated on LB-agar dishes supplemented with ampicillin. For this purpose, 40 g LB-agar powder according to Lennox were dissolved in 1000 mL H_2O. 100 µg mL^{-1} ampicillin were added and approximately 20 mL LB-agar were poured in each dish. For the growth of transformed bacteria in LB-media supplemented with ampicillin, 25 g LB-medium powder according to Miller were dissolved in 1000 mL H_2O. 100 µg mL^{-1} ampicillin was added.

Media for cell culture

Used eukaryotic cell types require different culture media and suitable components according to their needs. In table 2.11 cell types and the composition of their culture media is listed.

Table 2.11 Overview of culture media with appropriate components for eukaryotic cell types

Eukaryotic cell type	Components	Comments
(a) Cell lines		
Adherent cells: DMEM10 - 293T / 17 SF	Gibco® D-MEM GlutaMAX™ 10 % FBS (v/v) 50 U mL^{-1} penicillin 50 µg mL^{-1} streptomycin	Storage at 4 °C, referred to as DMEM10
Suspension cells: RPMI10 - CEMx174-M7R5-EGFP-Luc - PM-1	Gibco® RPMI 1640 GlutaMAX™ 10 % FBS (v/v) 50 U mL^{-1} penicillin 50 µg mL^{-1} streptomycin	Storage at 4 °C, referred to as RPMI10 add 1 µg mL^{-1} puromycin for selection of CEMx174-M7R5-EGFP-Luc
(b) Primary cells		
Negative fraction of positive selected $CD14^+$ monocytes	Gibco® RPMI 1640 GlutaMAX™ 5 % human serum (v/v) 50 U mL^{-1} penicillin 50 µg mL^{-1} streptomycin 20 U mL^{-1} IL2	Storage at 4 °C, add IL-2 freshly
$CD14^+$ monocyte derived dendritic cells	Gibco® RPMI 1640 GlutaMAX™ 1 % human serum (v/v) 50 U mL^{-1} penicillin 50 µg mL^{-1} streptomycin 1000 U mL^{-1} GM-CSF 200 U mL^{-1} IL-4	Storage at 4 °C Every second day 100-200 µL of R1 GM-CSF/IL-4 needs to be added
Co-cultures of moDCs and $CD8^+$ T or $CD16^+CD56^+$ NK cells	Gibco® RPMI 1640 GlutaMAX™ 5 % human serum (v/v) 50 U mL^{-1} penicillin 50 µg mL^{-1} streptomycin 1000 U mL^{-1} GM-CSF 200 U mL^{-1} IL-4 20 U mL^{-1} IL-2	Storage at 4 °C Every second day 100-200 µL of R1 GM-CSF/IL-4 needs to be added

2.10 Devices and Consumables

Consumables made from plastics or glass were obtained from Eppendorf, Hamburg, Germany; Falcon, Heidelberg, Germany; Greiner, Frickenhausen, Germany; Sarstedt, Nümbrecht, Germany; Millipore, Eschborn, Germany; Starlab, Ahrensburg, Germany; TPP, Trasadingen, Schweiz; Roche Applied Science, Mannheim, Germany; Thermo Fisher Scientific, Schwerte, Germany; Diversified Biotech, Dedham, MA, USA; ratiolab, Dreieich, Germany; Roth, Karlsruhe, Germany; VWR, Darmstadt, Germany; Schott, Mainz, Germany and Corning Incorporated, Wiesbaden, Germany. Table 2.12 lists the devices.

Table 2.12 Devices

Device	Specification	Manufacturer
Microcentrifuge		
S2	5417C	Eppendorf, Hamburg, Germany
	2K15	Sigma, Osterode am Harz, Germany
S3	Z216MK	Hermle, Wehingen, Germany
Medium bench centrifuge		
S2 (bacteria)	Megafuge® 1.OR	Heraeus, Hanau, Germany
S3 (cell culture)	Z383K	Hermle, Wehingen, Germany
Plate centrifuge		
S2	Typ 415	Sigma, Osterode am Harz, Germany
	Z300	Hermle, Wehingen, Germany
Incubator		
S2 (bacteria)	Innova™ 4900	New Brunswick, Nürtingen, Germany
S3 (cell culture)	CO_2 Incubator MCO-2OAIC	Sanyo, Wiesloch, Germany
Electrophoresis Devices:		
BioRad Power Pac 300 Sub-Cell® GT		Biorad, München, Germany
Sub-Cell® GT Cell		
Gel Doc™		
Fluorescence Microscope		
S3	CKX41	Olympus, Düsseldorf, Germany
	IX81	
Hood		
S2 (Real-time PCR)	Hera Safe	Heraeus, Hanau, Germany
S3 (cell culture)	Biowizard Xtra	Kojair, Vilppula, Germany
Other Devices:		
ABI 3130XL Genetic Analyzer		Applied Biosystems, Weiterstadt, Germany
Architect i2000SR		Abbott Diagnostics, Wiesbaden, Germany
ELx50 Microplate Strip Washer		BioTek®, Bad Friedrichshall, Germany
Eppendorf BioPhotometer plus		Eppendorf, Hamburg, Germany
LightCycler® 480		Roche Diagnostics, Mannheim, Germany
Luminex® SD™		Luminex Corporation, Austin, TX, USA
m2000™		Abbott Diagnostics, Wiesbaden, Germany
MACSQuant® Analyzer		Miltenyi, Bergisch Gladbach, Germany
Nanodrop ND-1000 Spectrophotometer		Peqlab, Erlangen, Germany
PCR-Thermoblock TRIO		Biometra, Göttingen, Germany
Thermomixer 5436		Eppendorf, Hamburg, Germany

2.11 Software

Software is needed to run certain devices but also to analyse data. Table 2.13 shows the software used including its application.

Table 2.13 Software

Software	Company	Application
FlowJo 7.6.5	Tree Star, Inc., Ashland, OR, USA	Analysis of flow cytometry data
Geno2pheno	geno2pheno.org	Alignment of HIV-1 sequences with reference strain HXB2
Lasergene® SeqMan Pro™	DNASTAR, Madison, WS, USA	Editing of sequencing data
LightCycler® Software release 1.5.0 SP3	Roche Applied Science, Mannheim, Germany	Analysis of real-time PCR data
Luminex 100IS Software 2.3.182	Luminex Corpoation, Austin, TX, USA	Analysis of luminex data
MACSQuantify®	Miltenyi, Bergisch Gladbach, Germany	Analysis of flow cytometry data
MATLAB R2010b	The MathWorks Inc., Natick, MA, USA	Statistical assessment of associations between tRAMs and HLA alleles
Microsoft Office Excel and Word 2003	Microsoft, Unterschleißheim, Germany	Analysis and presentation of data
Origin 7.5 SR4	Northhampton, MA, USA	Analysis and presentation of luminex data
QuickChange Primer Design	Agilent Technologies, Waldbronn, Germany	Design of mutagenic primer for QuickChange site-directed mutagenesis
SPSS 16.0	IBM, Ehningen, Germany	Statistical analysis of HIV-1 and HLA data

2.12 Databases

Databases contain a huge number of sequences or other data generated by the scientific community. Table 2.14 summarizes those databases used.

Table 2.14 Databases

Database	URL / reference	Application
Arevir Database	Local HIV database	Access to patient HIV-1 and HLA data
IMGT / HLA Database	http://www.ebi.ac.uk/ipd/imgt/hla/	Use of basic local alignment search tool (BLAST) for the analysis of HLA sequences
IAS-USA drug resistance mutation list	[149]	Identification of resistance associated mutations (RAMs)

3. Methods

3.1 Standard laboratory methods

Generation of competent E.coli JM109

100 mL antibiotic-free LB-medium were inoculated with 5 mL freshly grown JM109 culture and grown at 37 °C under permanent shaking until reaching an OD_{600} of 0.6-0.9. Bacteria were centrifuged at 3000 g and 4 °C for 15 min, the bacterial pellet was resuspended in 5 mL ice-cold TSB. Aliquots of competent JM109 were stored at -80 °C for further use.

Transformation of JM109 and Top10

50 µL competent bacteria (JM109 and Top10) stored at -80 °C, were thawed on ice and 1 µL plasmid-DNA (JM109), 5 µL ligation mix (JM109) or 2 µL TOPO® cloning reaction product (Top10) were added, respectively. After incubation for 30 min on ice, bacteria were heat shocked at 42 °C for 30 sec and again put on ice for 2 min before 250 µL S.O.C. medium was added. In order to permit the expression of selectable markers, bacteria were incubated for 60 min at 37 °C under permanent shaking. Transformation approaches were plated on preheated LB-agar dishes and incubated over night at 37 °C. Single colonies were picked to be cultured in the appropriate volume of LB-media for the isolation of plasmid-DNA.

Maintenance of cell lines and primary cells

Adherent cells (e.g. 293T / 17 SF, (293T)) were grown in continuous culture as monolayers on 10 cm tissue culture plates. They were split twice weekly 1:10 – 1:20 depending on their density. A confluent plate of cells was split as follows: media was removed by aspiration and the cells washed with D-PBS. Cells were overlaid with 0.25 % Trypsin-EDTA (1x), Phenol Red and incubated at 37 °C for 2-3 min. Cells were harvested by adding D-PBS and, after centrifugation for 10 min at 300 g, resuspended in DMEM10 (table 2.11a). The appropriate volume was transferred in a fresh 10 cm plate and incubated for 3-4 days at 37 °C with 5 % of CO_2.

Cells grown in suspension (e.g. CEMx174-M7R5-EGFP-Luc and PM-1) were resuspended in RPMI10 (table 2.11a) and cultured in cell culture flask. They were split every other week 1:20 – 1:50 depending on their density. The appropriate volume of cell suspension was transferred into a fresh cell culture flask and RPMI10

was added. For the selection of CEMx174-M7R5-EGFP-Luc 1 µg mL^{-1} puromycin was added to the medium. Cells were incubated at 37 °C with 5 % of CO_2.
$CD14^+$ primary cells were cultured in the appropriate cell culture medium (table 2.11b) in cell culture flasks at a density of $1*10^6$ cells mL^{-1} at 37 °C with 5 % of CO_2. Every other day GM-CSF and IL-4 were added freshly to the culture. $CD8^+$ and $CD16^+CD56^+$ primary cells were purified from the negative fraction of $CD14^+$ cells on day eight, just before co-culturing with moDCs. The negative fraction was cultured at a density of $5*10^6$ 0.5 mL^{-1} in the appropriate medium containing IL-2 at 37 °C with 5 % of CO_2.

Isolation of plasmid-DNA

Isolation of plasmid-DNA (Mini-preparation using 5 mL culture, Maxi-preparation using 200 mL culture, extracting DNA from gel electrophoresis) was performed using reagent kits according to the manufacturers' protocol. DNA concentration was determined, assessing the adsorption at a wavelength of 260 nm. The ratio of absorbance at λ=260 nm and λ=280 nm gives the degree of DNA quality. A quotient of OD_{260} / OD_{280} > 1.8 implies pure DNA.

Isolation of genomic DNA from cultured cells

Isolation of genomic DNA from cultured cells was performed using the NucleoSpin®Tissue reagent kit. When isolating genomic DNA and total RNA from the same sample of cultured cells the AllPrep DNA/RNA Mini Kit was used according to the manufacturers' protocol. Concentration and quality were determined as described above.

Isolation of total RNA from cultured cells / blood

Total RNA from EDTA-blood was isolated using NucleoSpin®RNA Blood according to the manufacturers' protocol. 400 µL whole blood, supplemented with 1.2-2 mg EDTA mL^{-1} blood was used to isolate total RNA. Concentration and quality were determined, aiming a OD_{260} / OD_{280} ratio of 2.
As mentioned above, total RNA from cultured cells was isolated using the AllPrep DNA/RNA Mini Kit according to the manufacturers' protocol.

Transfection of 293T cells

For the transfection of 293T cells the FuGENE® HD Transfection Reagent was used according to the manufacturers' protocol. $2.5*10^6$ cells were plated in 100 mm dishes and incubated overnight. For the transfection of single plasmids (pHR'SINcPPT-SEW, pHR'SINcPPT-SEW_HLA-A*02:01 and pHR'SINcPPT-SEW_HLA-B*44:03, pADA, pADA_V82A, pADA_L210F) 10 µg of DNA was used. For the co-transfection of pHR'SINcPPT-SEW / pHR'SINcPPT-SEW_HLA-A*02:01 / pHR'SINcPPT-SEW_HLA-B*44:03, pCMVΔR8.91 and pM.DG 20 µg, 15 µg and 6 µg were used, respectively.

Restriction digest

For a preparative digest, 4 µg of DNA and for an analytical restriction digest 1 µg DNA were used. Reagents were added to the DNA as listed in table 3.1. Restriction digest was performed at 37 °C for one hour and DNA was loaded on an agarose gel for electrophoresis.

Table 3.1 Pipetting scheme of analytical and preparative restriction digest

Reagent	Analytical restriction digest	Preparative restriction digest
DNA	1 µg	4 µg
Enzyme	1 U	4 U
Enzyme specific-buffer	1 µL	4 µL
Optional BSA 1:10	1 µL	4 µL
H_2O for analysis	add to a final volume of 20 µL	add to a final volume of 40 µL

Ligation of DNA-fragments, TOPO® Cloning Reaction

Before the ligation of a DNA-fragment (insert) into a plasmid, the 5' end of the enzymatically restricted plasmid was dephosphorylated by using 2 U shrimp alkaline phosphatase (SAP), 40 µL preparative digest, as well as 2 µL (v / v) SAP-buffer in a total volume of 50 µL (supplemented with H_2O). Incubation was performed as described above.

For the ligation, the Quick Ligation™ Kit was used according to the manufacturers' protocol. Plasmid-DNA and insert were incubated in a ratio 1:3, which was calculated according to the following formula:

$$\text{insert [ng]} = 3 \times \text{plasmid [ng]} \times (\text{insert [bp]} / \text{plasmid [bp]}).$$

Ligation mixture was mixed as described in table 3.2 and the ligation reaction was completed over night at room temperature.
The TOPO® Cloning Reaction was performed according to the manufacturers' protocol of the TOPO®TA Cloning® Kit.

Table 3.2 Pipetting schemes using the Quick Ligation™ Kit and the TOPO®TA Cloning® Kit

Quick Ligation™ Kit	
Reagent	**Amount**
T4-DNA-.Ligase	5 U
10x T4-Ligase-buffer	1 µL
Plasmid	3
Insert	1
H_2O for analysis	add to a final volume of 10 µL

TOPO®TA Cloning® Kit	
Reagent	**Amount**
Fresh PCR Product	4 µL
Salt Solution	1 µL
pCR2.1®-TOPO®TA	1 µL

Site directed mutagenesis (SDM)

For SDM the QuikChange™ Site-Directed Mutagenesis Kit was used according to the manufacturers' protocol. Reagents were combined and PCR conditions were performed as listed in table 3.3. This protocol permits site-specific mutagenesis in plasmids. It was used to generate point mutations leading to a switch in amino acids on proteins level.

Table 3.3 Pipetting scheme and PCR-Thermoblock TRIO conditions for SDM

Reagent	Amount
10x reaction-buffer	5 µL
DNA template	5-50 ng
Oligonucleotide #1	125 ng
Oligonucleotide #2	125 ng
dNTP mix	1 µL
H_2O for analysis	add to a final volume of 50 µL
PfuTurbo (2.5U)	1 µL

Temperature [°C]	Time [mm.ss]
95	00.30
95	00.30 I
55	01.00 I 18 cycles
68	02.00 I

Polymerase chain reaction (PCR)

The PCR serves as a rapid and selective amplification of small amounts of DNA fragments [150]. All PCR reactions discussed herein, were performed using the HotStarTaq DNA Polymerase Kit using the reaction mixture as listed in table 2.18. Reaction mixtures were placed into a PCR-Thermoblock TRIO for 45 cycles using the conditions listed in table 3.4.

Table 3.4 Pipetting scheme and PCR-Thermoblock TRIO conditions for PCR

Reagent	Amount
10x PCR-buffer	10 µL
5x Q-Solution	20 µL
dNTPs (10µM)	2 µL
5' forward primer (10 µM)	1 µL
3' reverse primer (10 µM)	1 µL
Template DNA	1-2 µg
HotStarTaq Polymerase (4 U / µL)	0.5 µL
Ampuwa, *aqua ad injectabilia*	add to a final volume of 100 µL

Temperature [°C]	Time [mm.ss]		
95	15.00		
95	00.30		
65	00.45		
72	03.00		
95	00.30		
60	00.45		
72	03.00		
95	00.30	I	
55	00.45	I	45 cycles
72	03.00	I	

Complementary DNA (cDNA) synthesis by reverse transcriptase PCR

By means of the application of an enzyme, the reverse transcriptase, RNA can be transcribed in vitro in cDNA. For the reverse transcription 400 ng of total RNA isolated from blood was transcribed with MAXIMA® reverse transcriptase and Oligo(dt)18-primer in the presence of a RNAse Inhibitor. The mixture was generated as described in table 3.5.

Table 3.5 cDNA synthesis using MAXIMA reverse transcriptase

Reagent	Amount
Template RNA	400 ng
Oligo(dT) (100 pM)	1 µL
dNTP Mix (10 mM)	1 µL
Nuclease-free H_2O	add to a final volume of 14.5 µL
5x RT-buffer	4 µL
RNase Inhibitor	0.5 µL (20 U)
Maxima® Reverse Transcriptase	1 µL (200 U)

Temperature [°C]	Time [mm.ss]
50	30.00
85	05.00

Total RNA isolated from cell lines was transcribed using the High Capacity cDNA Reverse Transcription Kit, using 800 ng of total RNA, following the scheme listed in table 3.6.

Table 3.6 cDNA synthesis using the High Capacity cDNA Reverse Transcription Kit

Reagent	Amount
10x RT-buffer	2 µL
25x dNTP Mix (100 mM)	0.8 µL
10x RT Random Primers	2 µL
MultiScribe™ Reverse Transcriptase	1 µL
RNase Inhibitor	1 µL
Nuclease-free H_2O	3.2 µL
Template RNA in 10 µL	800 ng

Temperature [°C]	Time [mm.ss]
25	10.00
37	120.00
85	05.00

Real-time PCR

Using the real-time PCR technique, DNA of interest (template DNA) cannot only be amplified but also quantified. Oligonucleotide primers located at the 3'- and 5'-terminus of the target DNA facilitate its amplification. Hybridized sequence-specific fluorescent labelled probes emit fluorescence when degraded by the 5' nuclease activity of the polymerase in the course of elongation. Fluorescence is detected and measured in each PCR cycle in the LightCycler®480 and its increase is corresponding to the exponential increase of the PCR product. The real-time PCR can be divided into three phases, the early phase, the exponential growth phase and a plateau phase. In the early phase, the background noise exceeds the fluorescence emitted by the probe. At some point the amount rises significantly above the background, the cycle number is defined as the crossing point (cp). Comparing cp values of samples to those of standards with known copy numbers, PCR products can be quantified. Table 3.7 lists ingredients of the reaction as well as the incubation conditions.

Table 3.7 Pipetting scheme and LightCycler®480 conditions for Real-Time PCR

Reagent	Amount
Nuclease-free H_2O	7 µL
Forward primer (10 µM)	1 µL
Reverse primer (10 µM)	1 µL
Probe	1 µL
Light Cycler® 480 Probes Master	10 µL
Genomic DNA / cDNA	5 µL

Temperature [°C]	Time [mm.ss]
95	10.00
95	00.15 I 40 cycle
60	01.00 I ← measurement

Designing standard/reference for RT-PCR

Here, the real-time PCR technique is used to determine the transducing units (TU) of lentiviral vectors and the lentiviral transgene expression in transduced target cells and is based on a protocol published by [144]. Lentiviral transgene expression is enhanced by the woodchuck hepatitis virus posttranscriptional regulatory element (WPRE), which is included in the 3' untranslated region of the transfer plasmid pHR'SINcPPT-SEW. This allows the quantification of lentiviral vectors at the level of integrated proviral DNA and cellular lentiviral vector-mediated gene (mRNA) expression. To obtain accurate TU and to monitor lentiviral transgene expression in transduced cells, copy numbers were normalized to genomic DNA albumin and β-actin mRNA copy number.

The cp values of standards are used to calculate the concentration of target genomic DNA and cDNA of transduced cell samples. Standards were generated for albumin, β-actin and WPRE and set up with six samples prepared in serial 1:10 dilutions of 10^6 copies. Dilutions were performed using plasmid maxi preparations and deoxyribonucleic acid, low molecular weight from salmon sperm (40 µg mL^{-1}, diluted in TE buffer). pCR2.1®-TOPO®TA_albumin and pCR2.1®-TOPO®TA_β-actin were generated, isolating genomic DNA of 293T cells, amplifying albumin and β-actin using primer sets (table 2.4d), which were also used in the Real-Time PCR assay and integrating these PCR products in pCR2.1®-TOPO®TA. pHR'SINcPPT-SEW was used to generate the WPRE standard curve (figure 3.1).

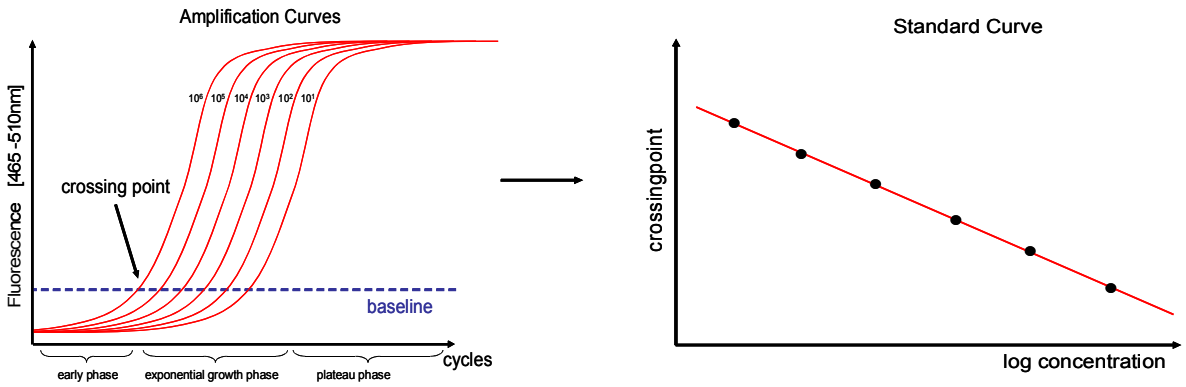

Figure 3.1 Example real-time PCR amplification plots of standards and generated standard curves by plotting cp against the number of plasmid copies to determine the copy number of an unknown sample

The calculation of DNA-based titers, representing the number of infectious particles, and mRNA-based titers, corresponding to mRNA expression of the transgene, was calculated as follows and is given in TU mL^{-1}.

TU mL^{-1} = WPRE concentration / 0.5 *albumin/β-actin concentration * total number of transduced cells * vector dilution factor(*)

(*) only the most dilute vector samples were used to calculate titers

Agarose gel electrophoresis

Agarose gel electrophoresis is used for the separation of DNA-fragments according to their length based on distinct velocities of migration in an electrical field. In order to identify the size of the DNA fragments, a DNA ladder, containing DNA fragments of defined length as reference facilitates the estimation of size of the applied DNA-fragment. Agarose gels used in this work are made of 1 % (w / v) agarose dissolved in Tris-acetate-EDTA-buffer (TAE). DNA was prepared in 6x loading dye to the digestion mixture or PCR product. Electrophoresis was performed in 1x TAE at 200 V for 40 min. DNA-fragments can be made visible using the intercalating chemical ethidium bromide (1 µg mL^{-1}), which fluoresces when exposed with UV light (λ = 250 - 310 nm). Pictures of agarose gels are documenting the fragmentation.

Sequencing reaction

For sequencing, the Sanger-method is used, which is based on chain breaks provoked by the assembly of dideoxynucleotides (ddNTPs) (instead of deoxynucleotides (dNTPs)) lacking the hydroxyl-group at their 3' terminus leading to an interrupted chain elongation. Here, ddNTPs, coupled to a fluorescent dye, are used, which enables the separation of fragments of different lengths in a capillary electrophoresis and excited by laser, nucleotide sequence can be concluded from emitted fluorescence profile.

For the sequencing of HIV pol, the HIV Genotyping Kit was used. A pre-mixture already contains the appropriate primer, the ddNTPs, dNTPs and the fluorescence dye and can be directly added to the sample. Here, 2 µL of sample are added to 3 µL of the respective primer mix (table 3.8).

Table 3.8 Pipetting scheme and PCR-Thermoblock TRIO conditions for sequencing reaction

Reagent	Amount	Temperature [°C]	Time [mm.ss]	
PCR Product / Plasmid- DNA	2 µL	96	00.10	
BigDye® Terminator v3.1	2 µL	96	00.10	I
5'- or 3' oligonucleotide (0.3 µM)	1 µL	60	03.00	I 29 cycles

Afterwards the sequence mix was purified to deplete factors from the sequencing reaction. To separate DNA fragments according to their molecular mass a sepharose column was used, following by applying the products on a gel matrix. While the fluorescent-marked DNA-fragments migrate through the column, the free ddNTPS were withheld. For the purification of the DNA of interest a Multi Screen Filter plate filled with Sephadex™ G-50 superfine was used. The sepharose was soaked with 300 µl water at 4 °C for at least 1 h and centrifuged at 910 g for 5 min. Template and Hi-Di™ Formamide, avoiding evaporation of the sample during the sequencing process, were added and centrifuged at 910 g for 5 min again. The purified product was thereby collected in the detection plate. After denaturating the DNA for 2 min at 90 °C the detection plate containing the purified sequencing product was placed into the sequencer ABI 3130XL Genetic Analyzer. The sequences were analyzed with the program Lasergene® SeqMan Pro™.

3.2 Protein detection

Flow cytometry, Permeabilization and Staining of cells for flow cytometry

Flow cytometry is used to identify the properties of cell subsets using specific antibodies to cellular proteins of interest. It is characterizing cells based on their granularity and size and, by using antibodies conjugated to a fluorescent dyes, intra- and extracellular proteins.

Using the MACSQuant® the detection of eight different fluorescence dyes could be performed according to manufacture's instructions.

In order to detect intracellular proteins, cells were permeabilized prior to flow cytometry. Cells were harvested, resuspended in D-PBS and BD Cytofix/Cytoperm™ Puffer according to manufacture's instructions for 20 min at 4 °C. Cells were washed prior to the staining with specific antibodies BD Perm/Wash™ Puffer (1:10). Staining of intracellular as well as extracellular proteins was performed as follows: 100 µL of cells [10^6 mL^{-1}] were stained with specific antibodies, using the appropriate dilution (table 2.6). After an incubation time of at least 30 min at 4 °C in the dark, cells were washed four times with FACS wash and run on the flow cytometer.

Bradford assay to determine protein content of lentiviral vector stocks and pADA based HIV-1 stocks

500 µL of Bradford reagent were added to 10 µL of lentiviral vector stocks / pADA based HIV-1 stocks and incubated for 5 min. Absorbance was detected at 595 nm with a spectrophotometer and protein concentration was calculated with the help of a standard curve. The standard curve was generated adding 0 µg, 10 µg, 20 µg, 40 µg, 80 µg and 100 µg BSA and 500 µL Bradford reagent.

3.3 Selection of patient cohort

The study on primary drug RESIstance in treatment-naïve HIV-1 infected patients (RESINA) is a multicentre study in North Rhine-Westphalia, Germany. Genotypic resistance testing was performed in therapy-naïve HIV-1 infected individuals prior to the start of antiretroviral treatment. Inclusion criteria for this analysis were documented HIV-1 infection, eligibility for application of HAART, the detection of transmitted resistance associated mutations (tRAMs) in either HIV-1 PR or RT and informed consent. Exclusion criteria were previous intake of antiretroviral drugs (as determined by self-report) and unwillingness to participate.

139 HIV-1 infected therapy-naïve patients were analysed: HIV-1 subtype (subdivision of group M of HIV-1) and HLA-A, -B and -C genotype.

Genomic DNA was extracted from patients' whole blood using the QiaAmp Blood Mini Kit according to the manufacturers' protocol. High-resolution HLA class I typing was performed by sequence-specific PCR [103, 151] at the Institute of Immunology and Genetics, Kaiserslautern, Germany.

3.4 Assessment of statistically significant associations between transmitted resistance associated mutations (tRAMs) and HLA class I alleles

The statistical analysis was performed with the help of Nico Pfeifer, Max Planck Institute for Informatics, Saarbrücken. Associations between tRAMs and HLA class I alleles were to be identified in order to identify potential immune escape variants within the well defined resistance associated mutations. Herefore, 139 HIV-1 infected HLA-typed therapy-naïve patients with detected transmitted resistance associated mutations (tRAMs) in either HIV-1 PR or RT were identified from the Arevir database (table 2.14).

Each individual of the cohort contributed a single HIV-1 sequence and a set of HLA class I genotypes to the analysis, resulting in a total of 6262 combinations of tRAM and HLA. Following Carlson et al. [152] a min count filter on the 2 x 2 contingency tables of all putative associations was applied, including only tests for which any bin in the contingency table had an observed and an expected value greater than three. After filtering in this way 236 putative associations remained. Statistical association between viral sequence and HLA class I genotypes were evaluated for these 236 combinations with Fisher's exact test using MATLAB R2010b. All p-values were two-sided. Additionally, false discovery rates (FDRs), q-values, and odds ratios (OR) together with the corresponding 95% confidence interval as a measure of the effect size were reported. ORs > 1 were considered relevant as this denotes that the chance for a mutation is higher to be found in the background of a given HLA type than the chance for a mutation without this HLA type. ORs were calculated according to Bland and Altman [153]. For contingency tables of tests that contained a bin with a zero entry, we followed the convention to add 0.5 to every bin. FDRs and q-values for all 236 tests of association between a specific HLA type and a particular tRAM. This was performed according to Storey and Tibshirani [154], while conservatively choosing $\pi 0$ equal to one. The q-value of an association test is the minimal FDR at which the test is accepted. All associations with FDR ≤ 0.10 were considered significant.

3.5 Generation of lentiviral vectors to produce recombinant monocyte derived dendritic cells (moDCs)

Recombinant DCs, over-expressing HLA class I alleles of interest, were generated using monocyte derived DCs transduced by a lentiviral vector described by Naldini and colleagues [147].

Lentiviral vectors allow the integration of genes of interest in non-dividing cells. To generate lentiviral vectors in 293T cells three plasmids were co-transfected: (1) a transfer plasmid (pHR'SINcPPT-SEW), encoding the gene of interest, (2) a helper plasmid (pCMVΔR8.91) facilitating the expression of viral proteins, which are necessary for the packaging of the gene of interest into a viral particle, and (3) an envelope plasmid (pM.DG), encoding the envelope protein VSV-g allowing the virus to enter most cell types (figure 3.2). Here, the genes of interest were: eGFP (control), HLA-A*02:01 and HLA-B*44:03, which were chosen according to the statistical analysis and isolated from healthy HLA-typed donors.

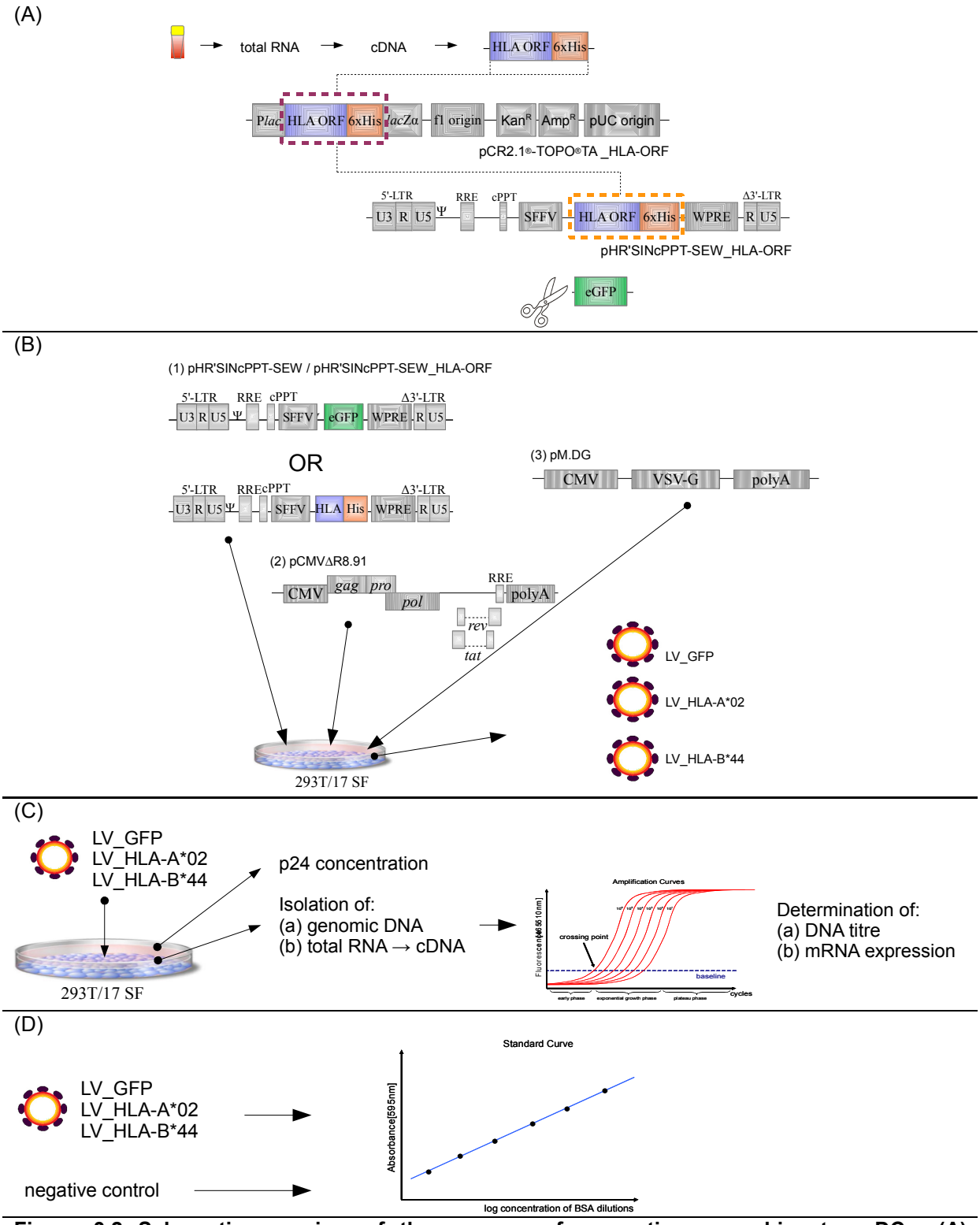

Figure 3.2 Schematic overview of the process of generating recombinant moDCs. (A) Generation of transfer plasmids introducing HLA-A or -B specific ORF. (B) Generation of lentiviral vectors LV_GFP, LV_HLA-A*02:01 and LV_HLA-B*44:03. (C) Determination of the infectious titer of the lentiviral vectors LV_GFP, LV_HLA-A*02:01 and LV_HLA-B*44:03. (D) Determination of the protein content within lentiviral vector stocks: LV_GFP, LV_ HLA-A*02:01 and LV_HLA-B*44:03 and a negative control

Generation of transfer plasmids introducing HLA-A or -B specific ORF

cDNA was generated from total RNA isolated from whole blood of HLA-typed healthy donors. In order to generate HLA-A or -B specific PCR products, a PCR was performed using the appropriate primer pairs (table 2.4a). The addition of the sequence of a BamHI restriction site at the 5' terminus and a NsiI restriction site on the 3'-end allowed cloning of the generated PCR product into the pCR2.1®-TOPO®TA cloning plasmid. In order to distinguish cell own HLA proteins from delivered HLA proteins, a sequence encoding for six Histidins (6his tag) was added using the PCR technique. Fresh PCR products were used for the Topo cloning reaction prior to clone the verified HLA fragment of interest into the transfer plasmid pHR'SINcPPT-SEW using BamHI and NsiI restriction sites.

Again, a sequencing reaction was performed to verify the presence of HLA ORF within the transfer plasmid. In order to confirm the expression of the proteins, 293T cells were transfected with the appropriate transfer plasmid. Flow cytometry permits to distinguish between cell own and delivered HLA proteins by measuring intracellular HLA-ABC and His antigens. Cells were permeabilized and stained for HLA-ABC and His for flow cytometric analysis.

*Generation of lentiviral vectors LV_GFP, LV_HLA-A*02:01 and LV_HLA-B*44:03*

Seven 100 mm dishes seeded with 293T cells were prepared for co-transfection pCMVΔR8.91, pM.DG and either pHR'SINcPPT-SEW, pHR'SINcPPT-SEW_HLA-A*02:01 or pHR'SINcPPT-SEW_HLA-B*44:03. Five days post transfection, supernatants containing the lentiviral vectors (LV_GFP, LV_HLA-A*02:01 and LV_HLA-B*44:03) were harvested and cell debris was removed by centrifugation at 300 g for 10 min at 4 °C and filtering using a 0.45 µm filter.

*Determination of the infectious titer of the lentiviral vectors LV_GFP, LV_HLA-A*02:01 and LV_HLA-B*44:03*

The number of viral particles was determined by measuring p24-antigen using the Architect HIV Ag / Ab Combo. This assay can be used for the qualitative detection of HIV-1 and HIV-2 p24 core protein antigen and antibodies and is based on the ELISA technique. The chemiluminiscent signals of each sample are compared to an integrated reference control. Results are given as the ratio of sample (S) and the control (CO). Values greater or equal to 1.00 are considered positive. The lentiviral

expression vector pCMVΔR8.91 encodes among others for HIV-1 gag the structural polyprotein, which is processed into several functional proteins, including CA, the capsid protein p24.

One cannot conclude the infectious titer determining p24 expression, therefore a real-time PCR assay was established according to [144]. The integration of the gene of interest was verified and lentiviral expression of the gene of interest in transduced cells demonstrated. 2 mL of 293T cells were seeded in six-well plates at a concentration of $1*10^4$ mL^{-1}. 24 hours later cells were transduced with 1:10 serial dilutions of lentiviral vectors starting with 100 µL undiluted lentiviral vector. On day five cells were harvested and genomic DNA as well as total RNA were isolated using the same samples. cDNA was generated prior to real-time PCR assay. The DNA-based titer as well as the mRNA-based titer were calculated.

*Determination of the protein content within lentiviral vector stocks: LV_GFP, LV_HLA-A*02:01 and LV_HLA-B*44:03*

A standard curve was designed, by measuring the absorbance at 595 nm of known BSA concentrations. The slope was used to calculate the concentrations of the lentiviral stocks and a negative control, by determining their absorbance.

3.6 Generation of infectious recombinant HIV-1 ADA: ADA_V82A, ADA_L210F

Recombinant ADA (ADA_V82A, ADA_L210F) were generated according to the statistical analysis (section 2.2.4), on the basis of the well characterized HIV-1 subtype B macrophage-tropic laboratory strain ADA [148]. Recombinant viral strains included the drug resistance associated mutations (RAMs) V82A in the PR and L210F in the RT. pADA pol ORF, comprising PR and RT was cloned in the pCR2.1®-TOPO®TA cloning plasmid to enable an in vitro site-directed mutagenesis of position 82 (PR) and 210 (RT), respectively. Mutagenised pADA pol ORF was cloned back into the pADA backbone for the generation of infectious viral particles via the transfection of 293T and subsequent infection of PM-1 cells.

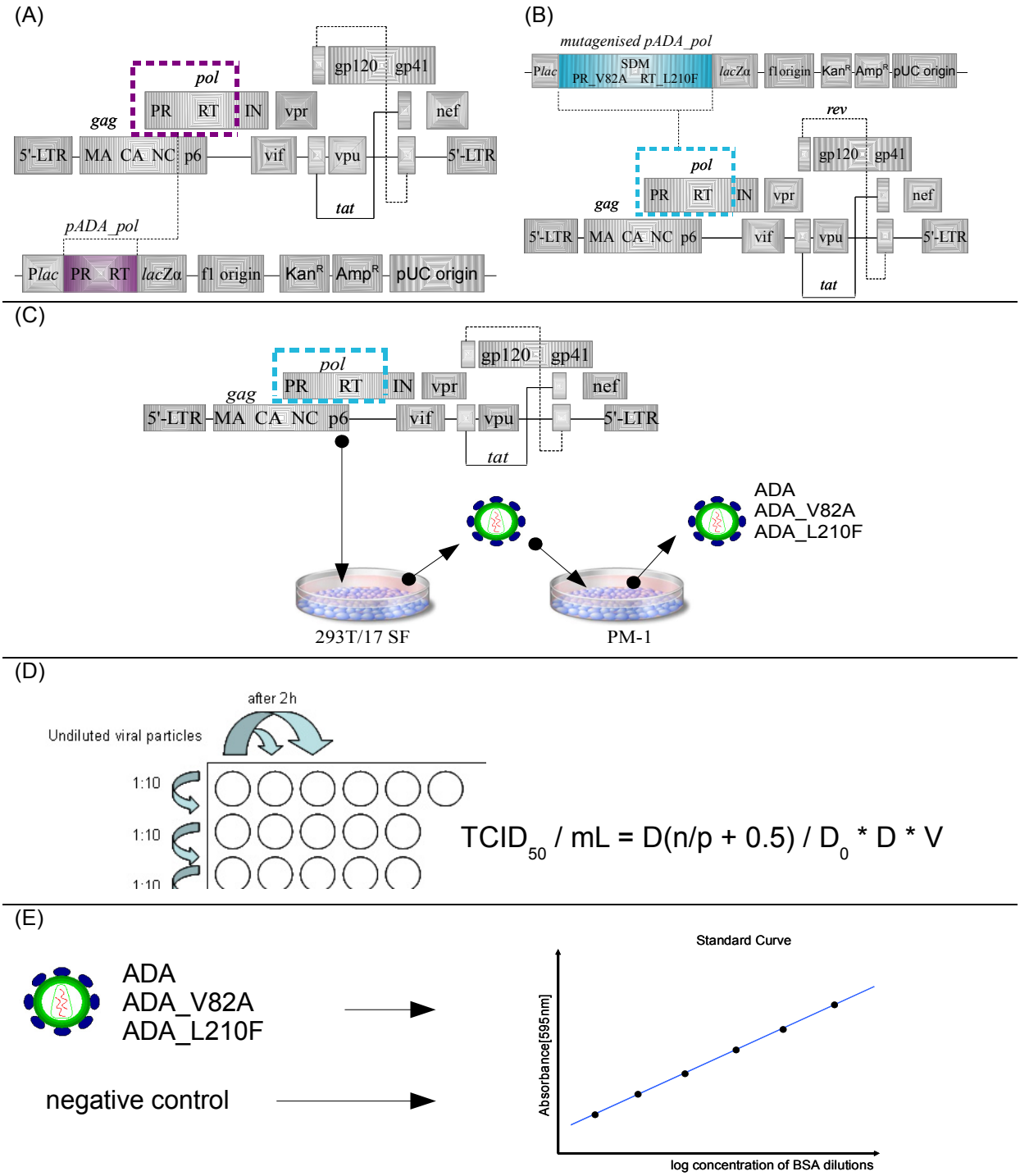

Figure 3.3 Stepwise description of the generation of infectious recombinant HIV-1 ADA: ADA_V82A, L210F. (A) Cloning of pADA-pol in pCR2.1®-TOPO®TA. (B) Introduction of specific RAMs (V82A and L210F) via SDM and cloning mutagenised pols (deriving from pCR2.1®-TOPO®TA-pol_V82A and pCR2.1®-TOPO®TA-pol_L210F) in pADA backbone. (C) Generation of infectious HIV-1 particles: ADA, ADA_V82A, ADA_L210F via the transfection of 293T and PM-1 cells. (D) Determination of infectious titer of ADA, ADA_V82A, ADA_L210F. (E) Determination of the protein content of the HIV-1 ADA stocks: ADA, ADA_V82A and ADA_L210F.

Cloning of pADA-pol in pCR2.1®-TOPO®TA

For the preparative digest of pADA-pol, pADA was digested using the restriction enzymes SpeI and EcoRI in EcoRI-buffer and BSA. In order to facilitate the ligation of pADA-pol in pCR2.1®-TOPO®TA, pCR2.1®-TOPO®TA was digested using the same conditions and was additionally treated with SAP. The complete reaction mixes were loaded onto an agarose gel and DNA-fragments of interest (pADA-pol and pCR2.1®-TOPO®TA backbone) were extracted. Ligation was performed, generating pCR2.1®-TOPO®TA-pol and transformation accomplished using E.coli JM109 chemically competent bacteria.

Introduction of specific tRAMs (V82A and L210F) via SDM

pCR2.1®-TOPO®TA-pol was used for each SDM using primer pairs: PR_V82A_5'/_3' and RT_L210F_5'/_3' (table 2.4c), followed by a DpnI digestion. SDM products (pCR2.1®-TOPO®TA-pol_V82A and pCR2.1®-TOPO®TA-pol_L210F) were transformed in JM109 chemically competent bacteria. Isolated plasmid-DNA was analyzed using the TOPO-5'/-3' primer set (table 2.4b), verifying the integration of mutagenised pADA-pol. A sequencing reaction was carried out using the same primer set to confirm the presence of the respective introduced mutation in pADA-pol.

Cloning mutagenised pols (deriving from pCR2.1®-TOPO®TA-pol_V82A and pCR2.1®-TOPO®TA-pol_L210F) in pADA backbone

For the preparative digest of mutagenised pCR2.1®-TOPO®TA-pol, each pCR2.1®-TOPO®TA-pol SDM was digested using SpeI and EcoRI restriction enzymes in EcoRI-buffer and BSA. In order to ligate mutagenised pol into the pADA backbone, pADA was digested using the same conditions including a SAP-treatment. The complete reaction mix was loaded onto an agarose gel and DNA-fragments (mutagenised pols and pADA backbone) were purified. Ligation was performed and E.coli JM109 chemically competent bacteria were transformed. Using PCR with isolated plasmid-DNA as template, the integration of mutagenised pol in the pADA backbone using the primer set: HIV-pol-5'/-3' (table 2.4b) was verified. These PCR products were used to confirm the presence of the respective inserted mutations in a sequencing reaction using the ViroSeq® HIV-1 Genotyping System.

Generation of infectious HIV-1 particles ADA, ADA_V82A, ADA_L210F

$1.25*10^6$ 293T cells were seeded in a 25 cm cell culture flask. 24 hours later cells were transfected with either 10 µg pADA, pADA_V82A or pADA_L210F. Three days post-transfection 1 mL of supernatant was used to infect 10^6 PM-1 cells at a concentration of 10^5 cell mL^{-1} in a 25 cm cell culture flask. Infection was facilitated during an incubation at 37 °C for one hour and 5 % CO_2. After adding 9 mL RPMI10, PM-1 cells were cultured for 24 h at the same conditions. Supernatant of 10 mL PM-1 cell suspension was collected when cytopathic effect (CPE) was visible (figure 3.5, Results). Cell debris was removed by centrifugation at 300 g for 10 min followed by filtering supernatant through a 0.45 µm filter.

Determination the infectious titer of ADA, ADA_V82A, ADA_L210F

The number of viral particles in the supernatant was determined by means of two routine diagnostical tests. (1) Architect HIV Ag / Ab Combo to determine p24 expression and (2) Real-Time HIV-1 Assay, targeting the integrase region of the polymerase gene, calculating HIV-1 RNA levels. Prior, to the determination of p24 expression and mRNA integrase expression, infectious ADA, ADA_V82A, and ADA_L210F viral particles were inactivated using 0.1% (v/v) Empigen® BB detergent. Nevertheless, one could not conclude viral infectivity using these two tests. Therefore, 75 µL CEMx174-M7R5-EGFP-Luc cells were seeded in each well of a flat bottom 96 well plate at a concentration of $2*10^6$ cell mL^{-1} in the first column. Cells were infected with serial dilutions (1:10) of ADA, ADA_V82A, and ADA_L210F viral particles, starting with 75 µL undiluted virus. Two hours post-infection, cells from one well were split into triplicates to start with the same infection conditions. Three days post-infection the infectious status of the cells with respect to eGFP expression were evaluated using fluorescence microscopy. Infected CEMx174-M7R5-EGFP-Luc cells express the reporter gene eGFP under the control of SIV-LTR, which is transactivated via the viral tat protein.

The infectious titer of cells was calculated according to the Kärber equation [155]:

$$TCID_{50} / mL = D(n/p + 0.5) / D_0 * D * V,$$

where D is the dilution factor, D_0 the first dilution step, n the number of positive wells and V the volume of the undiluted viral stock.

Determination of the protein content of the HIV-1 ADA stocks: ADA, ADA_V82A and ADA_L210F

A standard curve was designed, by measuring the absorbance at 595 nm of known BSA concentrations. The slope was used to calculate the concentrations of the HIV-1 ADA stocks and a negative control, by determining their absorbance.

3.7 Establishment of a cell culture model to determine the innate and adaptive immune response

A cell culture model was established, based on the in silico obtained results, assessing significant associations between HLA class I alleles and HIV-1 RAMs. Lentiviral vectors were produced, to generate recombinant moDCs, over-expressing HLA alleles of interest. These recombinant moDCs were than infected with recombinant HIV-1 carrying RAMs in RT and PR. Co-cultures with $CD16^+CD56^+$ NK cells as part of the innate immune system and $CD8^+$ T cells as part of the adaptive immune system were analyzed for differences in cytokine and chemokine release, indicating cell to cell interactions leading to immune escape.

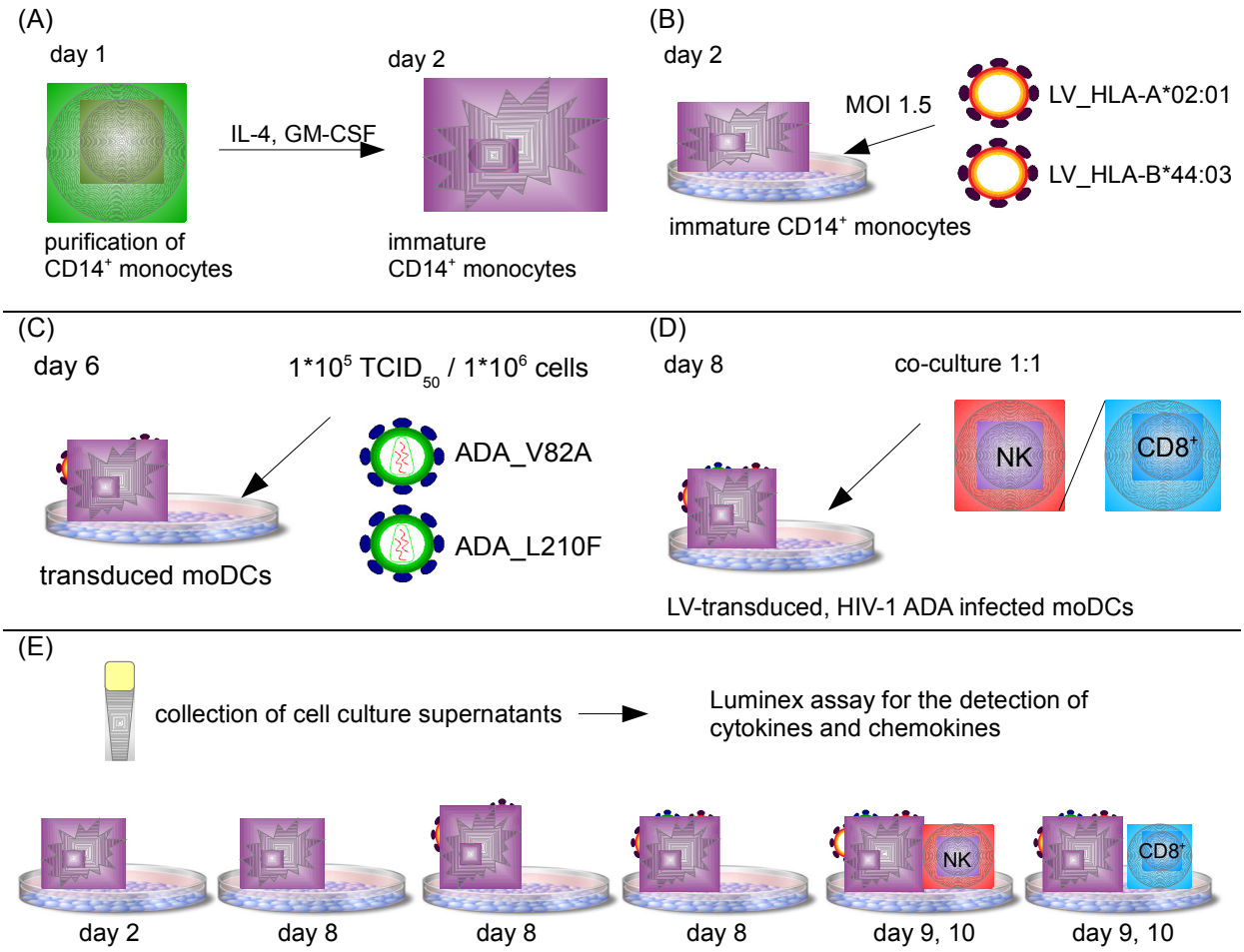

Figure 3.4 Schematic overview of the establishment of a cell culture model to determine the innate and adaptive immune response. (A) Generation of CD14$^+$ monocytes. (B) Transducing CD14$^+$ monocytes with the lentiviral vectors LV_GFP, LV_HLA-A*02:01 and LV_HLA-B*44:03. (C) Infection of transduced moDCs with ADA, ADA_V82A and ADA_L210F. (D) Co-culture of HIV-1 infected LV-transduced moDCs with CD16$^+$CD56$^+$ NK cells or CD8$^+$ T cells. (E) Determination of cytokine and chemokine release.

Purification of CD14$^+$ monocytes

PBMCs were obtained by Ficoll-Hypaque density gradient centrifugation from a total of 500 mL whole blood. Herefore, 20 mL of whole blood mixed with 17 mL D-PBS each were loaded on top of 12 mL Ficoll-Paque^{TM} plus. After centrifugation at 400 g for 20 min at room temperature, the PBMCs containing cushion was harvested and PBMCs were washed twice with 30 mL D-PBS. CD14$^+$ cells were isolated from these PBMCs using CD14 MicroBeads according to the manufacturers' protocol. In general, CD14$^+$ cells are magnetically labeled with CD14 MicroBeads and loaded onto MACS® LS columns and placed in a magnetic field. The magnetically labeled cells are retained within the column and the unlabeled cells run through. After

removing the column from the magnetic field, the retained $CD14^+$ monocytes can be eluted as the positively selected cell fraction. PBMCs, the flow trough and the positively selected $CD14^+$ monocytes were stained for CD3 and CD14 surface markers to monitor $CD14^+$ monocyte purification via flow cytometry. $CD14^+$ cells were cultured in the appropriate medium (table 2.11b) at 37 °C with 5 % of CO_2. Cell maturation status can be followed staining $CD14^+$ monocytes for CD25, CD80, CD83 and CD86. Purified $CD14^+$ monocytes were referred to as $CD14^+$ monocytes until day six of culture, from day six onward they were termed moDCs.

*Transducing $CD14^+$ monocytes with the lentiviral vectors LV_HLA-A*02:01 and LV_HLA-B*44:03*

Day two $CD14^+$ monocytes were transduced with lentiviral vectors LV_HLA-A*02:01 and LV_HLA-B*44:03 at a MOI of 1.5 (DNA-based titer). Herefore, $1*10^6$ mL^{-1} moDCs were pelleted in an FCS coated (3 min 4 °C) 15 mL tube and incubated with $1.5*10^6$ TU / $1*10^6$ moDCs of lentiviral vector. Afterwards, cells were cultured at a density of $1*10^6$ mL^{-1} in the appropriate medium (table 2.11b) at 37 °C with 5 % CO_2.

Infection of LV-transduced moDCs with ADA, ADA_V82A and ADA_L210F

On day six, LV-transduced moDCs were pelleted in an FBS coated 15 mL tube and incubated at 10^5 $TCID_{50}$ / 10^6 cells for one hour at 37 °C with 5 % CO_2 with HIV-1 ADA_V82A and ADA_L210F. Afterwards, cells were cultured at a density of $1*10^6$ mL^{-1} in the appropriate medium (table 2.11b) at 37 °C with 5 % CO_2.

Purification of $CD16^+CD56^+$ NK cells and $CD8^+$ T to co-culture with HIV-1 ADA infected LV-transduced moDCs

The negative fraction of $CD14^+$ monocytes was used for the purification of $CD8^+$ T and $CD16^+CD56^+$ NK cells. The $CD14^+$ monocyte negative fraction was cultured in the appropriate medium (table 2.11b) at 37 °C with 5 % CO_2 until day eight, the day of the co-culture. $CD16^+CD56^+$ NK cells were purified using the $CD56^+CD16^+$ NK Cell Isolation Kit. Cells were stained for CD16 and CD56 to monitor $CD16^+CD56^+$ NK cell purification via flow cytometry. $CD8^+$ T cells were isolated from the negative fraction of $CD14^+$ monocytes and $CD16^+CD56^+$ NK cells using CD8 MicroBeads according to the manufacturers' protocol. $CD8^+$ T cells were stained for CD3 and CD8 to monitor $CD8^+$ T cell purification via flow cytometry.

Co-culture of moDCs with either $CD16^+CD56^+$ NK or $CD8^+$ T cells

Purified $CD16^+CD56^+$ NK and $CD8^+$ T cells were added in a 1:1 ratio to the LV-transduced HIV-1 ADA infected moDCs. Afterwards, cells were cultured at a density of $1*10^6$ mL^{-1} in the appropriate medium (table 2.11b) at 37 °C with 5 % CO_2.

Determination of the cytokine and chemokine release in HIV-1 infected patients

A patient cohort was chosen, including 40 HIV-1 infected patients with pVL < 50 (therapy-experienced) and ten with pVL > $0.5*10^6$ (therapy-naïve), randomly selected. 50 µL of plasma was used to detect cytokine and chemokine secretion, using the human 25-plex panel, detecting several cytokines (GM-CSF, IFN-α / -γ, IL-1β / 1RA / 2 / 2R / 4 / 5 / 6 / 7 / 8 / 10 / 12 / 13 / 15 / 17, TNF-α) and chemokines (eotaxin, IP-10, MCP-1, MIG, MIP-1α / 1β, RANTES) and the LUMINEX®SD™ according to the manufacturers' protocol. Data was evaluated using Luminex 100IS Software 2.3.182.

As a control, the plasma of nine healthy lab volunteers was analyzed. Statistical analysis was performed using Origin 7.5 SR4, assessing significant differences in the secretion of healthy volunteers and HIV-1 infected patients ($p < 0.05$ in student t test). Error bars were calculated as the standard error of the mean.

Influence of the infection of moDCs with HIV-1 ADA_V82A and ADA_L210F on the cytokine and chemokine release of moDCs

The influence of HIV-1 ADA infection on the cytokine and chemokine release of moDCs, was determined using the human 25-plex panel and the LUMINEX®SD™ according to the manufacturers' protocol. Data was evaluated using Luminex 100IS Software 2.3.182. Here for, cell culture supernatants were harvested of single cell $CD14^+$ monocytes cultures on day two, as well as supernatants of uninfected, HIV-1 ADA_V82A and ADA_L210F infected moDCs on day eight. Supernatants were diluted 1:10 before the application in the luminex assay.

Values below the limit of detection were set to the lower limit of detection and values equal to and above the limit of detection were set to upper limit of detection. Error bars were calculated as the standard error of the mean.

Influence of the transduction of CD14$^+$ monocytes on the cytokine and chemokine release of moDCs

The influence of LV-transduction on the cytokine and chemokine release of moDCs was determined using the human 25-plex panel and the LUMINEX®SD™ according to the manufacturers' protocol. Data was evaluated using Luminex 100IS Software 2.3.182. Here for, cell culture supernatants were harvested of single cell CD14$^+$ monocytes cultures on day two, as well as supernatants of untransduced and LV-transduced moDCs on day eight. The influence of the two different lentiviral vectors on cytokine and chemokine secretion was not observed separately. Supernatants were diluted 1:10 before the application in the luminex assay.

Values below the limit of detection were set to the lower limit of detection and values equal to and above the limit of detection were set to upper limit of detection. Error bars were calculated as the standard error of the mean.

Determination of cytokine and chemokine release in the co-culture of HIV-1 ADA infected moDCs with either CD16$^+$CD56$^+$ NK cells or CD8$^+$ T cells indicating an immune escape of V82A (PR) or L210F (RT) in the respective HLA backgrounds

Cell culture supernatants were harvested of day eight untransduced, uninfected moDCs; untransduced, HIV-1 ADA infected moDCs; LV-transduced, uninfected moDCs and LV-transduced, HIV-1 ADA infected moDCs. Again, cell culture supernatants were harvested on day ten, of the above described cell fractions, co-cultured with either CD16$^+$CD56$^+$ NK cells or CD8$^+$ T cells.

The release of cytokines and chemokines was determined in 1:10 diluted supernatants using the cytokine human 25-plex panel and the LUMINEX®SD™ according to the manufacturers' protocol. Data was evaluated using Luminex 100IS Software 2.3.182.

Values below the limit of detection were set to the lower limit of detection and values equal to and above the limit of detection were set to upper limit of detection. Error bars were calculated as the standard error of the mean. Fold differences were calculated, normalizing to untransduced, uninfected moDCs and LV-transduced, uninfected moDCs. The ratios of fold differences were determined, for HLA-A*02:01 positive donor: ADA_L210F : ADA_V82A and for HLA-B*44:03 positive donor: ADA_V82A : ADA_L210F.

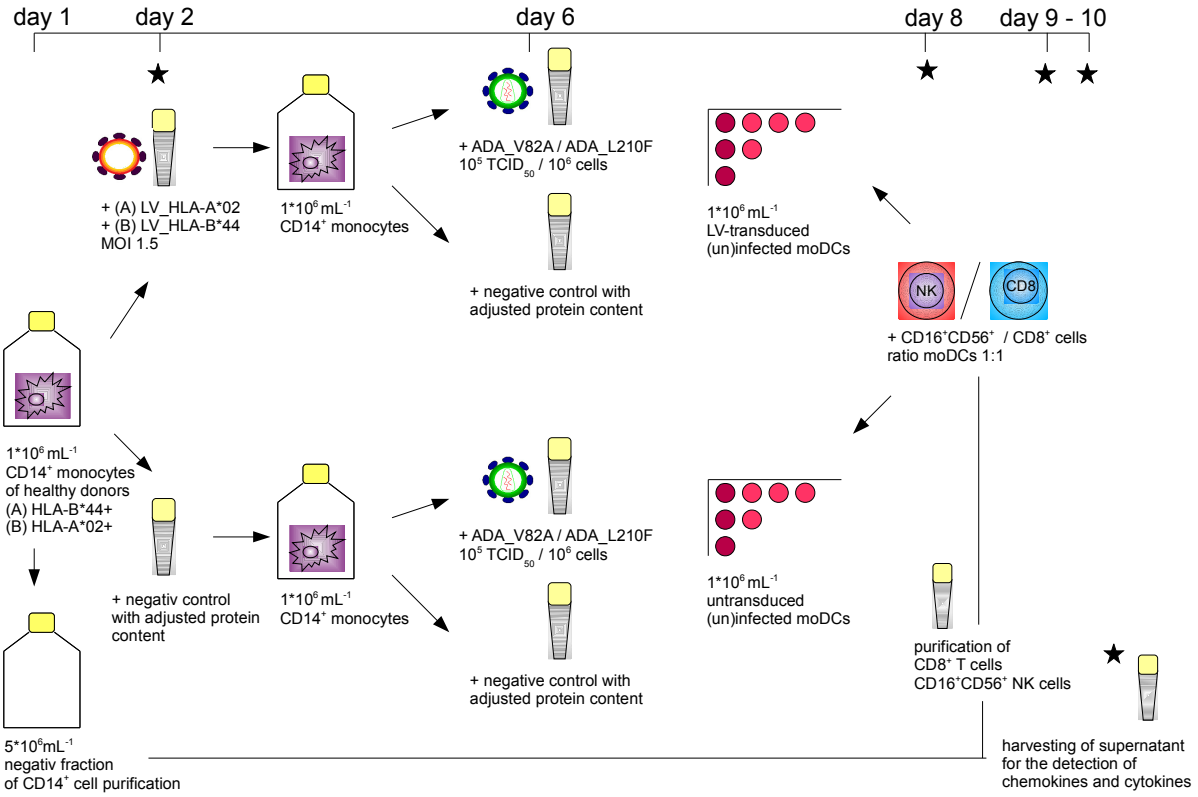

Figure 3.5 Schematic overview of the determination of cytokine and chemokine release in the co-culture of HIV-1 ADA infected moDCs with either $CD16^+CD56^+$ NK cells or $CD8^+$ T cells indicating an immune escape of V82A (PR) or L210F (RT) in the respective HLA backgrounds

4. Results

This study aimed to identify an influence of tRAMs within HIV-1 PR and RT on host specific innate and adaptive immune responses. A statistical analysis associating tRAMs within viral strains of a patient cohort of therapy-naïve HIV-1 infected individuals with the patients' HLA-A, -B and –C alleles was performed to identify potential immune escape mutations among tRAMs. V82A (PR), a tRAM, which is associated with resistance to several PR inhibitors was shown to be significantly associated with HLA-A*02:01 and was therefore chosen for further analysis. As a control, L210F (RT), a mutation which has already been described to have an impact on the patients' immune response in the background of HLA-B*44:03 was analyzed (data not shown [156]).

A cell culture model was established, in which recombinant moDCs, over-expressing HLA alleles of interest were infected with recombinant ADA based HIV-1 incorporating the respective tRAMs and responses of $CD16^+CD56^+$ NK cells and $CD8^+$ T cells determined. Recombinant moDCs were generated using a lentiviral vector system, delivering HLA alleles of interest, here HLA-A*02:01 and HLA-B*44:03 (figure 3.2). Transduced moDCs were subsequently infected with recombinant ADA based HIV-1 either comprising mutation V82A (PR) or L210F (RT) (figure 3.4). Innate immune responses were determined, co-culturing the transduced and infected moDCs with $CD16^+CD56^+$ NK cells and detecting cytokine and chemokine levels, while the adaptive immune response was detected in moDC / $CD8^+$ T cell co-cultures (figure 3.5).

4.1 Selection of patient cohort

In order to identify potential immune escape mutations among tRAMs in HLA-restricted epitopes, an appropriate patient cohort needed to be selected. 139 therapy-naïve HIV-1 infected patients from the RESINA study with tRAMs in either PR and / or RT were enrolled. 87.7 % of these patients were of Caucasian origin and 79.0 % were infected with HIV-1 subtype B (subtype A: 11.6 %, D: 1.4 %, G: 1.4 %, C: 1.4 %, F: 0.7 %, URF: 4.5 %). According to the IAS-list [125], 40 different PI tRAMs were detected, 10 different NRTI tRAMs and 14 different tRAMs conferring resistances to NNRTIs (table 4.1).

Table 4.1 Frequencies of PI, NRTI and NNRI tRAMs of 139 therapy-naïve patients

HXB2 reference strain	Mutation in the PR associated with PI Resistance	Number of patients
L10	F	1
	I	25
	V	4
G16	E	11
K20	I	7
	M	3
	R	13
	T	2
L24	I	1
V32	I	1
L33	F	4
	I	2
	V	3
M36	I	54
	L	3
	V	2
M46	I	8
	L	6
F53	L	3
Q58	E	1
D60	E	9
I62	V	46
L63	P	69
I64	L	2
	V	25
H69	K	22
	R	1
A71	T	11
	V	12
A77	I	35
V82	A	8
	I	9
	L	1
	T	1
I84	V	3
I85	V	1
L89	M	21
	V	1
L90	M	7
I93	L	47

HXB2 reference strain	Mutation in the RT associated with NRTI Resistance	Number of patients
M41	L	9
D67	N	6
K70	R	1
L74	V	1
L75	I	2
M184	V	3
L210	W	1
T215	Y	1
K219	E	3
	Q	6

HXB2 reference strain	Mutation in the RT associated with NNRTI Resistance	Number of patients
V90	I	3
K101	E	3
K103	N	14
V106	A	2
	I	10
V108	I	4
E138	A	8
	G	1
	K	2
V179	D	6
	T	2
V181	C	7
Y190	A	5
P225	H	2

HLA-typing of these patients revealed, that the HLA-A, -B and -C genotype of all patients showed the highest frequencies for: HLA-A*02:01, HLA-A*03:01, HLA-

A*01:01, and HLA-A*24:02; HLA-B*07:02, HLA-B*08:01, HLA-B*44:02, and HLA-B*51:01; HLA-C*07:02, HLA-C*07:01, HLA-C*04:01, HLA-C*06:02 (table 4.2).

Table 4.2 Frequencies of HLA-A, -B and –C alleles of 139 therapy-naïve patients

HLA-A*	Allele frequency
02:01	19.34
03:01	13.99
01:01	12.76
24:02	10.29
11:01	6.58
68:01	5.35
26:01	4.94
30:01	3.29
32:01	3.29
23:01	2.06
29:02	2.06
31:01	2.06
03:02	1.65
25:01	1.65
02:02	1.23
68:02	1.23
02:03	0.82
02:05	0.82
29:01	0.82
33:01	0.82
66:01	0.82
01:03	0.41
02:06	0.41
02:17	0.41
24:03	0.41
24:07	0.41
30:02	0.41
33:03	0.41
69:01	0.41
74:01	0.41
74:05	0.41

HLA-B	Allele frequency
07:02	11.55
08:01	9.16
44:02	7.57
51:01	7.17
15:01	6.77
35:01	6.37
18:01	5.98
13:02	3.19
27:05	3.19
38:01	3.19
40:01	2.79
15:03	2.39
35:02	1.99
35:03	1.99
44:03	1.99
14:02	1.59
42:01	1.59
57:01	1.59
40:02	1.20
44:05	1.20
50:01	1.20
52:01	1.20
55:01	1.20
56:01	1.20
58:01	1.20
13:01	0.80
14:01	0.80
15:02	0.80
15:17	0.80
35:08	0.80
39:01	0.80
45:01	0.80
46:01	0.80
53:01	0.80
07:05	0.40
15:16	0.40
15:32	0.40
27:02	0.40
27:14	0.40
37:01	0.40
39:10	0.40
41:01	0.40
49:01	0.40
54:01	0.40
58:02	0.40

HLA-C	Allele frequency
07:02	12.72
07:01	11.84
04:01	11.40
06:02	9.21
12:03	7.02
05:01	6.58
03:04	6.14
01:02	5.70
02:02	5.26
03:03	4.82
15:02	3.95
16:01	3.07
07:04	2.19
02:10	1.75
08:02	1.75
14:02	1.32
17:01	1.32
08:01	0.88
04:03	0.44
04:29	0.44
05:09	0.44
12:02	0.44
15:05	0.44
16:04	0.44
17:03	0.44

4.2 Assessment of statistically significant associations between tRAMs and HLA class I alleles

In order to identify potential immune escape mutants among tRAMs, significant associations between tRAMs and HLA-A, -B and –C alleles were assessed.

Of all 236 combinations of tRAMs in PR and RT and HLA-A, -B, and –C alleles, a total of 29 relevant associations were identified by Fishers exact test (explorative p-value ≤ 0.05; OR > 1). 24 relevant associations were found between tRAMs in PR and different HLA alleles plus five tRAMs in RT and HLA alleles (data not shown). After correcting for multiple testing according to Storey and Tibshirani [154] allowing FDR ≤ 0.10, nine associations remained significant (table 4.3). Another approach for correcting for multiple tests is the Bonferroni correction. This correction is in general more conservative, because it requires a p-value of 0.05 / n or smaller, where n is the number of tests performed. Nevertheless, the two strongest associations were still significant after Bonferroni correction (p-value < 0.0002). These two associations were the combinations of V82A (PR) and HLA-A*02:01 as well as I93L (PR) and HLA-B*15:01.

Table 4.3 Statistical significant associations between tRAMs and HLA-A, -B and –C alleles after correcting for multiple testing according to Storey and Tibshirani [154]

tRAMs in PR	Associated HLA allele	p-value	FDR	q-value	odds ratio	95% confidence interval	
						lower limit	upper limit
M36I	B*15:03	0.002876	0.084848	0.084848	$2.29*10^{7}$	$1.26*10^{6}$	$4.16*10^{8}$
	C*12:03	0.002275	0.076699	0.076699	$5.92*10^{7}$	$1.78*10^{6}$	$1.97*10^{7}$
M46L	A*03:01	0.003403	0.089246	0.089246	$1.79*10^{7}$	$2.01*10^{6}$	$1.60*10^{8}$
	C*02:10	0.000659	0.038895	0.038895	$5.27*10^{7}$	$2.72*10^{6}$	$1.02*10^{9}$
V82A	A*02:01	0.000112	0.026362	0.018934	$3.98*10^{7}$	$2.24*10^{6}$	$7.07*10^{8}$
	C*02:10	0.000534	0.041982	0.038895	$5.65*10^{7}$	$2.90*10^{6}$	$1.10*10^{9}$
I93L	B*15:01	0.000160	0.018934	0.018934	$8.41*10^{6}$	$2.56*10^{6}$	$2.76*10^{7}$

tRAMs in RT	Associated HLA allele	p-value	FDR	q-value	odds ratio	95% confidence interval	
						lower limit	upper limit
V179D	A*02:01	0.001196	0.056440	0.056440	$2.90*10^{7}$	$1.59*10^{6}$	$5.26*10^{8}$
	C*07:01	0.001893	0.074476	0.074476	$2.16*10^{7}$	$2.40*10^{6}$	$1.94*10^{8}$

V82A (PR) was highly associated with HLA-A*02:01 and therefore selected for further analysis. L210F (RT) is a well characterized immune escape mutation in the background of HLA-B*44:03 and was found at a frequency of 5.0 % (7 / 139) in the

therapy-naïve patients. No statistically significant associations could be found (p = 0.231) however the two-digit HLA-B*44 was significantly associated with L210F (RT) (p = 0.027). Thus, L210F (RT) was the second mutation used to establish the cell culture model.

4.3 Generation of lentiviral vectors to produce recombinant monocyte-derived dendritic cells (moDCs)

This part focuses on the generation of lentiviral vectors to produce recombinant moDCs, over-expressing either HLA-A*02:01 or HLA-B*44:03. Herefore, a lentiviral vector system was chosen to facilitate a stable integration of the gene of interest and the expression in non-dividing moDCs.

Generation of transfer plasmids introducing HLA-A or -B specific ORF

cDNA was generated from total RNA of HLA-A*02:01 and HLA-B*44:03 positive donors. A PCR, using appropriate primer pairs (table 2.4a) was performed to amplify a product containing the HLA-A*02:01 ORF with a size of 1098 bp and HLA-B*44:03 ORF with a size of 1089 bp, introducing in addition a His-tag at the 3'end (figure 4.1).

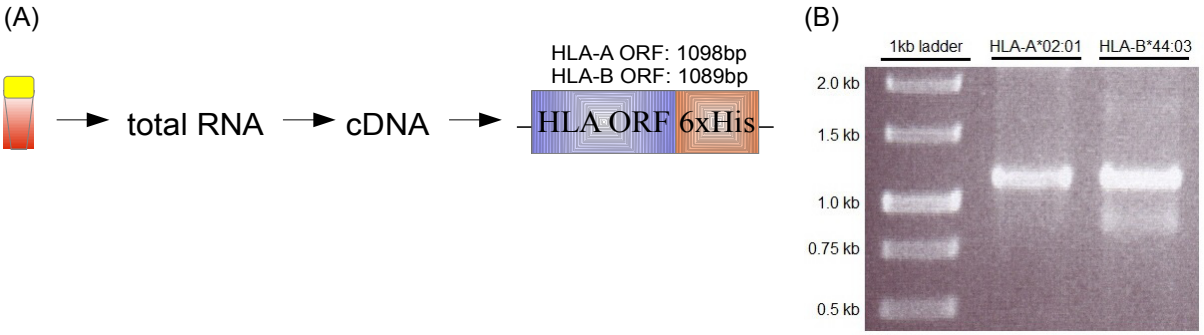

Figure 4.1 Amplification of HLA ORF. (A) cDNA generated from total RNA of whole blood of an HLA-A*02:01 and an HLA-B*44:03 positive donor. HLA-A and –B specific PCR products were generated using HLA-A and –B specific primer sets, introducing a His-tag at the 3' end of the HLA-ORF. (B) HLA-A*02:01 and HLA-B*44:03 ORF PCR products were visualized using gel electrophoresis.

After cloning HLA-A*02:01 and HLA-B*44:03 ORF in pCR2.1®-TOPO®TA cloning plasmid (data not shown), HLA ORFs were ligated in the pHR'SINcPPT-SEW transfer plasmid, forming the product pHR'SINcPPT-SEW_HLA. A PCR was

performed using SEW-5'-HLA-ORF and SEW-3'-HLA-ORF (table 2.4b) to verify the successful integration of the inserted HLA-ORF (figure 4.2, data not shown).

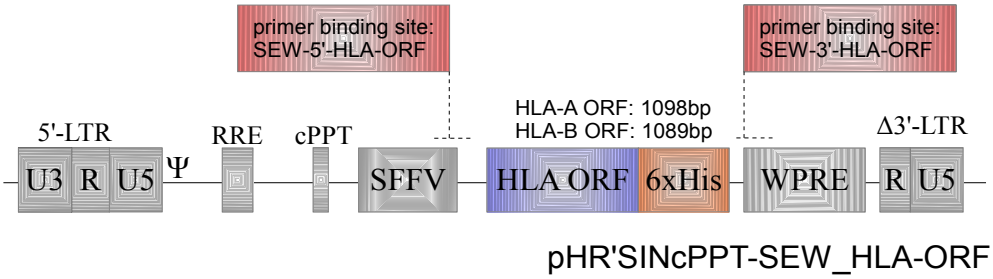

Figure 4.2 Verification of the integration of HLA-ORF in pHR'SINcPPT-SEW, analyzing pHR'SINcPPT-SEW_HLA-ORF clones using pHR'SINcPPT-SEW specific primer (data not shown).

To further confirm the presence of HLA-A*02:01 and HLA-B*44:03 ORFs in the transfer plasmid pHR'SINcPPT-SEW, a sequencing reaction was performed using the same primer set (SEW-5'-HLA-ORF and SEW-3'-HLA-ORF) and as a template the PCR product. Sequences were aligned to published HLA sequences [93], showing a sequence identity ranging from of 99 % for HLA-A*02:01 to 100 % for HLA-B*44:03 (figure 9.1).

In order to verify the ability of an expression of the HLA proteins HLA-A*02:01 and HLA-B*44:03, 293T cells were transfected with the transfer plasmids: pHR'SINcPPT-SEW_HLA-A*02:01 and pHR'SINcPPT-SEW_HLA-B*44:03. Using flow cytometry cells were permeabilized and stained for His and HLA-ABC to evaluate the expression of the His-tagged HLA proteins. The percentages of cells expressing both, HLA and His-tagged (HLA-) proteins were quantified by the mean fluorescence intensity (MFI) of both fluorescence dyes labelling the respective antibody. The dot plots show an increase in double positive cells, showing those His-tagged HLA alleles transfected by the transfer plasmid (figure 4.3).

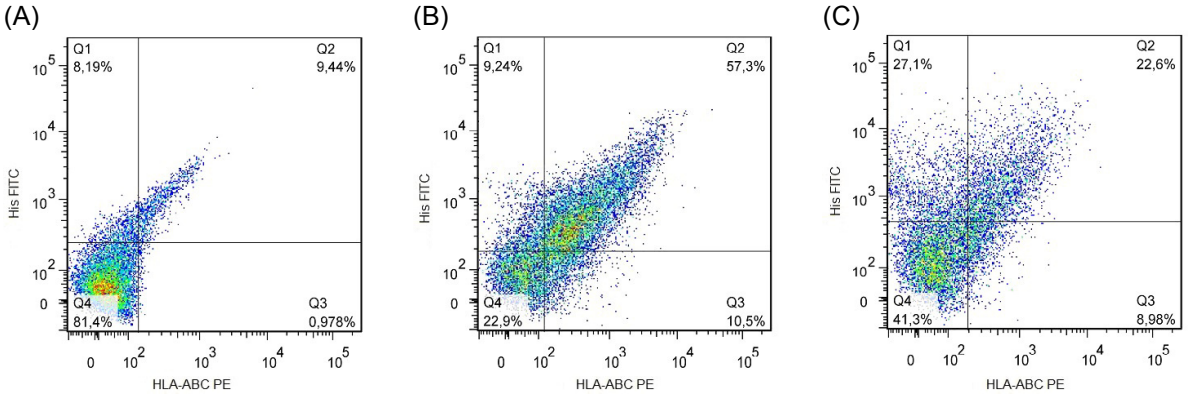

Figure 4.3 Flow cytometry analysis to identify 293T transfected His-tagged HLA proteins. 293T cells were permeabilized and stained for His-FITC and HLA-ABC-PE to identify the His-tagged HLA proteins (A) untransfected, stained with isotype control, (B) transfected with pHR'SINcPPT-SEW_HLA-A*02:01 and (C) with pHR'SINcPPT-SEW_HLA-B*44:03.

Table 4.4 summarizes the flow cytometry data of MFI (FITC and PE) of un-transfected and transfected 293T cells, indicating the expression of both His-tagged HLA proteins, HLA-A*02:01 and HLA-B*44:03.

Table 4.4 Summary of flow cytometry results of 293T cells transfected with pHR'SINcPPT-SEW_HLA-A*02:01 and pHR'SINcPPT-SEW_HLA-B*44:03

Transfectant	His–FITC and HLA-ABC–PE		
	% - T	MFI (FITC)	MFI (PE)
Un-transfected	9.4	885	240
pHR'SINcPPT-SEW_HLA-A*02:01	57.3	612	369
pHR'SINcPPT-SEW_HLA-B*44:03	22.6	1511	537

*Generation of lentiviral vectors LV_GFP, LV_HLA-A*02:01 and LV_HLA-44:03*

Based on the protocol of Naldini et al. [147] lentiviral vectors were generated by co-transfecting (1) pHR'SINcPPT-SEW / pHR'SINcPPT-SEW_HLA-A*02:01 / pHR'SINcPPT-SEW_HLA-B*44:03, (2) pCMVΔR8.91 and (3) pM.DG. To quantify lentiviral vector particles HIV-1 p24 expression was determined. The infectious titer was evaluated based on the integration and expression of the gene of interest after the transduction of 293T cells determined by real-time PCR.

*Determination of the infectious titer of the lentiviral vectors LV_GFP, LV_HLA-A*02:01 and LV_HLA-B*44:03*

DNA- and mRNA based titer were determined based on a real-time PCR assay, established according to Lizée et al., 2003 [144]. The integration of the gene of interest as well as the lentiviral expression of the gene of interest in transduced cells was analyzed. The integration was ensured by the detection of WPRE specific DNA, while the expression of the gene of interest was ensured by the detection of WPRE specific mRNA. Table 9.1 and 9.2 summarize albumin, β-actin and WPRE concentrations. Table 4.5 summarizes HIV-1 p24 concentrations and the calculated lentiviral vector titers. For the transduction of $CD14^+$ monocytes a MOI of 1.5 was used (DNA-based titer).

Table 4.5 DNA- and mRNA-based titer of lentiviral vectors: LV_GFP, LV_HLA-A*02:01 and LV_HLA-B*44:03

Lentiviral vector	DNA-based titer [TU / mL] → infectious particles	mRNA-based titer [TU / mL] → mRNA expression	Architect i2000SR [S / CO*] → p24 expression
LV_GFP	$3.88*10^8$	$1.56*10^6$	1084.10
LV_HLA-A*02:01	$4.59*10^8$	$4.56*10^6$	1226.01
LV_HLA-B*44:03	$3.18*10^8$	$8.36*10^6$	1196.65

* <1.00 nonreactive

*Determination of the protein content within lentiviral vectors: LV_GFP, LV_ HLA-A*02:01 and LV_HLA-B*44:03*

The protein content of lentiviral vectors: LV_GFP, LV_HLA-A*02:01, LV_HLA-B*44:03 and a control (untransfected 293T supernatant, microvesicle control) was determined using the Bradford protein assay and measuring absorbance at 595 nm. A standard curve was generated using known concentrations of BSA. Using the slope, protein contents of the lentiviral vectors and the negative control were calculated. Figure 4.4 shows the standard curve.

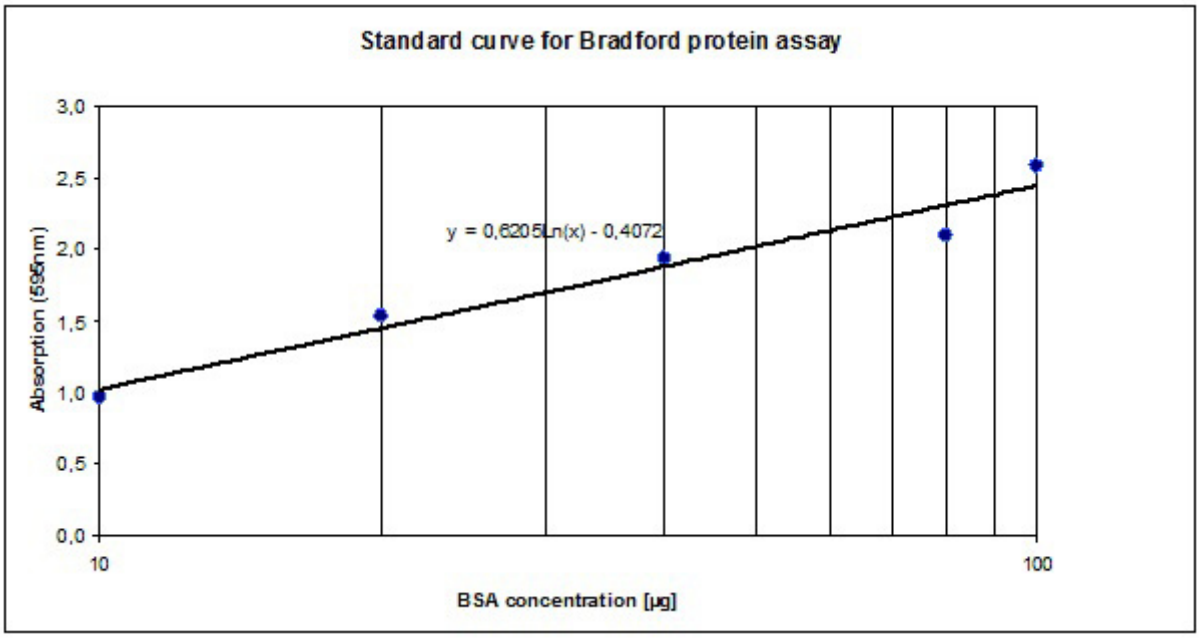

Figure 4.4 Standard curve generated by the measurement of known concentrations of BSA. The slope y=0.6205ln(x)-0.4072 is used to calculate the total protein concentration of lentiviral vectors and the negative control.

Table 4.6 summarizes the calculated protein concentrations of each lentiviral vector. The control was used as the negative control in the transduction of $CD14^+$ monocytes and was applied adjusted to the lentiviral vector protein content.

Table 4.6 Calculated total protein concentrations of lentiviral vector stocks

Lentiviral vector	Absorbance (595 nm)	Total protein concentration [µg / mL]
LV_GFP	1.550	2026
LV_HLA-A*02:01	1.654	2378
LV_HLA-B*44:03	1.570	2089
control (293T supernatant)	1.446	1727

4.4 Generation of infectious recombinant HIV-1 ADA: ADA_V82A, ADA_L210F

This part focuses on the generation of recombinant pADA-based HIV-1, including either the mutation V82A (PR) or L210F (RT). ADA is a well characterized laboratory HIV-1 strain, subtype B, macrophage-tropic [148].

Cloning of pADA-pol in pCR2.1®-TOPO®TA

In order to generate recombinant pADA-based HIV-1, the pADA-pol region was cloned in the cloning plasmid pCR2.1®-TOPO®TA, resulting in the product pCR2.1®-TOPO®TA-pol. The integration of pADA-pol was verified performing a restriction

digest of pCR2.1®-TOPO®TA-pol and the subsequent identification of products via gel electrophoresis (data not shown).

Introduction of specific tRAMs (V82A and L210F) via SDM

Specific tRAMs (V82A (PR) and L210F (RT)) were integrated in pCR2.1®-TOPO®TA-pol via SDM. SDM products were transformed in JM109 for amplification. To characterize SDM clones, a PCR reaction was performed using the TOPO-5' / TOPO-3' primer set (table 2.4b), amplifying the pADA-pol ORF and visualizing via gel electrophoresis (data not shown).

Cloning mutagenised pols (deriving from pCR2.1®-TOPO®TA-pol_V82A and pCR2.1®-TOPO®TA-pol_L210F) in pADA backbone

To determine a successful integration of the different pADA-pol SDM products back in the pADA backbone, the respective plasmid DNA was isolated and a PCR was performed using primer HIV-pol-5' and HIV-pol-3' (table 2.4b) amplifying the pol ORF with a length of 1510 bp. The PCR product was visualized via gel electrophoresis as shown in figure 4.5.

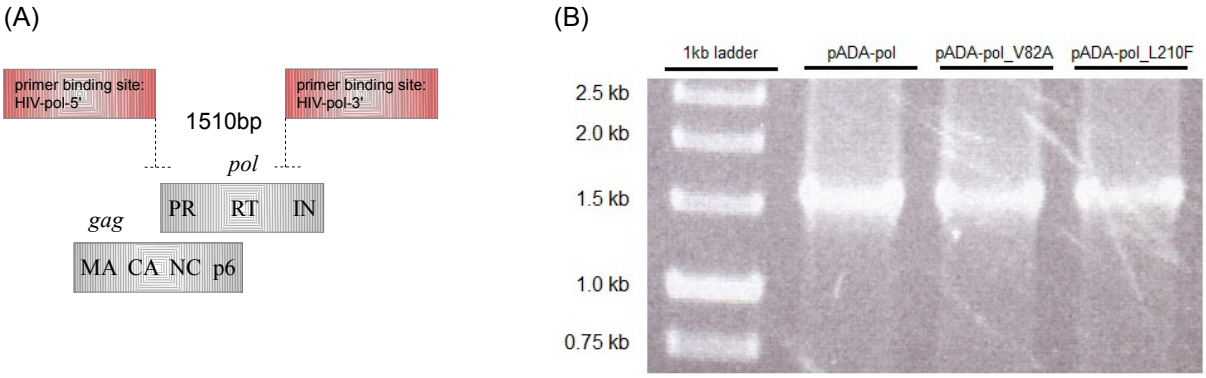

Figure 4.5 Determining the presence of pADA-pol back in pADA backbone using pol specific primer in a PCR. (A) Schematic overview of pADA and HIV-pol primer binding sites. (B) Identification of pADA-pol ORF using gel electrophoresis at 1510 bp.

A sequencing reaction of SDM pADA-pol PCR products was performed to verify the presence of integrated tRAMs V82A (PR) and L210F (RT) using the ViroSeq® HIV-1 Genotyping System. Sequences were edited and uploaded in geno2pheno (table 2.13) to identify substitutions in PR and RT compared to the diagnostic reference strain HXB2. As the ADA HIV-1 strain is in this study used as reference, the

substitutions of pADA-pol were also analyzed. Table 4.7 summarizes all substitutions found for each clone, all differing at the respective amino acid positions, where the tRAMs were integrated.

Table 4.7 Substitutions within pADA-pol SDM clones compared to HXB2

SDM clones	Substitution in PR (compared to HXB2 reference strain)	Substitution in RT (compared to HXB2 reference strain)
pADA-pol	V3I, S37N, R57G	K102Q, E122K, S162C, L214F, P272A, I293V
pADA-pol_V82A	V3I, S37N, **V82A**	K102Q, E122K, L214F, P272A, I293V
pADA-pol_L210F	V3I, S37N	K102Q, E122K, S162C, **L210F**, L214F, P272A, I293V

Generation of infectious HIV-1 particles: ADA, ADA_V82A and ADA_L210F

293T cells were transfected with pADA, pADA_V82A and pADA_L210F. Three days post transfection, the supernatant was used to infect PM-1 cells. Cells were observed using a light microscopy (figure 4.6) to detect CPE formation before harvesting viral particles on day four.

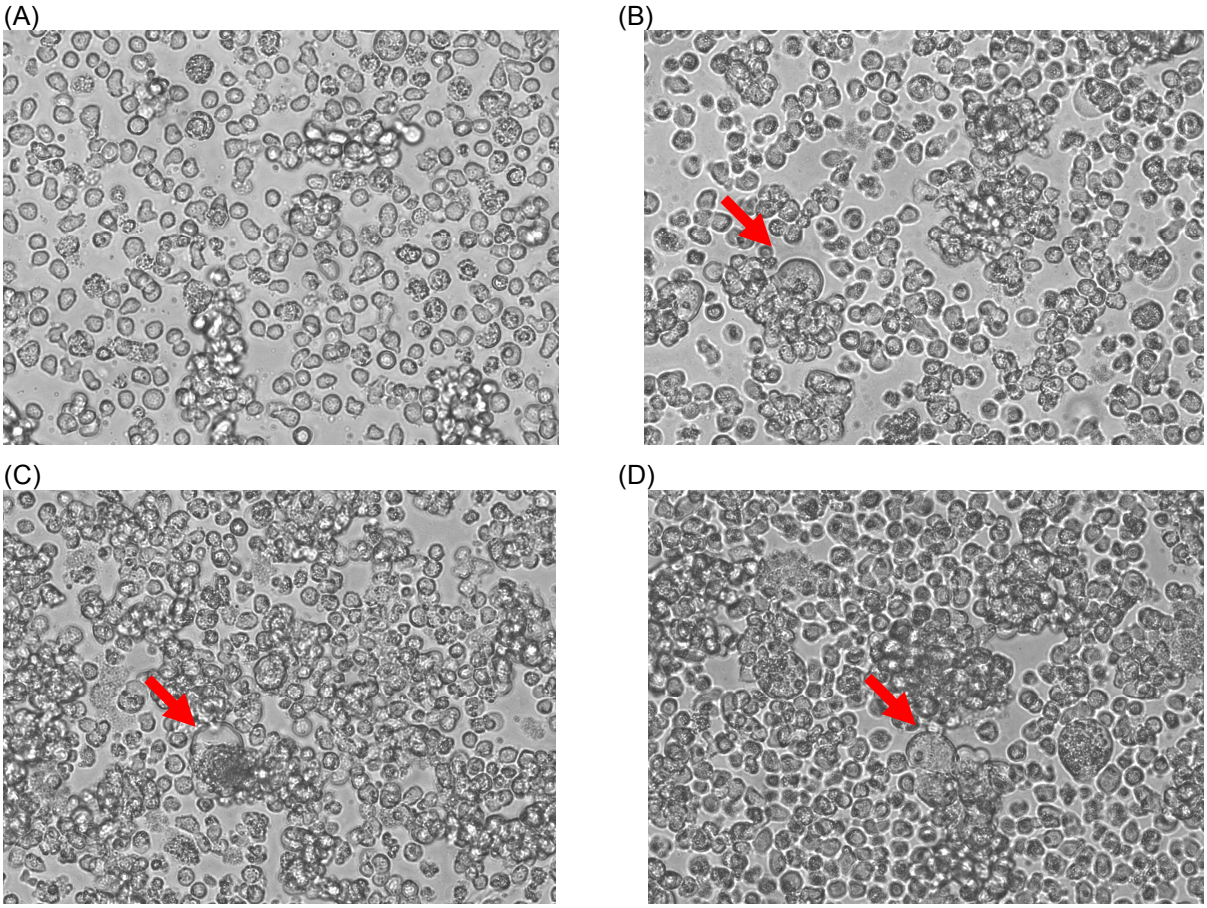

Figure 4.6 Light microscopic pictures (20x original magnification) of PM-1 cells infected or not with ADA, ADA_V82A and ADA_L210F on day four post infection. The arrows indicate CPE formation. (A) uninfected, (B) infected with ADA, (C) infected with ADA_V82A and (D) infected with ADA_L210F cells

Determination of the infectious titer of ADA, ADA_V82A and ADA_L210F

After the harvest, the number of the viral particles was determined measuring p24 concentrations and viral copy numbers were detected using the RealTime HIV-1 assay (table 4.8). However, in order to quantify the infectious units, CEMx174-M7R5-EGFP-Luc cells were infected with serial dilutions of ADA, ADA_V82A, and ADA_L210F. CEMx174-M7R5-EGFP-Luc cells carry the reporter gene eGFP that is expressed in response to the HIV-1 tat protein. The infectious status of the cells was evaluated with respect to eGFP expression and the titer can be calculated using the Kärber equation [155]. Table 4.8 summarizes the number of viral particles and the infectious units for each viral strain.

Table 4.8 Summary of HIV-1 ADA infectious particles, p24 antigen expression and HIV-1 integrase mRNA expression

Viral Strain	$TCID_{50}$ / mL → infectious particles	Architect i2000SR [S/CO*] → p24 expression	m2000™ copies / mL → mRNA expression of HIV-1 integrase
ADA	$1.17*10^5$	829.03	$6.09*10^7$
ADA_V82A	$1.17*10^4$	328.23	$2.40*10^7$
ADA_L210F	$1.17*10^6$	1149.78	$8.00*10^7$

* <1.00 nonreactive

Determination of the protein content of the HIV-1 ADA stocks: ADA, ADA_V82A and ADA_L210F

The protein contents of HIV-1 ADA: ADA; ADA_V82A, ADA_L210F and a control (uninfected PM-1 supernatant, microvesicle control) were determined using the Bradford protein assay and measuring the absorbance at 595 nm. According to a standard curve of known BSA concentrations (figure 4.4) protein concentrations of HIV-1 ADA and the negative control were calculated (table 4.9). The control was used as the negative control in the infection of moDCs and was applied, adjusted to HIV-1 ADA protein contents.

Table 4.9 Calculated total protein concentrations of HIV-1 ADA stocks

Viral strain	Absorbance (nm)	Total protein concentration [µg / mL]
ADA	1.913	3540
ADA_V82A	1.892	3428
ADA_L210F	1.984	3939
neg. control (PM-1 supernatant)	1.941	3696

4.5 Establishment of a cell culture model to determine the innate and adaptive immune response

The establishment of the cell culture model included the production of lentiviral vectors and the generation of recombinant moDCs, which over-express HLA alleles of interest. Recombinant moDCs were infected with recombinant HIV-1 (with RAMs in RT and PR). The supernatants of co-cultures with $CD16^+CD56^+$ NK and $CD8^+$ T cells were analyzed for differences in cytokine and chemokine levels.

Purification of CD14$^+$ monocytes

In order to generate moDCs, CD14$^+$ monocytes were purified from PBMCs of healthy donors. The number of PBMCs as well as the number of CD14$^+$ monocytes varied highly between the different donors. The number of CD14$^+$ monocytes decreased strongly from day one to day two. Table 4.10 summarizes the numbers of PBMCs, day one and day two CD14$^+$ monocytes. Day two CD14$^+$ monocytes were harvested for the transduction with lentiviral vectors.

Table 4.10 Numbers of PBMCs and purified day one and day two CD14$^+$ monocytes

Healthy donor	PBMCs	day 1 CD14$^+$ monocytes		day 2 CD14$^+$ monocytes	
		total	% of PBMCs	Total	% of PBMCs
1	5,736,000,000	90,400,000	1.58	32,500,000	0.57
2	7,441,500,000	63,200,000	0.85	22,500,000	0.30
3	6,471,000,000	44,100,000	0.68	29,400,000	0.45
4	3,573,000,000	67,200,000	1.88	26,200,000	0.73

The morphology of day one CD14$^+$ monocytes showed a spherical form with a grainy surface (figure 4.7 (A)). Adding GM-CFS and IL4 to the culture of CD14$^+$ monocytes led to differentiation of cells. Day two CD14$^+$ monocytes appeared elongated and started forming dendrite-like arms (figure 4.7 (B)).

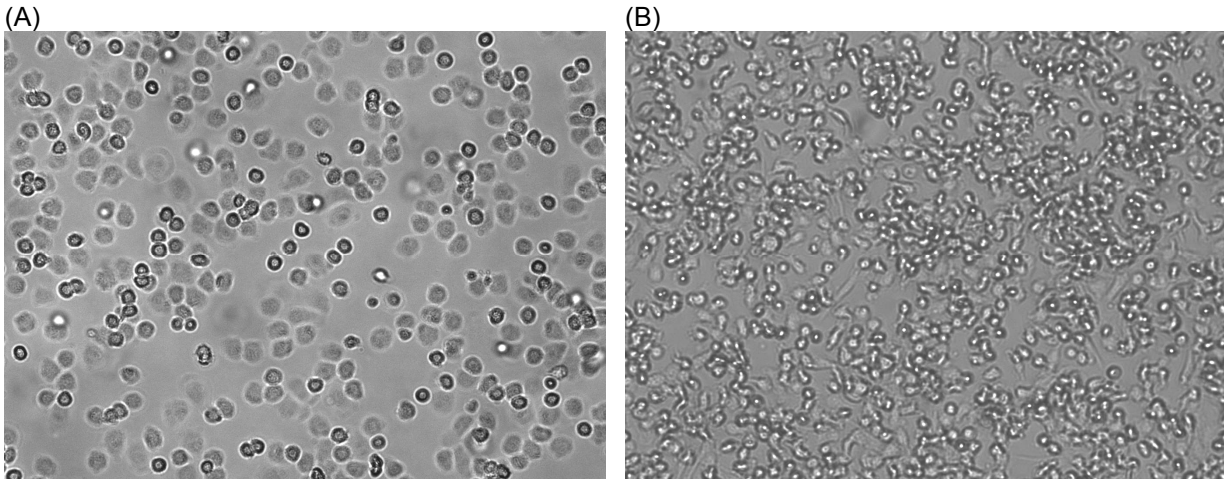

Figure 4.7 Light microscopic pictures (20x original magnification) of day one and day two CD14$^+$ monocytes. Exemplarily, showing one donor out of four. (A) CD14$^+$ monocytes on day one, (B) on day two.

The quantity and quality of purified CD14$^+$ monocytes was assessed, staining cells for CD3 and CD14 surface markers and flow cytometry. The maturation status was

monitored, staining cells for CD25, CD80, CD83, CD86 and HLA-DR (figure 4.8 / table 4.11).

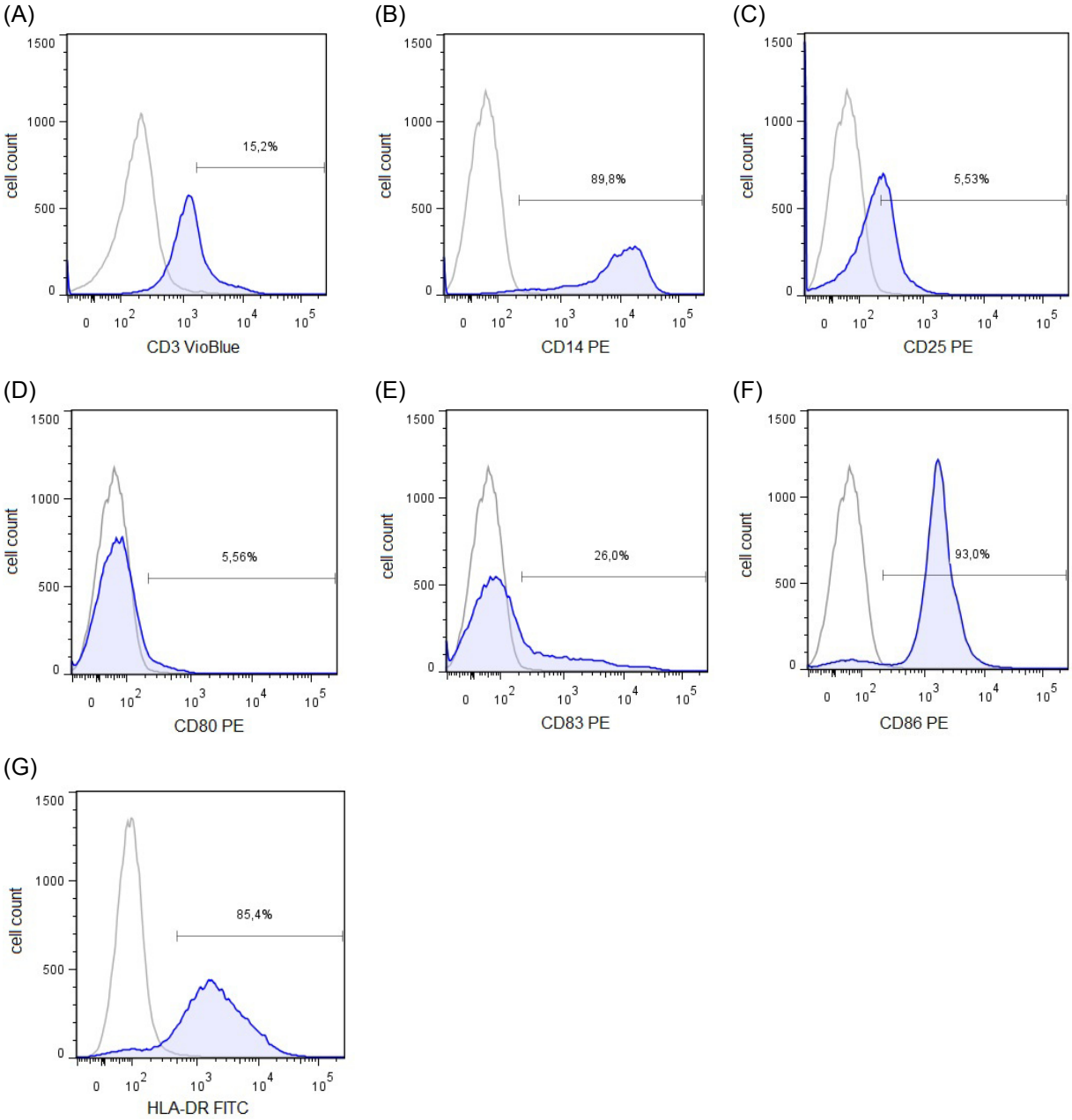

Figure 4.8 Flow cytometric analysis of the quantity, quality and maturation status, using well characterized surface markers, of purified CD14$^+$ monocytes. Exemplarily, showing one donor out of four. (A) shows the percentage of CD3$^+$ cells, (B) the percentage of CD14$^+$ cells, (C) the CD25 maturation marker, (D) CD80, (E) CD83, (F) CD86 and (G) HLA-DR. The grey curves show the isotype control, whereas the blue curves represent the stained surface markers.

The percentage of purified CD14$^+$ monocytes ranged from 57.44 % to 91.3 % with a percentage of CD3$^+$ cells of 1.21 % to 15.2 % between the different donors. No expression of CD25 and CD80 was detected and only little of CD83, indicating the

presence of immature $CD14^+$ monocytes. CD86, a marker for early monocyte maturation, and HLA-DR were up-regulated.

Table 4.11 Summary of the flow cytometry analysis of the quantity, quality and maturation status of purified $CD14^+$ monocytes

Maturation marker		Healthy donor			
		1	**2**	**3**	**4**
CD3	% - T	3.97 [0.994*]	15.2 [1.04*]	1.21 [0.94*]	1.88 [1.02*]
	MFI (VioBlue)	5353 [6411*]	3051 [2688*]	128 [32*]	130 [207*]
CD14	% - T	91.3 [1.02*]	89.8 [1.06*]	83.83 [1.04*]	57.44 [1.06*]
	MFI (PE)	11600 [618*]	8048 [349*]	64 [6*]	105 [22*]
CD25	% - T	1.78 [1.02*]	5.53 [1.06*]	3.07 [1.04*]	1.18 [1.06*]
	MFI (PE)	592 [618*]	330 [349*]	9 [6*]	16 [22*]
CD80	% - T	1.18 [1.02*]	5.56 [1.06*]	2.08 [1.04*]	1.26 [1.06*]
	MFI (PE)	577 [618*]	335 [349*]	4 [6*]	25 [22*]
CD83	% - T	12.4 [1.02*]	26.0 [1.06*]	28.69 [1.04*]	2.34 [1.06*]
	MFI (PE)	1175 [618*]	984 [349*]	32 [6*]	21 [22*]
CD86	% - T	94.2 [1.02*]	93.0 [1.06*]	70.56 [1.04*]	46.44 [1.06*]
	MFI (PE)	1996 [618*]	1630 [349*]	29 [6*]	30 [22*]
HLA-DR	% - T	58.0 [1.06*]	85.4 [0.989*]	46.94 [0.99*]	n.a.
	MFI (FITC)	1488 [1362*]	1982 [825*]	21 [22*]	n.a.

* neg. control

*Transducing $CD14^+$ monocytes with the lentiviral vectors LV_ HLA-A*02:01 and LV_HLA-44:03*

Day two $CD14^+$ monocytes were harvested for the transduction with lentiviral vectors LV_HLA-A*02:01 and LV_HLA-B*44:03 at a MOI of 1.5 (DNA-based titer). After transduction, on day four on day six of culture, the morphology of untransduced and LV-transduced cells was observed, all showed the typical dendrites. No differences could be noted between the morphology. Comparing cell viability, both untransduced and LV-transduced cells showed a reduction in cell number on day six (figure 4.9).

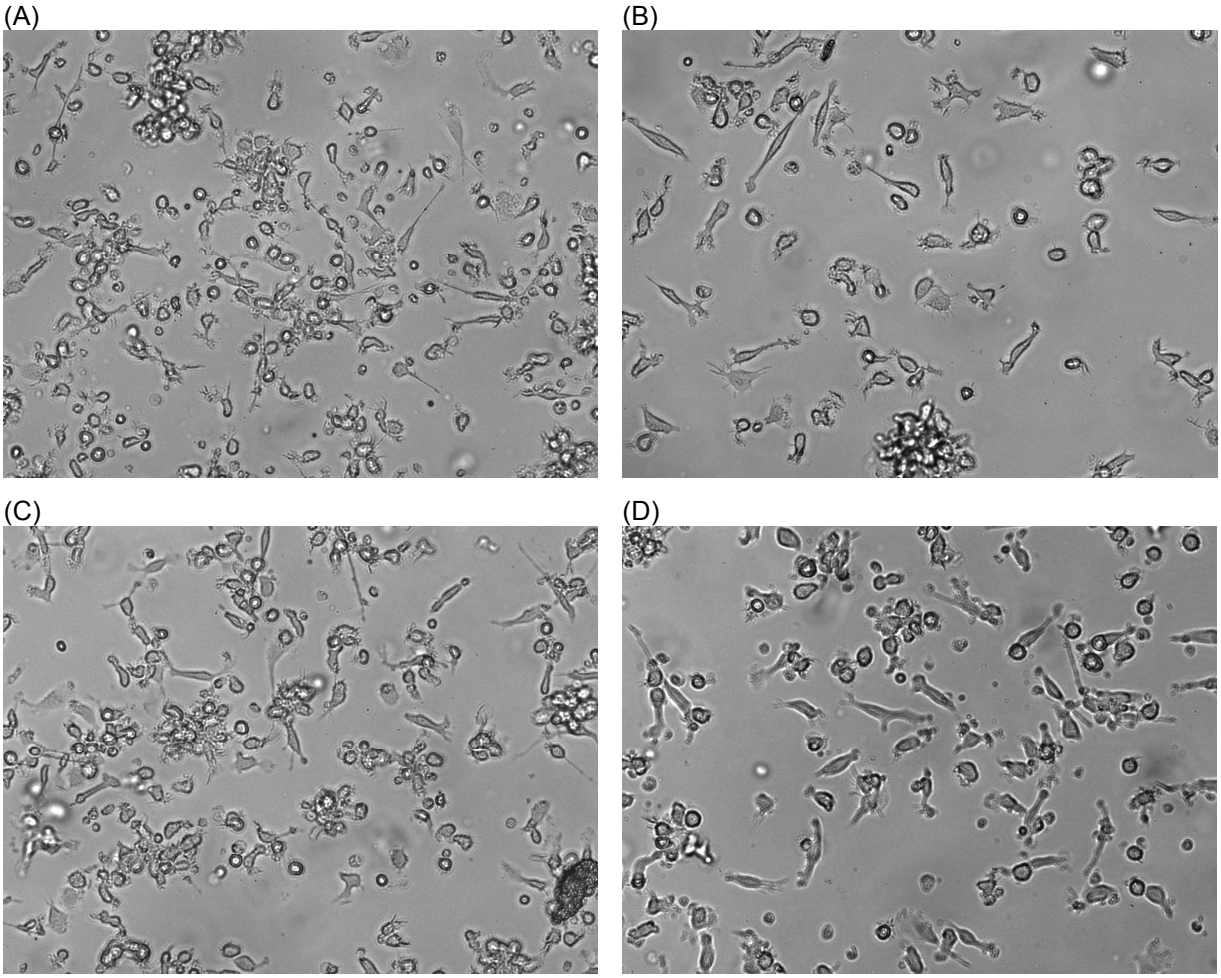

Figure 4.9 Light microscopic pictures (20x original magnification) of untransduced and LV-transduced cells. Exemplarily, showing one donor out of four. (A) untransduced $CD14^+$ monocytes on day four, (B) moDCs on day six, (C) LV-transduced $CD14^+$ monocytes on day four and (D) LV-transduced moDCs on day six.

To verify the successful transduction of $CD14^+$ monocytes, genomic DNA of day ten co-cultures, containing LV-transduced moDCs, was isolated. A real-time PCR was performed to detect WPRE, which integrates together with the genes of interest in transduced cells.

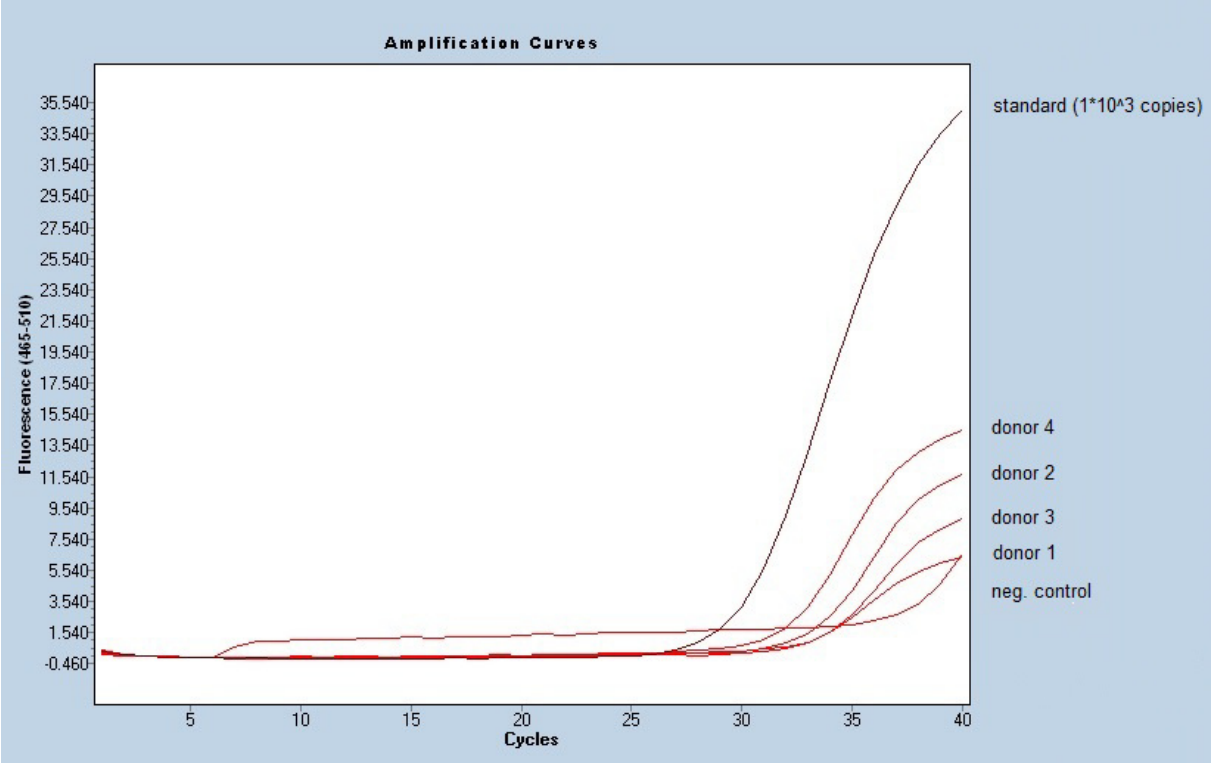

Figure 4.10 Real-time PCR amplification curves detecting integrated WPRE in moDCs of the four donors to conclude the transduction of CD14$^+$ monocytes.

Cycle numbers of amplification curves detecting WPRE were used to determine WPRE copy numbers (figure 4.10). The cell content of co-cultures containing transduced moDCs and CD16$^+$CD56$^+$ NK cells and CD8$^+$ T cells was determined measuring the housekeeping gene albumin. In all of the co-cultures integrated WPRE could be detected in moDCs, verifying the transduction with lentiviral vectors (table 4.12). Nevertheless, no conclusion could be drawn on the percentage of transduced CD14$^+$ monocytes, as DNA was isolated of day ten co-cultures.

Table 4.12 Cycle number of real-time amplification curves detecting WPRE, calculated WPRE copy numbers (according to standards) and the cell count determined by the detection of albumin

Donor	cycle number	Calculated WPRE copy number	Cell count (according to albumin concentrations)
1	33.13	104	3560
2	32.24	211	8700
3	32.59	160	3905
4	31.60	342	6750
neg. control	35.00	20.7	2.73

Infection of LV-transduced moDCs with HIV-1 ADA_V82A and ADA_L210F

On day six of culture, moDCs were infected with HIV-1 ADA_V82A and ADA_L210F, respectively, in order to analyze the effect of different HIV-1 ADA on moDCs. Prior to infection, no differences between the cell counts of moDCs could be observed, comparing untransduced and LV-transduced; indicating that lentiviral vectors did not have an impact on cell viability (table 4.13).

Table 4.13 Numbers of untransduced and LV-transduced moDCs used for the infection with HIV-1 ADA_V82A and ADA_L210F of all donors

Healthy donor	Day 6 moDCs		Day 6 LV-transduced moDCs	
	Total	% of PBMCs	total	% of PBMCs
1	2,600,000	0.05	2,850,000	0.05
2	2,650,000	0.04	2,850,000	0.04
3	1,950,000	0.03	1,800,000	0.03
4	2,900,000	0.08	2,350,000	0.07

Figure 4.11 shows the morphology of uninfected and HIV-1 ADA infected moDCs on day seven and eight. On day seven, no visible differences could be observed. However, while on day eight uninfected moDCs remain unchanged, HIV-1 ADA infected moDCs showed smaller roundish cells close by.

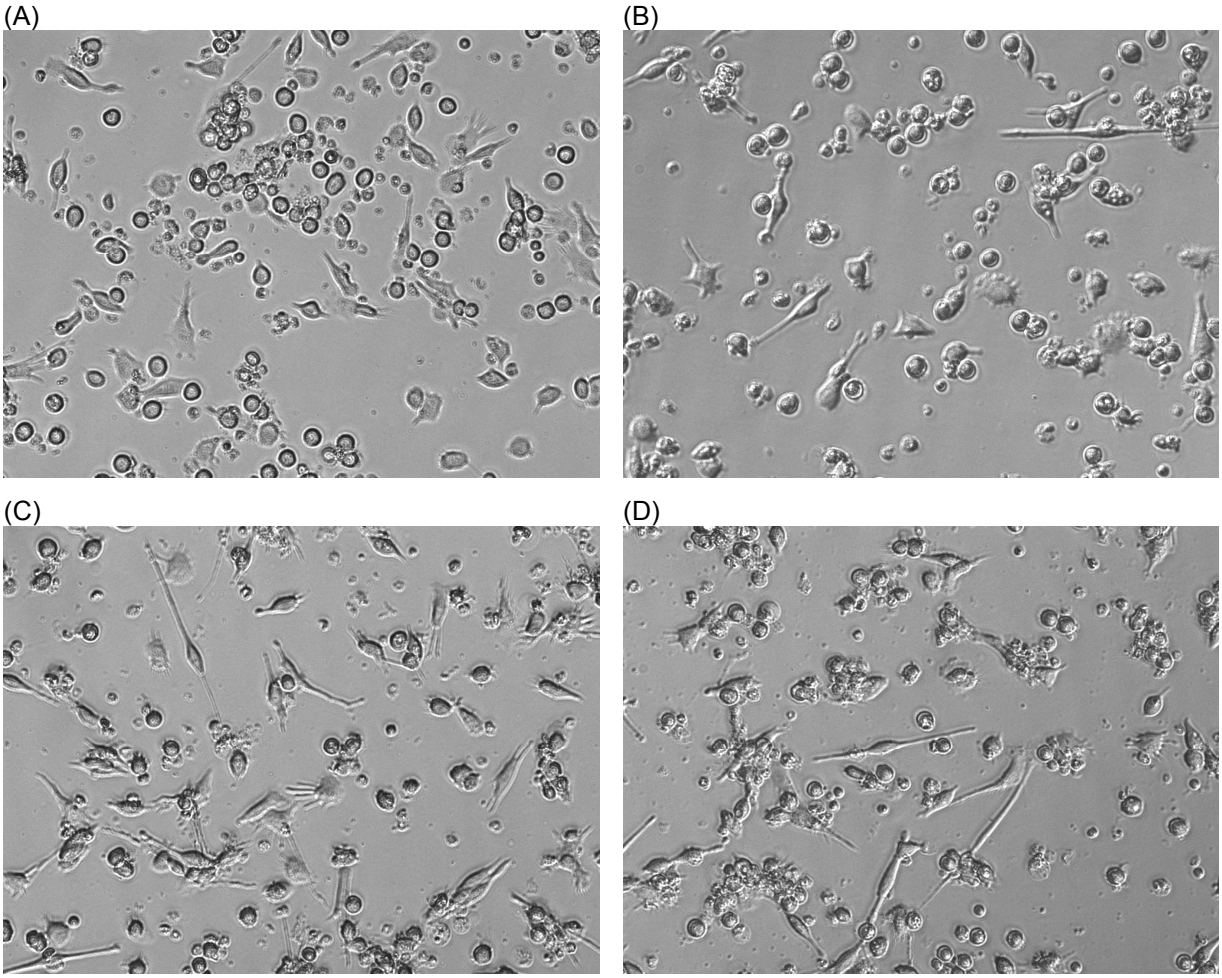

Figure 4.11 Light microscopic pictures (20x original magnification) of uninfected and HIV-1 ADA infected moDCs. Exemplarily, showing one donor out of four and only one of the used HIV-1 ADA (HIV-1 ADA_V82A). (A) uninfected on day seven, (B) uninfected on day eight, (C) HIV-1 ADA infected on day seven and (D) HIV-1 ADA infected on day eight.

Figure 4.12 shows in comparison to figure 4.11 LV-transduced moDCs. While no change in morphology could be observed between untransduced and LV-transduced moDCs on day seven, day eight cells showed spindle-like structures and smaller roundish shaped cells close by. No differences could be observed between day eight moDCs and the ADA infected LV-transduced moDCs of day seven and eight.

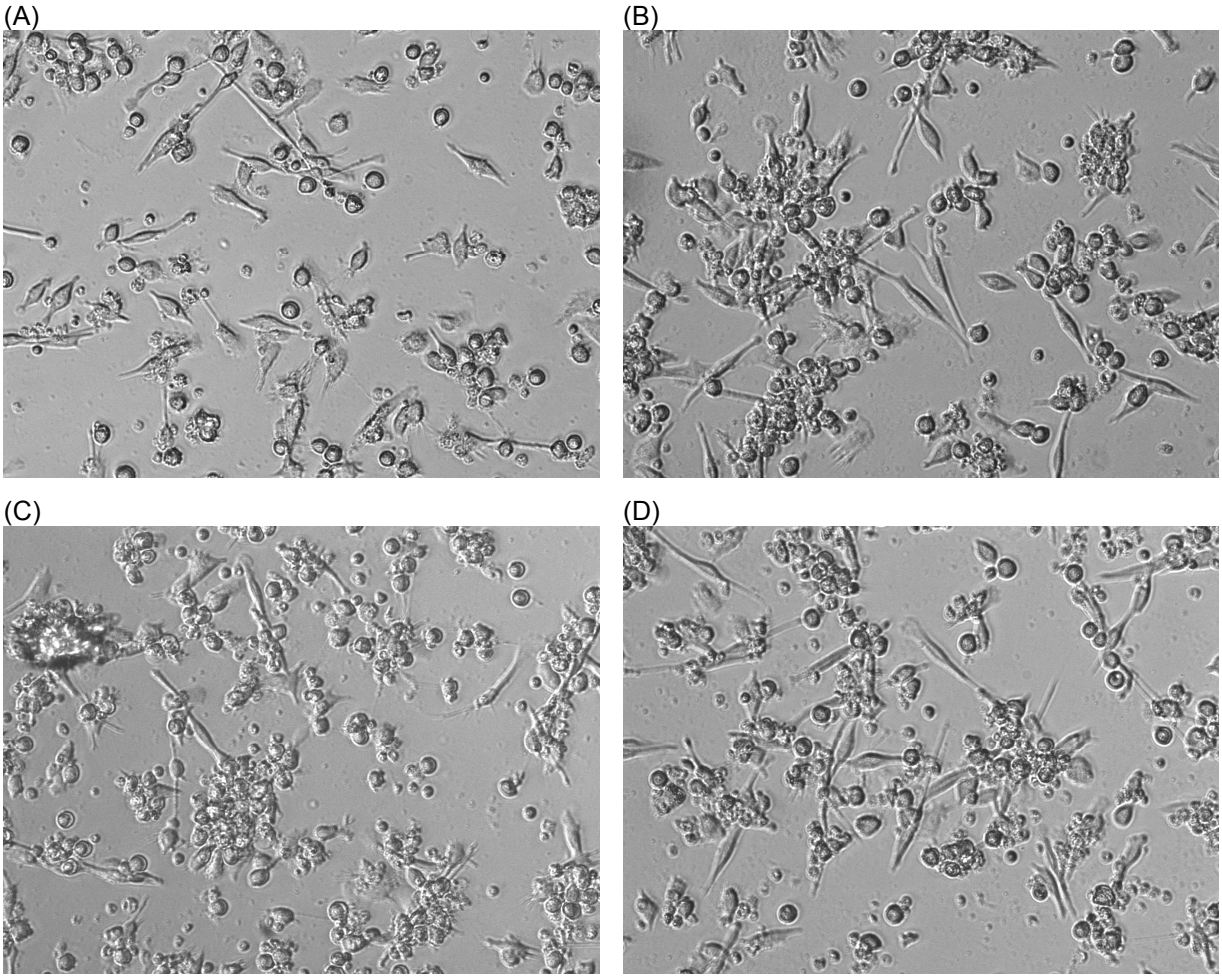

Figure 4.12 Light microscopic pictures (20x original magnification) of LV-transduced uninfected and HIV-1 ADA infected moDCs. Exemplarily, showing one donor out of four and only one of the used HIV-1 ADA (HIV-1 ADA_V82A) (A) uninfected on day seven, (B) uninfected on day eight, (C) HIV-1 ADA infected on day seven and (D) HIV-1 ADA infected on day eight.

To verify the infection of moDCs, genomic DNA was isolated of day ten co-cultures of HIV-1 ADA infected moDCs and $CD16^+CD56^+$ NK cells and $CD8^+$ T cells. The RealTime HIV-1 assay was performed to determine viral copy numbers.

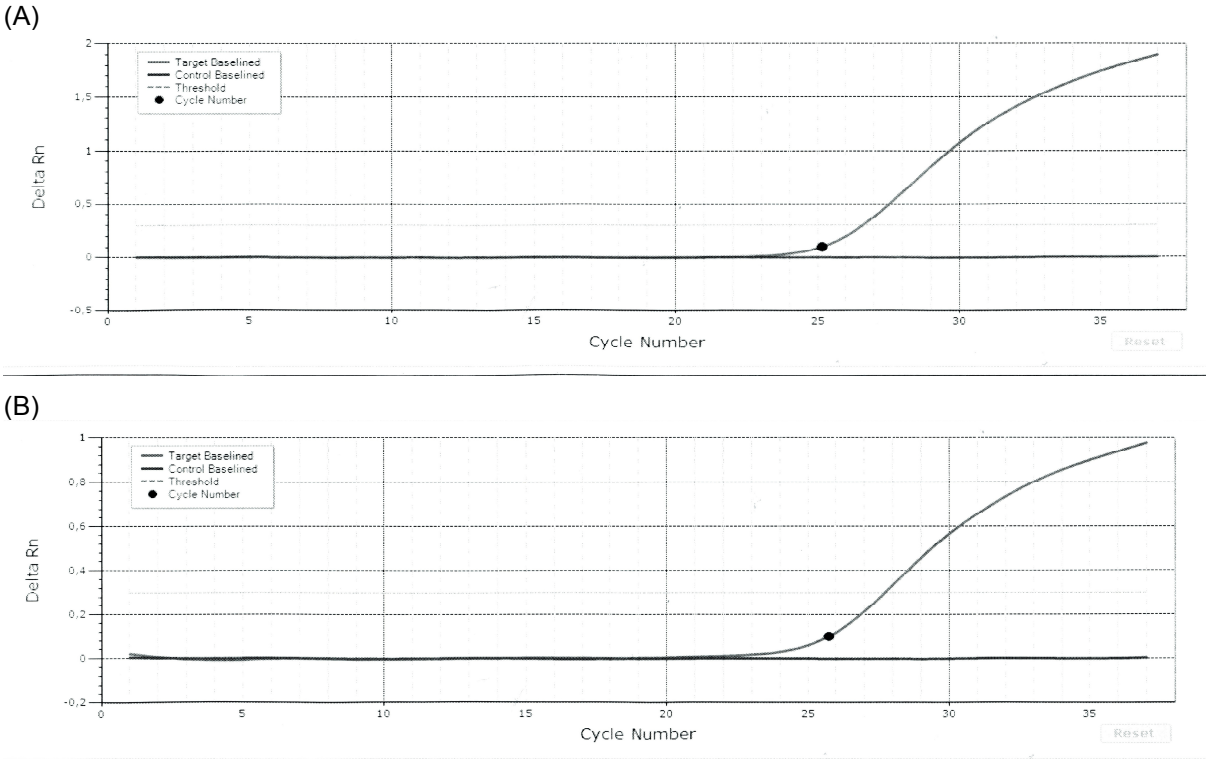

Figure 4.13 Real-time PCR amplification curves determining the presence of HIV-1 integrase to verify the infection with HIV-1 ADA of moDCs. Exemplarily, showing one donor out of four (A) infection with ADA_V82A and (B) with ADA_L210F

Amplification curves showed that moDCs were HIV-1 ADA infected. However, the percentage of infected moDCs could not be determined, as DNA was isolated from co-cultures, not only containing moDCs, but also $CD16^+CD65^+$ NK cells and $CD8^+$ T cells. Figure 4.13 shows exemplarily donor 1 (the amplification curves of donor 2-4 are shown in figure 9.2). Table 4.14 summarizes cycle numbers of real-time amplification curves detecting HIV-1 integrase of all four donors.

Table 4.14 Cycle numbers of real-time amplification curves detecting HIV-1 integrase of all donors

Donor	moDCs infected with ADA_V82A → cycle number	moDCs infected with ADA_L210F → cycle number
1	25.15	25.74
2	24.17	24.50
3	24.46	24.59
4	23.71	23.68

Purification of CD16$^+$CD56$^+$ NK cells and CD8$^+$ T to co-culture with HIV-1 ADA infected LV-transduced moDCs

On day eight of culture, CD16$^+$CD56$^+$ NK cells were purified from the negative fraction of CD14$^+$ monocytes. In order to monitor the purification of CD16$^+$CD56$^+$ NK cells, cells were stained for CD16 and CD56 surface markers (figure 4.15). The percentage of cells expressing both CD16 and CD56 were quantified by the MFI of both fluorescent dyes labelling the antibodies. The dot plots show the population of CD16$^+$CD56$^+$ NK cells (figure 4.14).

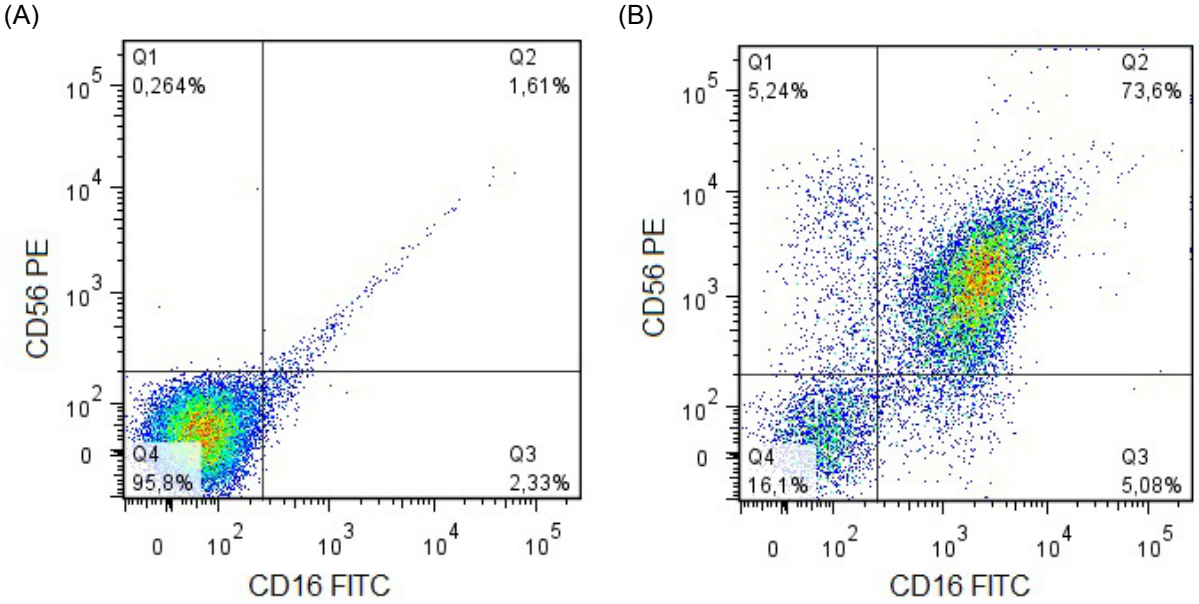

Figure 4.14 Flow cytometric analysis of the quantity and quality of purified CD16$^+$CD56$^+$ NK cells via flow cytometry. Exemplarily, showing one donor out of four. (A) isotype control as negative control, (B) CD16$^+$CD56$^+$ NK cells

The percentage of CD16$^+$CD56$^+$ NK cells ranged from 73.6 % to 80.2 % (table 4.15) between the different donors.

Table 4.15 Summary of flow cytometry results to analyze quantity and quality of purified CD16$^+$CD56$^+$ NK cells of all donors.

Healthy donor	CD16 FITC / CD56 PE		
	% - T	MFI (FITC)	MFI (PE)
1	77.9 [26.6*]	773 [196*]	833 [103*]
2	80.2 [4.27*]	1658 [876*]	1781 [296*]
3	32.9 [4.49*]	17.04 [4.96*]	15.53 [1.32*]
4	73.6 [1.61*]	1999 [773*]	1367 [368*]

* neg. control

Subsequently, $CD8^+$ T cells were isolated from the negative fraction of $CD16^+CD56^+$ NK cells. The number of purified $CD16^+CD56^+$ NK cells ranged from $1.7*10^6$ – $5*10^6$ cells, while the numbers of $CD8^+$ T cells ranged from $48.1*10^6$ – $90.3*10^6$ cells. Comparing $CD16^+CD56^+$ NK cell and $CD8^+$ T cell numbers, $CD8^+$ T cells were present in much greater numbers (13.4 – 53.1 times higher).

Table 4.16 Number of purified $CD16^+CD56^+$ NK and $CD8^+$ T cells of all donors.

Healthy donor	Number of $CD16^+CD56^+$ cells		Number of $CD8^+$ cells	
	Total	% of PBMCs	Total	% of PBMCs
1	1,700,000	0.03	90,250,000	1.57
2	5,000,000	0.07	71,950,000	0.97
3	2,900,000	0.04	48,050,000	0.74
4	4,900,000	0.14	80,300,000	2.25

Light microscopic pictures of figure 4.15 show the different cell morphologies of $CD8^+$ T cells and $CD16^+CD56^+$ NK cells.

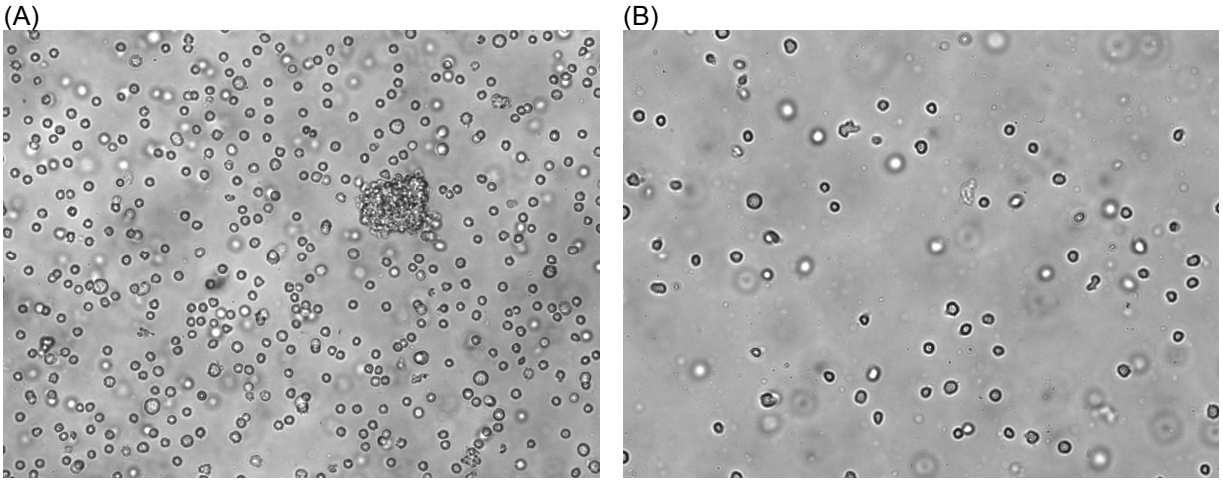

Figure 4.15 Light microscopic pictures (20x original magnification) of (A) $CD8^+$ T cells and (B) $CD16^+CD56^+$ NK cells. Exemplarily, showing one donor out of four.

To monitor the purity of $CD8^+$ T cells, cells were analyzed via flow cytometry staining for CD3 and CD8 surface markers (figure 4.16).

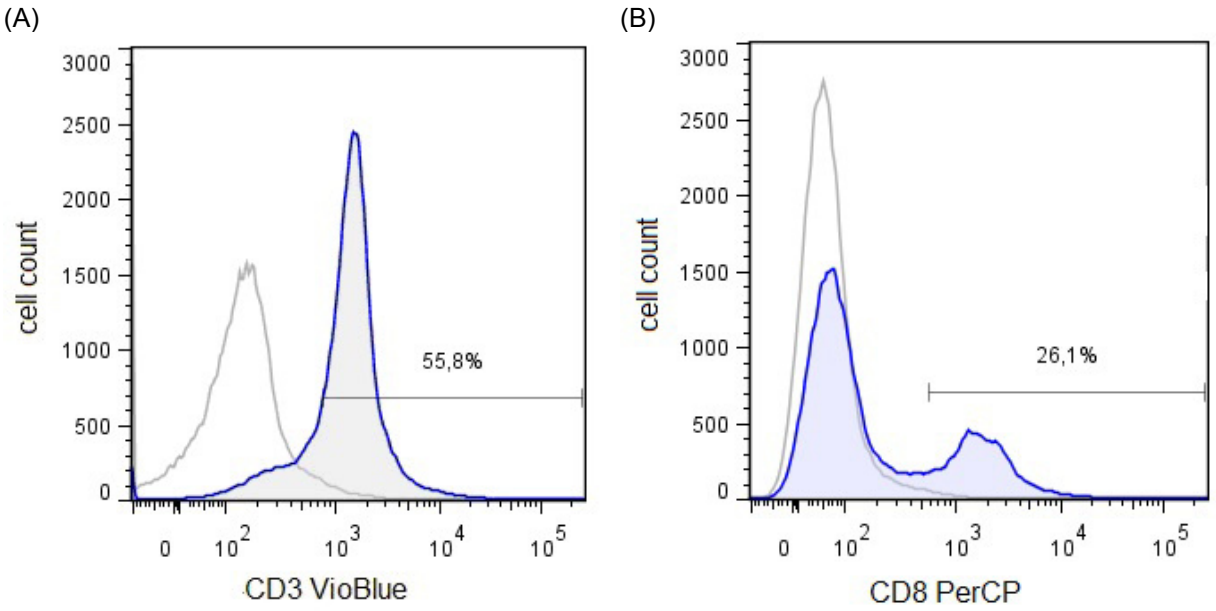

Figure 4.16 Flow cytometric analysis of the quantity and quality of purified CD8$^+$ cells. Exemplarily, showing one donor out of four. The grey curves show the isotype control, whereas the blue curves represent the stained surface markers. (A) percentage of CD3$^+$ cells, (B) percentage of CD8$^+$ cells

CD3$^+$ cell counts ranged from 7.18 - 55.8 % and CD8$^+$ T cells from 13.9 – 31.23 %. Table 4.17 summarizes cell counts of the different donors.

Table 4.17 Summary of flow cytometry results to analyze quantity and quality of purified CD8$^+$ T cells of all donors.

Healthy donor	anti-CD3 VioBlue		anti-CD8 PerCP	
	% - T	MFI (VioBlue)	% - T	MFI (PerCP)
1	47.8 [1.01*]	1142 [1376*]	28.2 [1.02*]	1733 [877*]
2	55.8 [1.07*]	1037 [1166*]	26.1 [1.05*]	1620 [813*]
3	39.24 [1.06*]	24.11 [8.65*]	31.23 [1.03*]	19.05 [14.16*]
4	7.18 [1.01*]	3349 [3457*]	13.9 [1.02*]	627 [428*]

*neg. control

Co-culture of moDCs with either CD16$^+$CD56$^+$ NK or CD8$^+$ T cells

Untransduced and LV-transduced moDCs, either infected with HIV-1 ADA_V82A or ADA_L210F were, on day eight of culture, co-cultured with CD16$^+$CD56$^+$ NK or CD8$^+$ T cells. The cell numbers of the different fractions of moDCs ranged from 50,000 to 210,000 and are summarized in table 4.18. The number of co-cultured CD16$^+$CD56$^+$ NK and CD8$^+$ T cells was adjusted accordingly and added in a 1:1 ratio.

Table 4.18 Summary of moDC numbers in the different cell fractions of all donors

Cell fraction	healthy donor 1		healthy donor 2		healthy donor 3		healthy donor 4	
	total # of cells	% of PBMCs	total # of cells	% of PBMCs	total # of cells	% of PBMCs	total # of cells	% of PBMCs
uninfected	9.5*	0.0017	8.5*	0.0011	5.0*	0.00077	21.0*	0.0059
ADA_V82A infected	12.5*	0.0022	10.5*	0.0014	6.5*	0.001	15.0*	0.0042
ADA_L210F infected	10.5*	0.0018	17.5*	0.0024	5.0*	0.00077	11.0*	0.0031
LV-transduced, uninfected	5.5*	0.0009	13.0*	0.0017	6.5*	0.001	12.0*	0.0034
LV-transduced, ADA_V82A infected	9.5*	0.0017	20.5*	0.0028	6.5*	0.001	15.0*	0.0042
LV-transduced, ADA_L210F infected	13.0*	0.0023	15.5*	0.0021	6.0*	0.00093	15.0*	0.0042

*10^4

Differences between the cultures of untransduced and LV-transduced cells could be observed in the morphology of the co-culture of moDCs with $CD16^+CD56^+$ NK cells on day nine. Comparing light microscopic pictures of co-cultures of day nine and ten of moDCs with $CD16^+CD56^+$ NK cells, revealed an activation of $CD16^+CD56^+$ NK cells and the killing of moDCs. There was no visible difference between untransduced and LV-transduced cells nor between uninfected and HIV-1 ADA infected moDCs (figure 4.17).

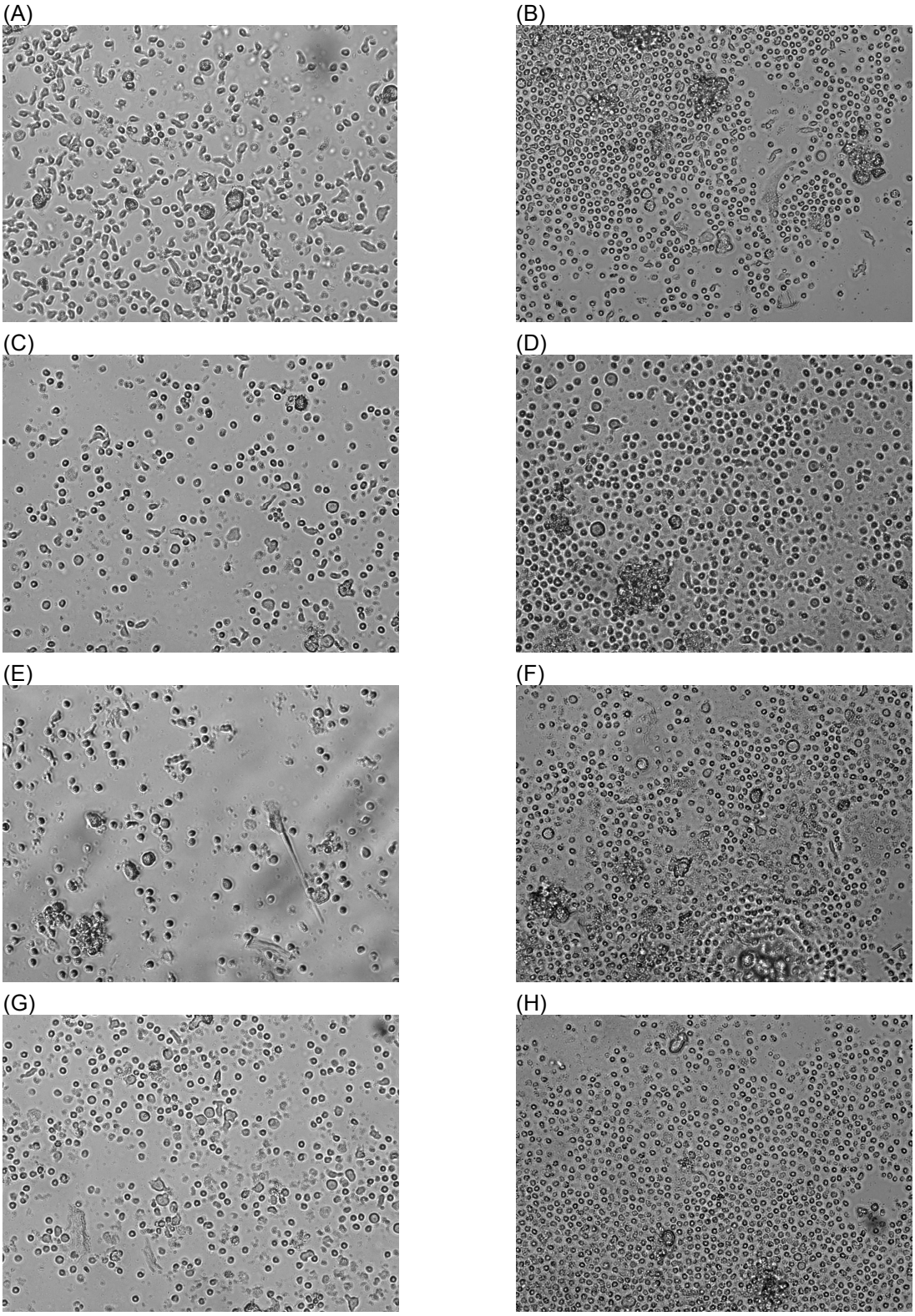

Figure 4.17 Light microscopic pictures (20x original magnification) of co-cultures of moDCs and $CD16^{+}CD56^{+}$ NK cells on day nine and ten. Exemplarily, showing one donor out of four. (A) moDCs on day nine, (B) moDCs on day ten, (C) LV-transduced moDCs on day nine, (D) LV-transduced moDCs on day ten, (E) LV-transduced HIV-1 ADA_V82A moDCs on day nine, (F) LV-transduced HIV-1 ADA_V82A moDCs on day ten, (G) LV-transduced HIV-1 ADA_L210F moDCs on day nine and (H) LV-transduced HIV-1 ADA_L210F moDCs on ten.

Figure 4.18 shows pictures of co-cultures of untransduced and LV-transduced moDCs with $CD8^+$ T cells on day nine and ten of culture. Light microscopic pictures of day ten showed no visible difference between uninfected untransduced and LV-transduced cells. But observing HIV-1 ADA_V82A and ADA_L210F infected moDCs, one could see that $CD8^+$ T cells accumulated.

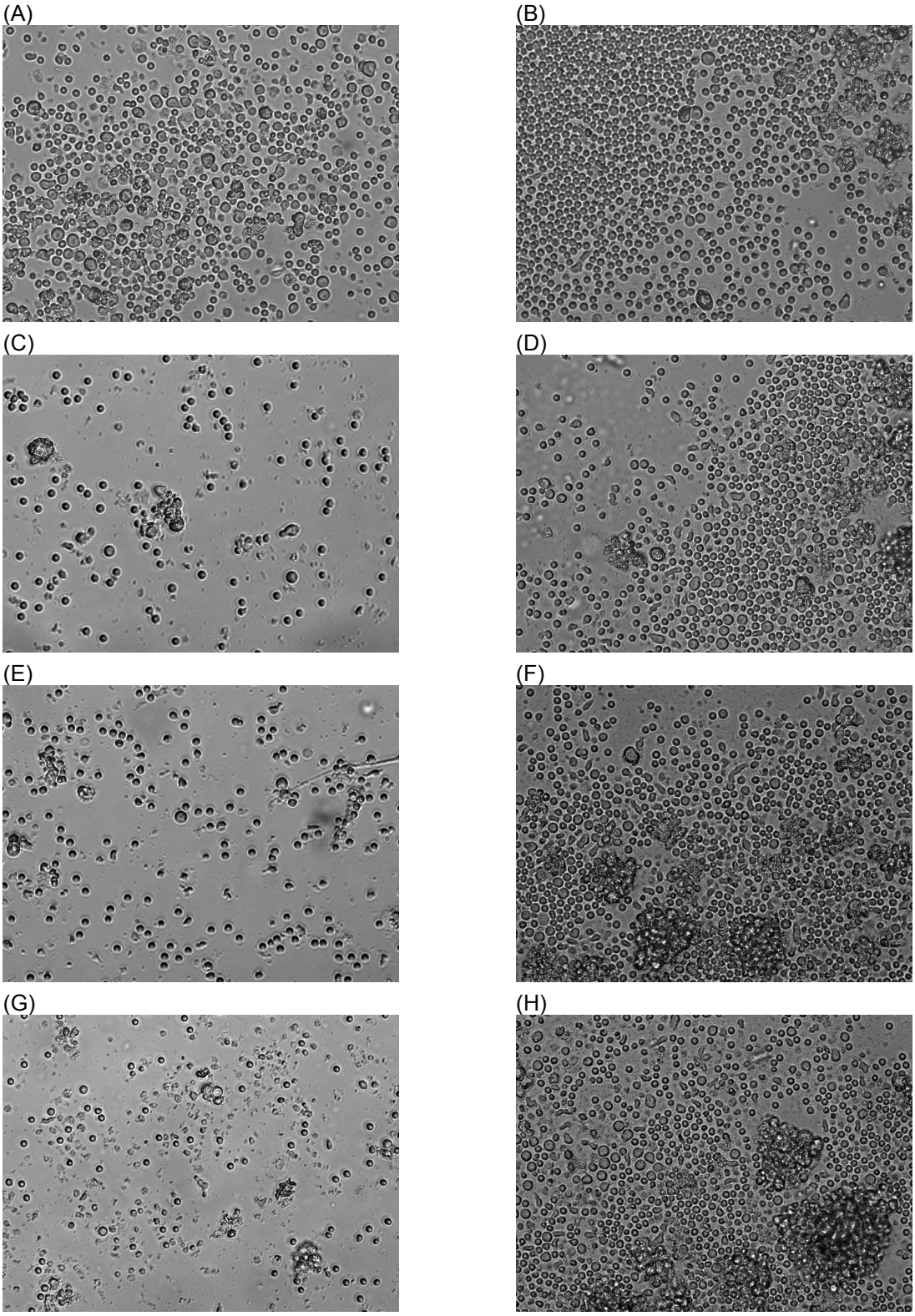

Figure 4.18 Light microscopic pictures (20x original magnification) of co-cultures of moDCs and $CD8^+$ T cells on day nine and ten. Exemplarily, showing one donor out of four. (A) moDCs on day nine, (B) moDCs on day ten, (C) LV-transduced moDCs on day nine, (D) LV-transduced moDCs on day ten, (E) LV-transduced HIV-1 ADA_V82A moDCs on day nine, (F) LV-transduced HIV-1 ADA_V82A moDCs on day ten, (G) LV-transduced HIV-1 ADA_L210F moDCs on day nine and (H) LV-transduced HIV-1 ADA_L210F moDCs on ten.

Light microscopic pictures of co-cultures suggested the presence of dead cells. To determine whether co-cultures with $CD8^+$ T or $CD16^+CD56^+$ NK cells contain more dead cells, untransduced and LV-transduced moDCs, co-cultured with either $CD16^+CD56^+$ NK cells or $CD8^+$ T cells, were stained with propidium iodide, which enters porous cells and intercalates with the DNA. Figure 3.19 shows histograms indicating the percentage of dead cells.

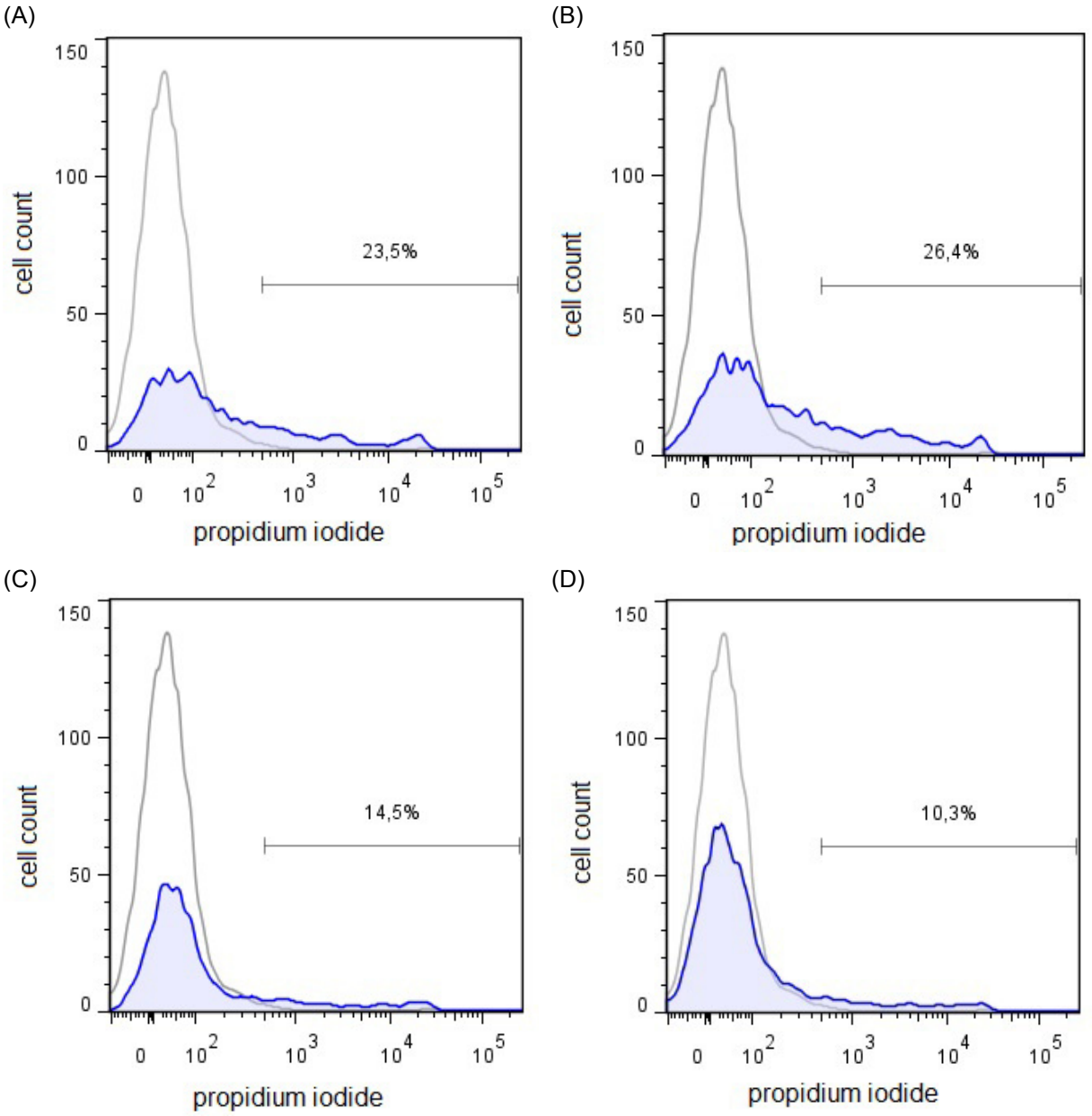

Figure 4.19 Flow cytometric analysis of the cell viability in co-cultures of moDCs / $CD8^+$ T cells and moDCs / $CD16^+CD56^+$ NK cells. The grey curves show the isotype control, whereas the blue curves represent the stained surface markers. (A) co-culture of moDCs and $CD16^+CD56^+$ NK cells, (B) co-culture of LV-transduced moDCs and $CD16^+CD56^+$ NK cells, (C) co-culture of moDCs and $CD8^+$ T cells, (D) co-culture of LV-transduced moDCs and $CD8^+$ T cells

Table 4.19 summarizes the data of %-T and MFI (PE) of propidium iodide stained cells, indicating the amount of dead cells. Co-cultures containing $CD16^+CD56^+$ NK cells contained between 23.5 – 26.4 % dead cells, whereas co-cultures with $CD8^+$ T cells contained 10.3 – 14.5 % . The amount of dead cells within co-cultures containing $CD16^+CD56^+$ NK cells was significantly higher than in $CD8^+$ T cells ($p = 0.0389$).

Table 4.19 Summary of flow cytometry results to analyze cell viability in co-cultures of moDCs / $CD8^+$ T cells and moDCs / $CD16^+CD56^+$ NK cells

co-culture	%-T	MFI (PE)
moDCs / $CD16^+CD56^+$ NK cells	23.5	1842
LV-transduced moDCs / $CD16^+CD56^+$ NK cells	26.4	2074
moDCs / $CD8^+$ T cells	14.5	2587
LV-transduced moDCs / $CD8^+$ T cells	10.3	2568
neg. control	0.998	1150

Determination of the cytokine and chemokine release in HIV-1 infected patients

The killing of infected cells by $CD16^+CD56^+$ NK cells and $CD8^+$ T cells requires signaling between infected cells and effector cells for their differentiation and activation. This process can be executed by the secretion of cytokines and chemokines, and their binding to specific receptors and the activation of underlying signaling cascades.

In a first step, the cytokine and chemokine release associated with HIV-1 infection was determined. Here for, a cohort of patients with low (< 50, therapy-experienced) and high (> 500,000, therapy-naïve) plasma viral load (pVL) was analyzed for the release of cytokines and chemokines and was compared with healthy donors. Significant differences could surprisingly be observed both, between HIV-1 infected patients with low pVL and healthy donors and patients with high pVL and healthy donors. Levels of the cytokines IL-2R ($p = 0.00776$) and IL-12 ($p = 0.00011$) and the chemokines CCL2 ($p = 0.00357$), CCL11 ($p = 0.00026$), CXCL9 ($p = 0.00017$) and CXCL10 ($p = 0.00045$) were significantly elevated in HIV-1 infected patients with high pVL. In addition, in HIV-1 infected patients with pVL under the limit of detection (pVL < 50), levels of the cytokines IL-1β ($p = 0.01831$), IL-1RA ($p = 0.02746$), IL-2R ($p = 0.00011$), IL-4 ($p = 0.00112$), IL-8 ($p = 0.01928$), IL-13 ($p = 0.02977$), IL-15 ($p = 0.03651$), IL-17 ($p = 0.00284$) and TNF-α ($p = 0.02118$) were unexpectedly significantly lower than compared to the negative controls (figure 4.20). Levels of

IFN-γ and CCL5 were out of the upper and lower limit of detection, respectively and therefore not shown.

(A)

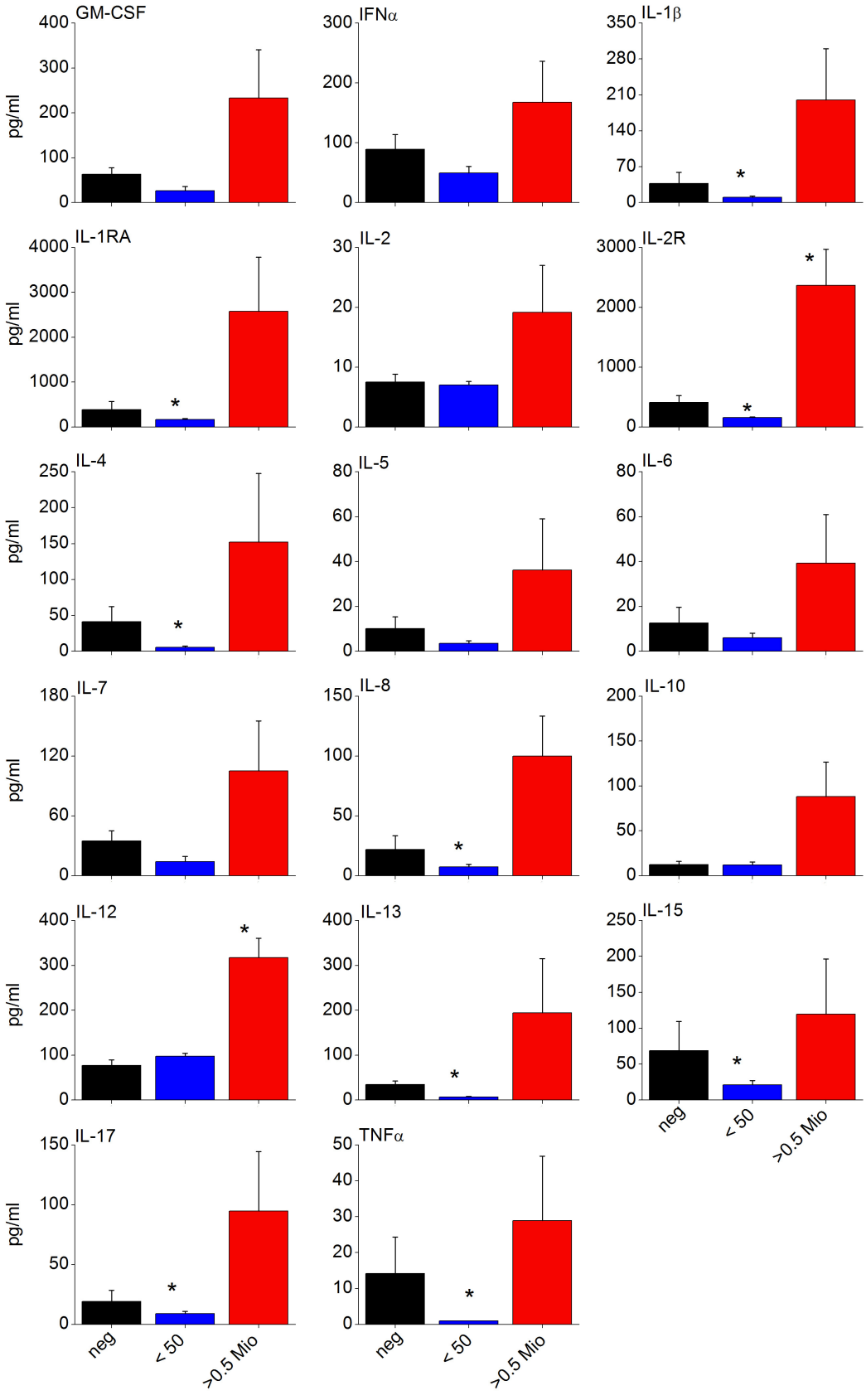
GM-CSF
IFNα
IL-1β
IL-1RA
IL-2
IL-2R
IL-4
IL-5
IL-6
IL-7
IL-8
IL-10
IL-12
IL-13
IL-15
IL-17
TNFα
pg/ml
neg
< 50
>0.5 Mio

(B)

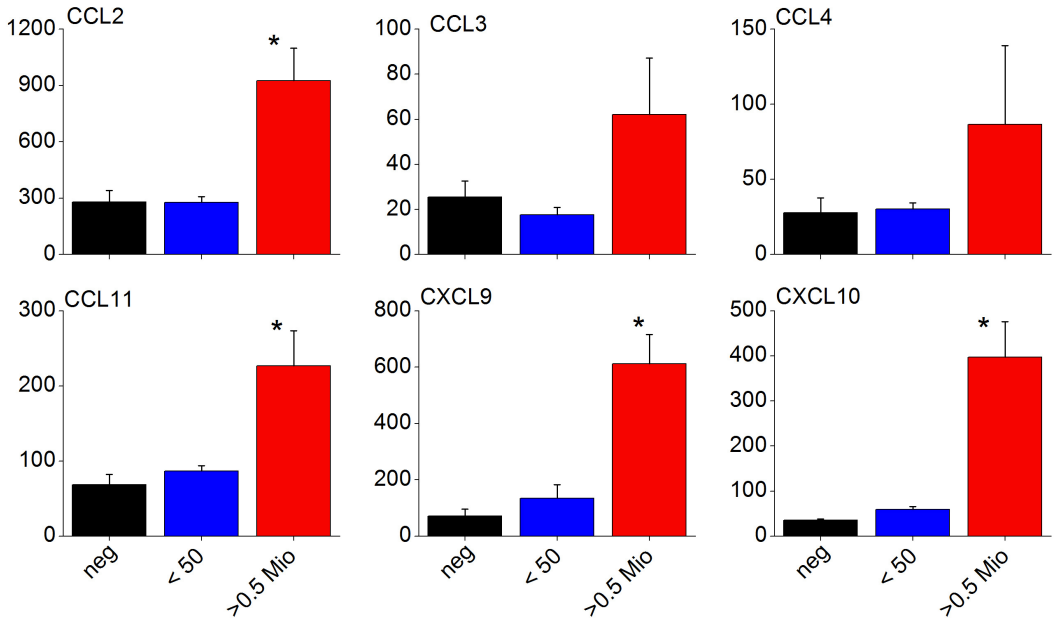

Figure 4.20 Evaluation in plasma of HIV-1 infected and uninfected (black bar, n = 9) individuals for (A) cytokine and (B) chemokine secretion. HIV-1 infected patients were classified in patients with pVL under the limit of detection (pVL< 50 (therapy-experienced), blue bar, n = 40) and pVL > 0.5*10^6 copies mL^{-1} ((therapy-naïve), red bar, n = 10). Asterisks show significant associations between the uninfected individuals and HIV-1 infected.

Influence of the infection of moDCs with HIV-1 ADA_V82A and ADA_L210F on the cytokine and chemokine release of moDCs

MoDCs were, on day six of culture, infected with HIV-1 ADA_V82A and ADA_L210F at 10^5 $TCID_{50}$ / 10^6 cells. The effect of infection on the secretion of cytokines and chemokines was analyzed, determining levels on day two of culture and day eight, before the co-culture with either $CD16^+CD56^+$ NK cells or $CD8^+$ T cells. Secretion upon infection with ADA_V82A and ADA_L210F was observed separately, and data were compared to the cytokine and chemokine secretion of uninfected cells. In various cases no differences in cytokine and chemokine release could be observed between uninfected and HIV-1 ADA infected moDCs, these cytokines include IFN-γ, IL-2, IL-5, IL-10, IL-13, IL-17 and the chemokines CCL11 and CXCL9. However, slightly elevated levels were determined in uninfected moDCs compared to HIV-1 ADA infected cells, observing the cytokines IL-4, IL-7, IL-15, TNF-α and the chemokines CCL2, CCL4 and CCL5. Cytokines GM-CSF, IL-1β, IL-12 and chemokine CXCL10 showed the least secretion in HIV-ADA_V82A infected cells,

uninfected and ADA_L210F infected moDCs showed similar slightly elevated levels. Contrary, cytokine IL-2R and the chemokine CCL3 showed the least secretion when infected with HIV-1 ADA_L210F and slightly elevated levels after infection with ADA_V82A and in uninfected cells. Levels of cytokines IL-1RA and IL-6 remained low in uninfected and HIV-1 ADA_L210F infected moDCs, but are elevated in ADA_V82A infected cells. Cytokines IFN-α and IL-8 showed elevated levels, in HIV-1 ADA_V82A and ADA_L210F moDCs, respectively, compared to uninfected moDCs. None of these differences reached significance (figure 4.21).

(A)

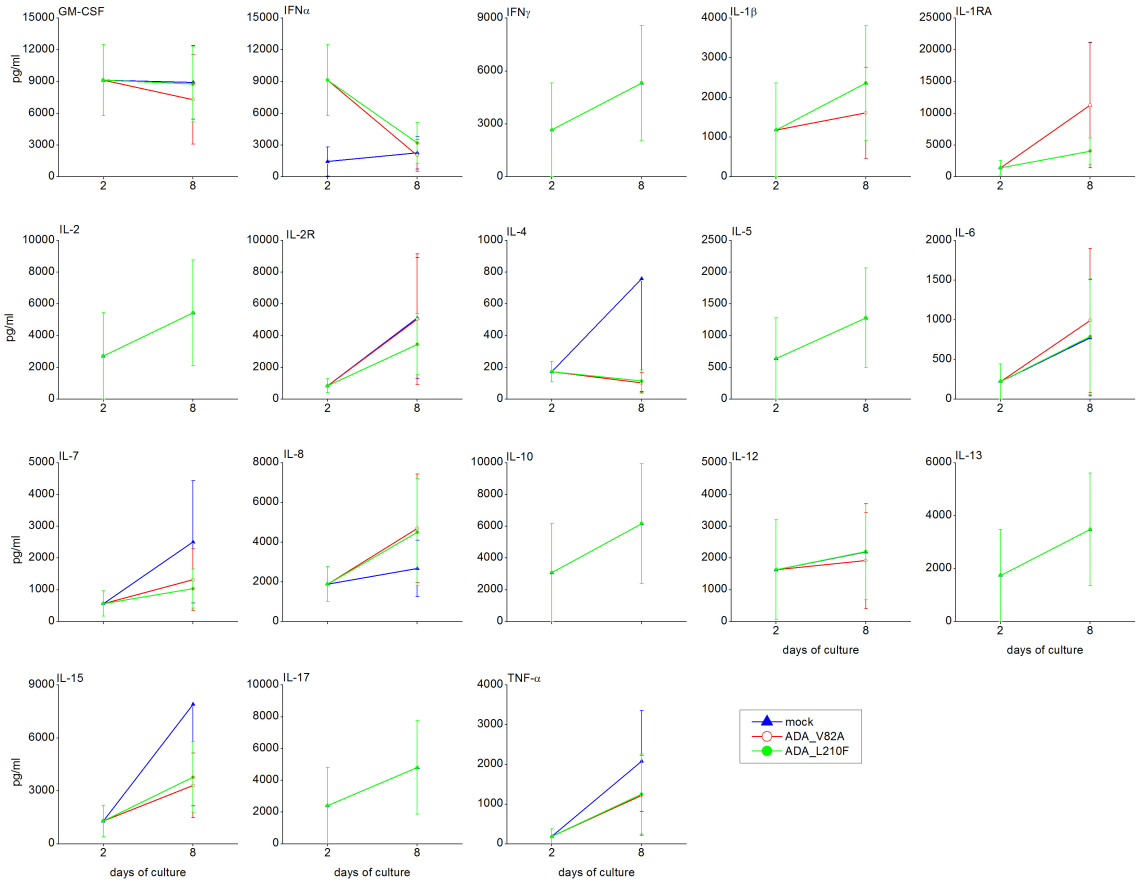

(B)

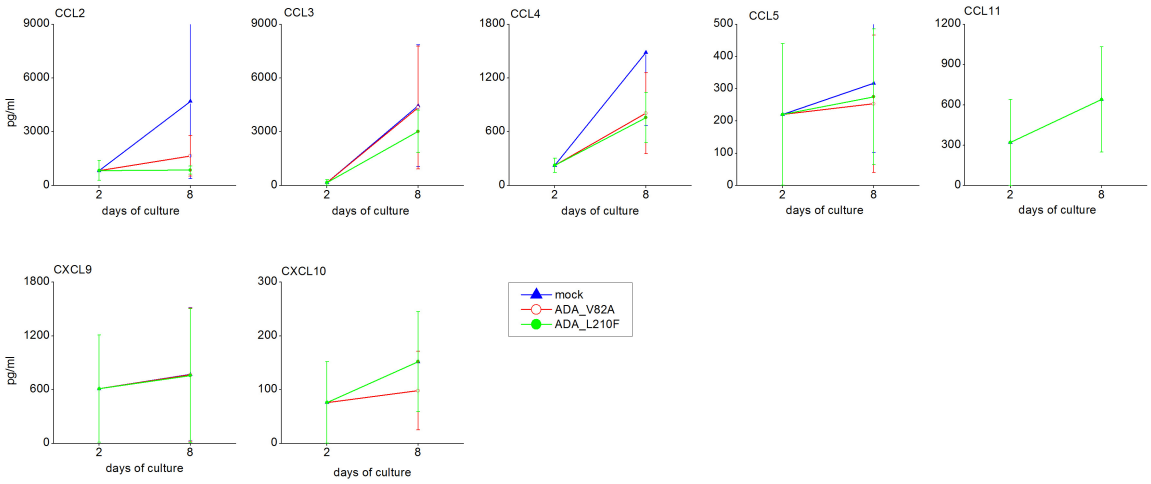

Figure 4.21 (A) cytokine and (B) chemokine secretion of day two CD14$^+$ monocytes (blue, mock) and day eight HIV-1 ADA infected moDCs (HIV-1 ADA_V82A, red; ADA_L210F, green).

Influence of the transduction of CD14$^+$ monocytes on the cytokine and chemokine release of moDCs

Before the infection of moDCs with HIV-1 ADA on day six of culture, day two CD14$^+$ monocytes were transduced with LV_HLA-A*02:01 and LV_HLA-B*44:03, respectively at MOI 1.5 (DNA-based titer). To determine an impact of LV-transduction on cytokine and chemokine release, their secretion was determined before the transduction of CD14$^+$ monocytes as well as on day eight of moDCs, before the co-culture with either CD16$^+$CD56$^+$ NK cells or CD8$^+$ T cells. In most cases, no differences in cytokine and chemokine release could be observed between untransduced and LV-transduced cells, these cytokines include IFN-γ, IL-1β, IL-2, IL-5, IL-10, IL-13, IL-17, TNF-α and the chemokines CCL11, CXCL9 and CXCL10. However, slightly higher levels of the cytokines IL-1RA, IL-6, IL-12 and the chemokine CCL5 could be detected in LV-transduced cells (figure 4.20), while the amounts of the cytokines GM-CSF, IFN-α, IL-2R, IL-4, IL-7, IL-15 and the chemokines CCL2, CCL3 and CCL4 were elevated in untransduced cells (figure 4.22). None of these differences reached significance.

(A)

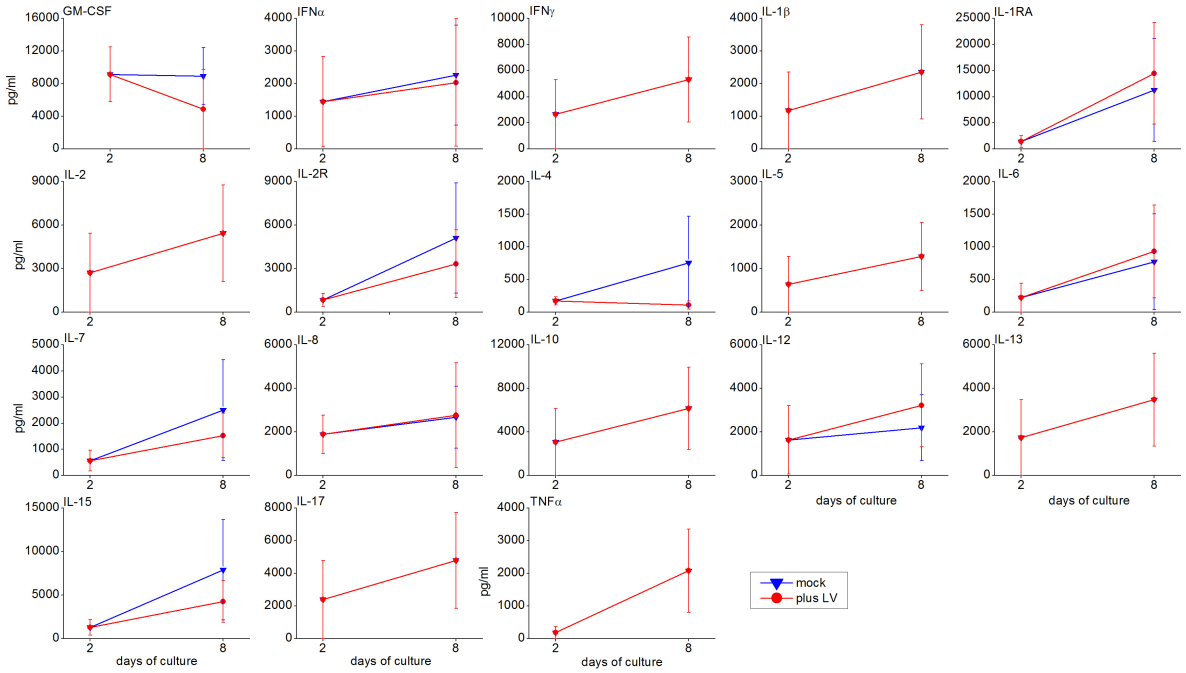

(B)

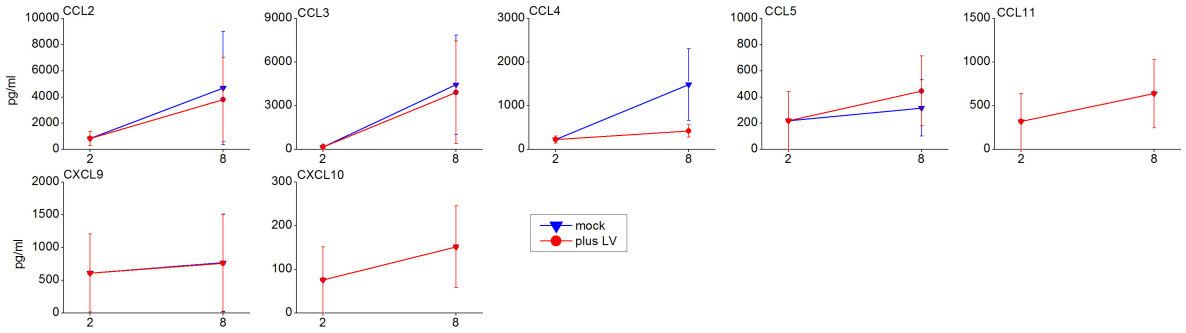

Figure 4.22 (A) cytokine and (B) chemokine release detected in the supernatant of un-transduced (blue) and LV-transduced (red) day two CD14$^+$ monocytes and day eight moDCs.

Determination of cytokine and chemokine release in the co-culture of HIV-1 ADA infected moDCs with either CD16$^+$CD56$^+$ NK cells or CD8$^+$ T cells indicating an immune escape of V82A (PR) or L210F (RT) in the respective HLA backgrounds

The effect of HIV-1 ADA_V82A and ADA_L210F on cytokine and chemokine release was determined in co-cultures of moDCs deriving from either HLA-A*02:01 or HLA-B*44:03 donor, with CD16$^+$CD56$^+$ NK cells and CD8$^+$ T cells, respectively. Prior to infection, lentiviral vectors were used to introduce HLA-B*44:03 in the HLA-A*02:01 donors and HLA-A*02:01 in the HLA-B*44:03 donors.

It was assumed, that moDCs deriving from an HLA-A*02:01 positive donor can modify their cytokine and chemokine release upon encountering HIV-1 ADA_L210F, resulting either in an increase of release, or a decrease. V82A (PR) was identified as a possible immune escape mutation in the background of HLA-A*02:01. In this HLA background, an infection with HIV-1 ADA_V82A should modify cytokine and chemokine secretion less than detected for infections with ADA_L210F. Introducing HLA-B*44:03, using a lentiviral vector, into CD14$^+$ monocytes deriving from HLA-A*02:01 positive donors, should have no impact on cytokine and chemokine levels upon infection with HIV-1 ADA_V82A. However, as L210F (RT) has been described to be an immune escape mutation in the background of HLA-B*44:03, infection with HIV-1 ADA_L210F should result in a less pronounced secretion profile.

Vice versa, moDCs of HLA-B*44:03 positive donor should show a modified cytokine and chemokine secretion pattern encountering HIV-1 ADA_V82A and less pronounced when infected with ADA_L210F. In transduced moDCs, introducing HLA-A*02:01, the infection with either ADA_V82A or ADA_L210F should have no effect on cytokine and chemokine levels.

In order to determine the impact of immune escape mutations, V82A (PR) and L210F (RT), cytokine and chemokine release in the co-cultures of HIV-1 ADA infected moDCs with either CD16$^+$CD56$^+$ NK cells or CD8$^+$ T cells was analyzed. To cover a broad range of cytokines and chemokines, the human 25-plex panel was used. In general, the presence of either CD16$^+$CD56$^+$ NK cells or CD8$^+$ T cells in moDC cultures resulted in higher levels of cytokine and chemokine release on day ten, compared to the absence on day eight. Independent of infection, an increase of cytokines and chemokines can be observed, comparing untransduced and LV-transduced cells.

With respect to HLA-A*02:01 positive donors, co-cultures of moDCs and $CD16^+CD56^+$ NK cells showed the release of cytokines IL-4, IL-7, IL-8, IL-12 and IL-15 as well as the chemokines CCL2, CCL4 and CCL5 (figure 4.23) according to model A2 (ratio ADA_L210F : ADA_V82A < 1 / ratio ADA_L210F : ADA_V82A $\geq$ 1, figure 1.8). Regarding, HLA-B*44:03 positive donor, co-cultures of moDCs and $CD16^+CD56^+$ NK cells showed the release of the cytokines IL-8 and IL-15 and the chemokines CCL2 and CCL3 (figure 4.24) according to model B2 (ratio ADA_V82A : ADA_L210F < 1 / ratio ADA_V82A : ADA_L210F $\geq$ 1, figure 1.8). Cytokines IL-4, IL-7 and the chemokine CCL4 (figure 4.24) were secreted according to model B1 (ratio ADA_V82A : ADA_L210F > 1 / ratio ADA_V82A : ADA_L210F $\leq$ 1, figure 1.8).

With respect to HLA-A*02:01 positive donors, co-cultures of moDCs and $CD8^+$ T cells showed the release of cytokines IL-6, IL-7 and IL-8 as well as the chemokine CXCL9 (figure 4.25) according to model A2 (ratio ADA_L210F : ADA_V82A < 1 / ratio ADA_L210F : ADA_V82A $\geq$ 1, figure 1.8).

Regarding, HLA-B*44:03 positive donor, co-cultures of moDCs and $CD8^+$ T cells showed the release of the cytokines IL-1RA, IL-7, IL-8 and the chemokines CCL2 and TNF-α (figure 4.26) according to model B2 (ratio ADA_V82A : ADA_L210F < 1 / ratio ADA_V82A : ADA_L210F $\geq$ 1, figure 1.8). Chemokine CXCL9 was secreted according to model B1 (ratio ADA_V82A : ADA_L210F > 1 / ratio ADA_V82A : ADA_L210F $\leq$ 1, figure 1.8).

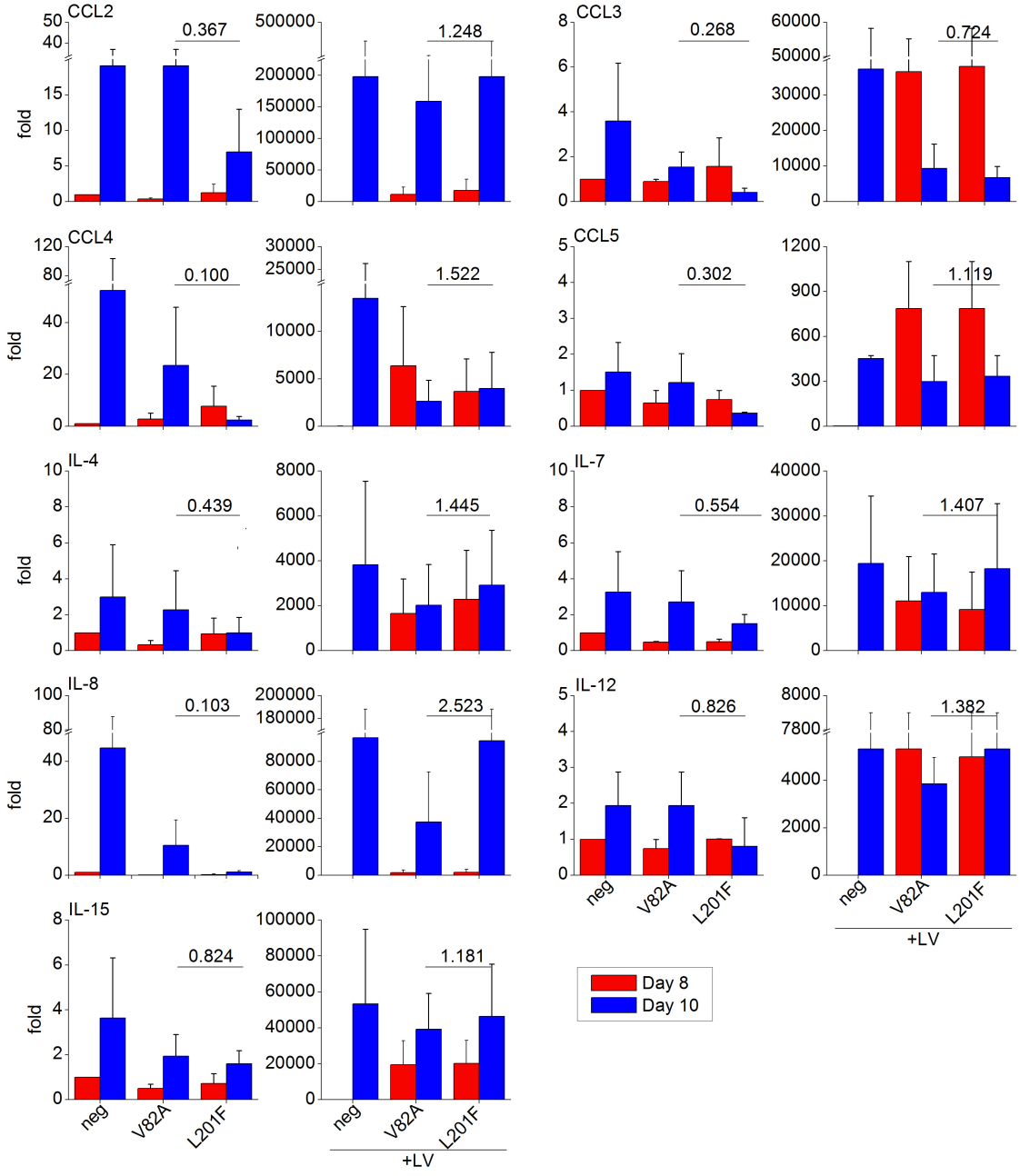

Figure 4.23 Fold difference in cytokine and chemokine release normalized to untransduced uninfected moDCs and transduced uninfected moDCs of HLA-A*02:01 in the absence (day eight, red) and presence of $CD16^{+}CD56^{+}$ NK cells (day ten, blue). Differences between cytokine and chemokine release upon encountering the two viral strains were calculated, dividing the fold differences of cytokine and chemokine release upon infection with ADA_L210F by the fold differences of cytokine and chemokine release upon infection with ADA_V82A.

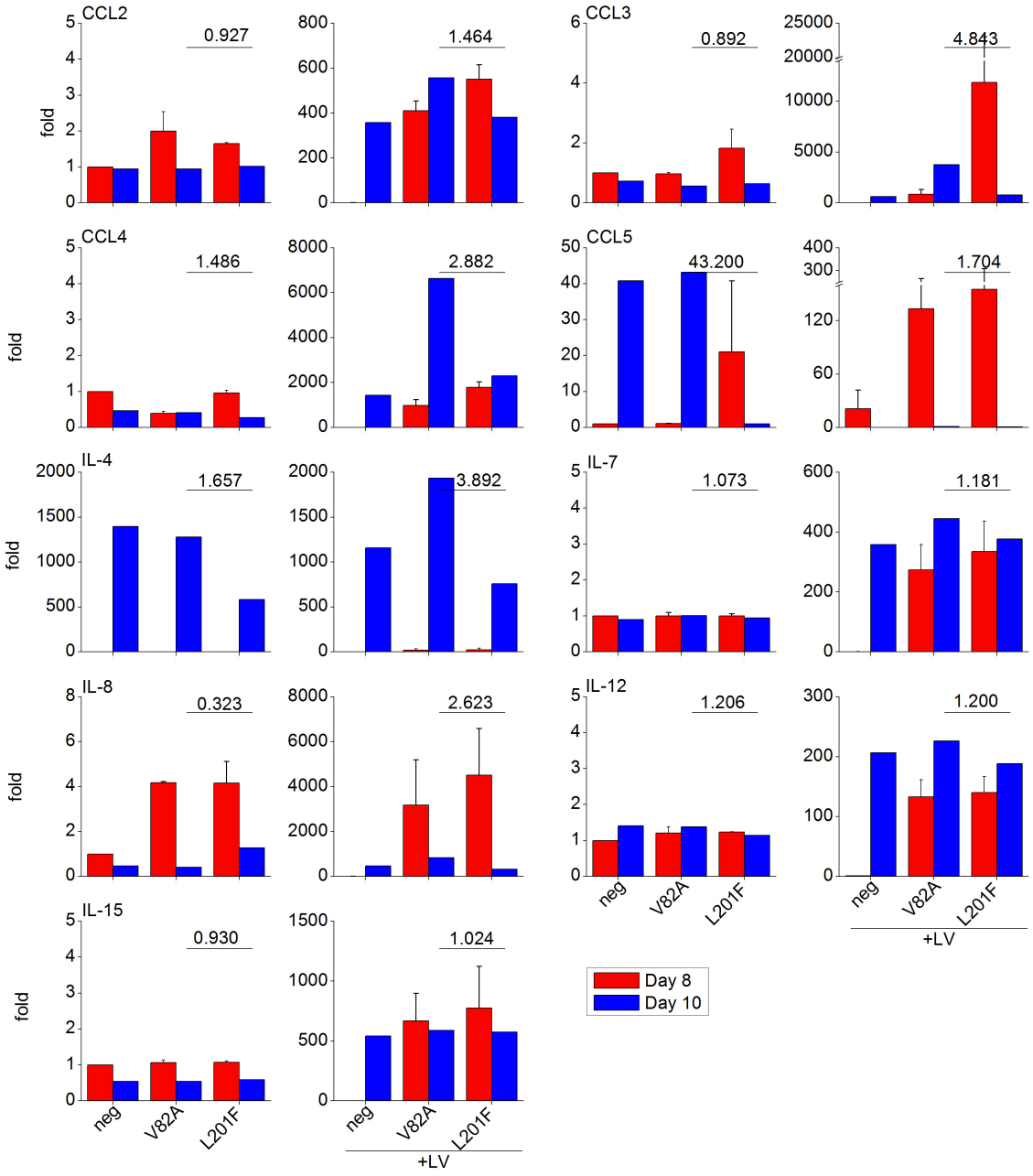

Figure 4.24 Fold difference in cytokine and chemokine release normalized to untransduced uninfected moDCs and transduced uninfected moDCs of HLA-B*44:03 in the absence (day eight, red) and presence of $CD16^{+}CD56^{+}$ NK cells (day ten, blue). Differences between cytokine and chemokine release upon encountering the two viral strains were calculated, dividing the fold differences of cytokine and chemokine release upon infection with ADA_V82A by the fold differences of cytokine and chemokine release upon infection with ADA_L210F.

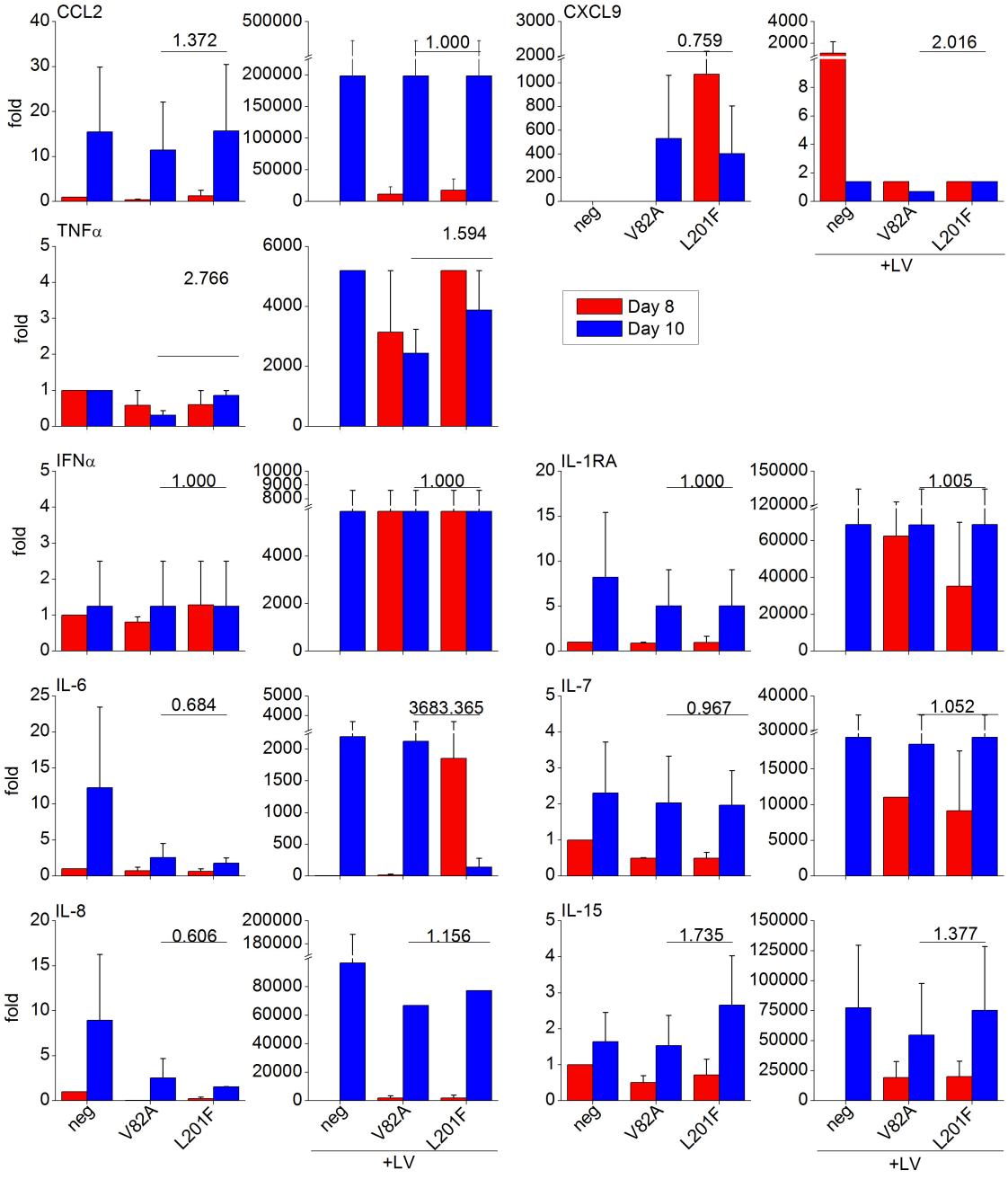

Figure 4.25 Fold difference in cytokine and chemokine release normalized to untransduced uninfected moDCs and transduced uninfected moDCs of HLA-A*02:01 in the absence (day eight, red) and presence of $CD8^+$ T cells (day ten, blue). Differences between cytokine and chemokine release upon encountering the two viral strains were calculated, dividing the fold differences of cytokine and chemokine release upon infection with ADA_L210F by the fold differences of cytokine and chemokine release upon infection with ADA_V82A.

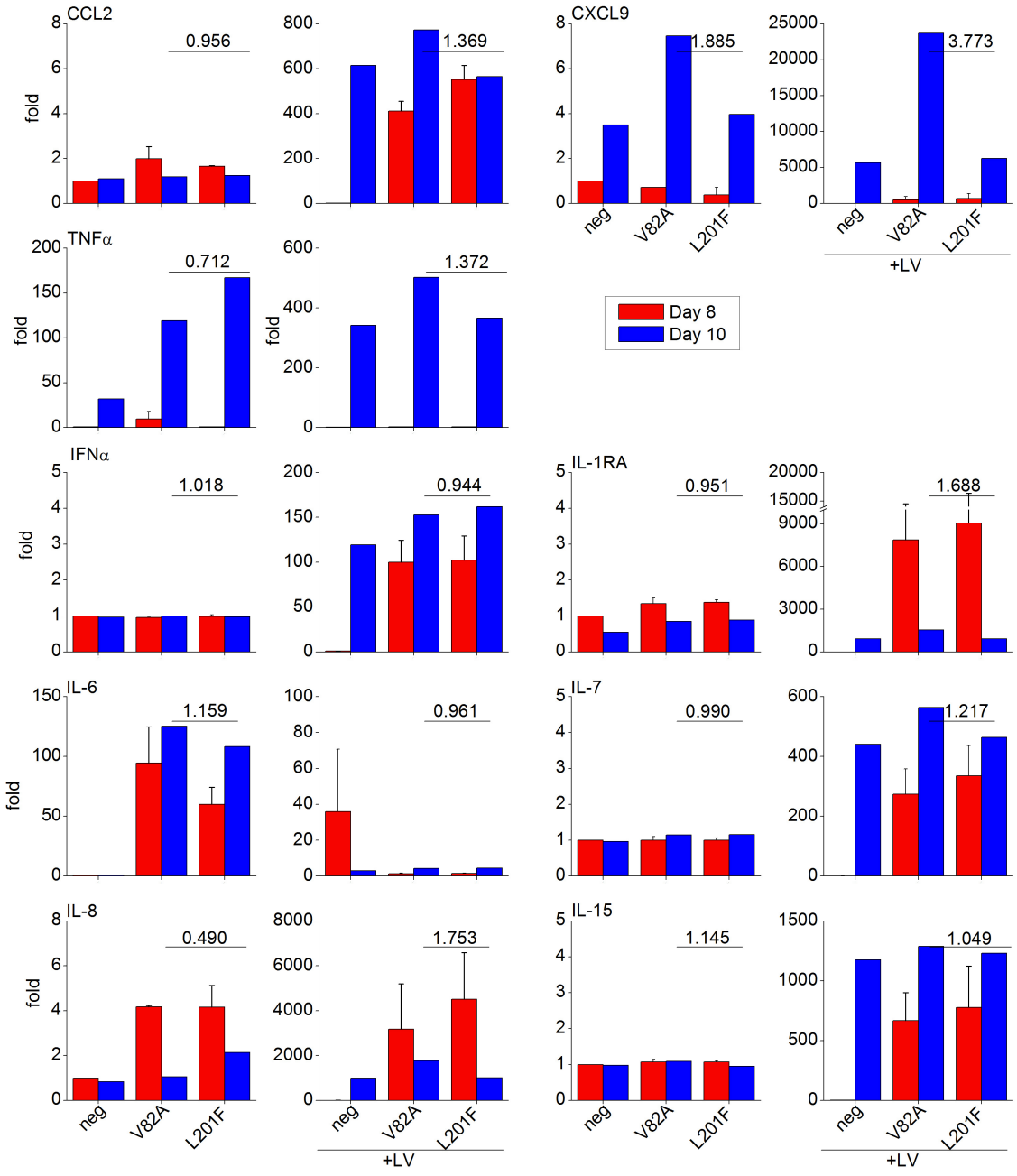

Figure 4.26 Fold difference in cytokine and chemokine release normalized to untransduced uninfected moDCs and transduced uninfected moDCs of HLA-A*02:01 in the absence (day eight, red) and presence of $CD8^+$ T cells (day ten, blue). Differences between cytokine and chemokine release upon encountering the two viral strains were calculated, dividing the fold differences of cytokine and chemokine release upon infection with ADA_V82A by the fold differences of cytokine and chemokine release upon infection with ADA_L210F.

In summary, co-cultures of moDCs and $CD16^+CD56^+$ NK cells showed a differential secretion of IL-4, IL-7, IL-8, IL-15 and CCL4. While, the levels of IL-4, IL-7 and CCL4 is decreased in HLA-A*02:01 positive donors with an introduced HLA-B*44:03 upon infection with HIV-1 ADA_L210F, the secretion of IL-4, IL-7 and CCL4 is increased in HLA-B*44:03 positive donors with an introduced HLA-A*02:01 upon infection with HIV-1 ADA_V82A. The secretion of IL-15 and IL-8 is decreased in the two above described settings, pointing to a possible involvement of V82A (PR) and L210F (RT) in their respective HLA-background, in immune escape. Co-cultures of moDCs and $CD8^+$ T cells showed a differential secretion of IL-7, IL-8 and CXCL9. CXCL9 is decreased in HLA-A*02:01 positive donors with an introduced HLA-B*44:03 upon infection with HIV-1 ADA_L210F and increased in HLA-B*44:03 positive donors with an introduced HLA-A*02:01 upon infection with HIV-1 ADA_V82A. In contrast, the secretion of IL-7 and IL-8 is decreased in the two above described settings and again could be involved in an immune escape.

Therefore, investigating immune escape, a reduction in the secretion of IL-7, IL-8 and IL-15 seems to be of importance.

5. Discussion

The initiation and selection of treatment for therapy-naïve patients is based on several aspects. There are not only HIV-1 plasma viral load (pVL) and $CD4^+$ T cell count to consider but also personal issues, like co-morbidities and likelihood of adherence. This work focuses on the consideration of the patients' HLA-alleles for therapy selection.

The host immune system is an important factor in the selection of mutations, causing the virus to adapt to the HLA type of the infected individual. The persistence of these mutations in a new host after transmission is influenced by the HLA alleles of the new host. If the relevant HLA allele, responsible for the selection of the mutation, is shared by donor and recipient, a reversion may not occur [157]. In general, mutations persist when they do not cause high viral fitness costs, because even minor enhancements in fitness can quickly lead to the replacement of less fit variants. Eventually high fitness costs can be overcome by additional compensatory mutations. Otherwise the reversion to the wild type sequence is most likely [158-162]. Several studies propose an adaptation of HIV-1 to common HLA alleles even on population level. These commonly found HLA alleles can shape the virus, leaving a genetic footprint of immune response, which could even influence the virus evolution leading to the replacement of the consensus sequence [133, 158, 162].

Mutations which are associated with resistances against certain drugs can possibly be located within HLA class I restricted epitopes. They can positively or negatively influence immunogenicity by hampering the binding of viral peptides to the restricting HLA class I allele, changing T cell recognition sites or altering peptide processing by the cellular proteasome [130-140]. This can possibly explain the persistence of transmitted drug resistance mutations (tRAMs) within the drug-free environment of about 10 % of the therapy-naïve patients of the RESINA study cohort.

A standard antiretroviral therapy without the consideration of HLA-allele mediated immune selection could include antiretroviral drugs that would promote a therapy failure by providing a selective pressure for tRAMs, conferring not only resistance to the drug but also immune escape. The consideration of the host immune response is especially important in the treatment of therapy-naïve patients already harbouring tRAMs. In these patients the treatment should be optimized using all available information regarding virus and host to facilitate a long lasting therapy success.

In order to identify the direct clinical impact of tRAMs and the individual HLA type on the antiretroviral regimen and therefore therapy outcome and progression of disease, a cell culture model was established.

This model allowed the study of immune function in the context of the whole viral particle and defined HLA alleles, independent of patient samples but still close to the in vivo environment. Previous work [163, 164] was based on ELISPOT (enzyme linked immuno spot) assays which however hold several disadvantages. ELISPOT assays depend on patients' blood samples which contain depending on the status of HIV-1 infection, very low cell numbers. Assays could occasionally not be evaluated. In addition, ELISPOT assays were based on PBMCs, making it impossible to observe the behaviour of single cell types. Consequently, in the cell culture model established in this work, distinct cell types were purified before their use in culture. The stimulation of PBMCs in ELISPOT assays was accomplished using several peptides comprising viral epitopes, allowing the study of presentation and recognition of viral peptides only. In the cell culture model, the use of whole viral particles, however, allowed the study of the influence of mutations on peptide processing by the cellular proteasome. IFN-γ was the only marker evaluated in ELISPOT assays. Nevertheless, literature suggests the involvement of several cytokines and chemokines in the innate and adaptive immune responses of HIV-1 infected patients [165-167].

To understand a possible association of cytokine / chemokine secretion and HIV-1 infection, a cohort of patients with low (therapy-experienced) and high pVL (therapy-naïve) was chosen to analyze cytokine and chemokine levels. Herefore the luminex assay was used, which is a high throughput method, facilitating the analysis of 25 different cytokines and chemokines from each sample. Levels of IL-2R, IL-12, CCL2, CCL11, CXCL9 and CXCL10 were significantly elevated in patients with high pVL, while levels of IL-1β, IL-1RA, IL-2R, IL-4, IL-8, IL-13, IL-15, IL-17 compared to healthy individuals and TNF-α were significantly lower in patients with low pVL. Unfortunately, detected levels of IFN-γ were out of the upper limit of detection. Published data investigating cytokine and chemokine secretion usually do not distinguish between different pVL of HIV-1 infected patients, but rather aim at the identification of cytokines and chemokines, which are associated with early HIV-1 infections or a progression of disease. Nevertheless, in early HIV-1 infection and during disease progression, HIV-1 infected patients show most likely high pVL. Literature data can, therefore, be compared to cytokine and chemokine secretion in

patients with high pVL of the here described cohort. Byrnes et al. described increased levels of IL-12 in early HIV-1 infection [168], whereas associations of IL-2R [169, 170], CCL2 [171], CXCL9 and CXCL10 [172, 173] with disease progression have been published.

The previous work, based on ELISPOT assays and the investigation of the secretion of cytokines and chemokines in HIV-1 infected patients, guided to the development of the here established cell culture model.

Starting with the assessment of significant associations between HLA class I alleles and HIV-1 tRAMs, possible immune escape mutants among tRAMs were identified. In total, nine associations were significant after correction for multiple testing. Of those nine associations, V82A (PR) which was in this study highly significantly associated with HLA-A*02:01, has also been found of significant high prevalence in the background of HLA-A*02:01 in another study, investigating 492 treated patients [174]. It is usually difficult to compare data of association studies between different patient cohorts, due to strong differences in the genetic background of patients. Even comparing associations found in this study and a patient cohort in Erlangen, Germany was not fully successful [175].

The in silico obtained results were used as the basis for the cell culture model: HLA alleles of interest (HLA-A*02:01 and HLA-B*44:03) were over-expressed on monocyte-derived DCs (moDCs), representing the most important antigen presenting cell type [176, 177]. A VSV-G-pseudotyped lentiviral vector system was chosen to ensure (1) the delivery of the gene of interest independent of receptor interaction and (2) a stable integration and expression of the gene of interest in these non-dividing cells. Lentiviral vectors were generated, carrying the two different HLA ORFs of interest, aiming at their delivery into moDCs to generate recombinant moDCs. These recombinant moDCs were later on infected with HIV-1 carrying tRAMs in RT and PR (V82A (PR) and L210F (RT)) to determine changes in immunogenicity. Immunogenicity was here investigated by observing changes in cytokine and chemokine release in the co-cultures of $CD16^+CD56^+$ NK cells or $CD8^+$ T cells and recombinant moDCs.

Several methods have been described to deliver genes into target cells. The transfection of $CD14^+$ monocytes using naked DNA has not been described. Instead, introducing genes into target cells using viruses as carrier are common [147, 178-180]. Here, target cells were $CD14^+$ monocytes, which are non-dividing cells,

requiring the integration of the HLA ORF using lentiviral vectors. Lentiviral vectors have the ability to integrate their genome into non-dividing cells. The viral genome, including the gene of interest, in form of RNA is reverse-transcribed, when entering the target cells [147]. Proviral DNA is then inserted into the cellular genome at a random position, having the disadvantage that the site of integration is unpredictable and function of cellular genes could be impaired [181, 182].

Lentiviral vectors were pseudotyped with VSV-G to enable a transduction of $CD14^+$ monocytes via endocytosis. In general, pseudotyping with VSV-G has the advantages to interact with a ubiquitous receptor on cells, giving the vector a broad host-cell range and in addition ensures lentiviral vector stability [183].

The aim of this study included the generation of immature recombinant moDCs over-expressing HLA alleles of interest, which were able to process and present HIV-1 peptides on their cell surface. For this purpose, $CD14^+$ monocytes were transduced with lentiviral vectors, at a preferred MOI (multiplicity of infection) of 1.5 to have a relatively high transduction efficacy, but at the same time, not causing maturation of $CD14^+$ monocytes. Immature moDCs are specialized for antigen uptake, but can, upon appropriate stimuli, terminally differentiate into mature moDCs. Mature moDCs are enrolled in T cell recruitment [178]. Breckpot et al. described a percentage of transduced moDCs of 32.3 ± 11.8 % at a MOI of 1.5. Transduction at MOIs of 15 and 150 increased transduction efficacies to 80.3 ± 11.5 % and 93.0 ± 2.8 %, but at the same time increased the expression of surface markers CD25, CD80, CD83, CD86, HLA class I and II [180]. However, in this study, the maturation status of moDCs was not followed investigating the expression of cell surface markers, due to small cell numbers. Instead, the release of cytokines and chemokines was determined in response to LV-transduction. Higher levels of the cytokines IL-1RA, IL-6, IL-12 and the chemokine CCL5 could be detected in LV-transduced cells. Nevertheless, this elevation was not significant and needs to be further evaluated.

In addition, the influence of HIV-1 ADA infection of moDCs on cytokine and chemokine secretion was investigated. For the release of several cytokines and chemokines no differences could be observed between uninfected and HIV-1 ADA infected moDCs. This finding is in accordance with literature, HIV-1 does not cause maturation of moDCs [178].

These results lead to the conclusion that neither LV-transduction, nor the infection with HIV-1 seemed to have a significant impact on viability and cytokine and

chemokine secretion of moDCs. Investigating co-cultures of moDCs with either $CD16^+CD56^+$ NK cells or $CD8^+$ T cells, cell morphologies showed that co-cultures rapidly accumulated high numbers of dead cells. Quantification of dead cells in both co-cultures staining with propidium iodide, revealed a significantly higher percentage in co-cultures with $CD16^+CD56^+$ NK cells than with $CD8^+$ T cells. This suggests a more rapid response of $CD16^+CD56^+$ NK cells than by $CD8^+$ T cells upon encountering moDCs. $CD16^+CD56^+$ NK cells are highly cytotoxic and play a major role in the innate immune response and they provide rapid responses to viral infection [184, 185] Activation of these cells does not necessarily require activating signals, but is also executed by missing self-antigens caused by a down-regulation of HLA class I molecules [186, 187]. In contrast, $CD8^+$ T cells form part of the adaptive immune response, but can also induce the cell death of virally infected cells [160, 188]. Activation of $CD8^+$ T cells is dependent on two separate signals the antigen, which is bound to HLA class I molecules, and a secondary signal that can be either CD80 or CD86 [189]. There are several ways to induce cell death of virally infected cells by $CD16^+CD56^+$ NK and $CD8^+$ T cells. The best known mechanisms are the secretion of cytotoxins such as perforin and granzyme and the engagement of death receptors (CD95 / CD95 ligand) [111, 190, 191]. However, these mechanisms require cell to cell interactions of HIV-1 infected moDCs and $CD16^+CD56^+$ NK cells or $CD8^+$ T cells. This can be facilitated by the secretion of cytokines and chemokines.

An impairment of the secretion of cytokines and chemokines is most likely involved in immune escape mechanisms [192]. In this study, the impact of the putative immune escape mutation V82A (PR) in the background of HLA-A*02:01 on cytokine and chemokine secretion was evaluated and compared to cytokine and chemokine levels detected investigating the already described immune escape variant L210F (RT) in the background of HLA-B*44:03. Co-cultures of $CD16^+CD56^+$ NK cells or $CD8^+$ T cells with moDCs infected with HIV-1 ADA_V82A and ADA_L210F, respectively, were analyzed for cytokine and chemokine secretion. An impairment of such secretion was detected for the cytokines IL-7, IL-8 and IL-15, which could be associated with immune escape. The infection with the viral strain, comprising the putative immune escape mutation V82A (PR) in the respective HLA background, led to similarly decreased levels of these three cytokines compared to L210F (RT). While levels of cytokine IL-8 were decreased within co-cultures of moDCs with $CD16^+CD56^+$ NK cells and $CD8^+$ T cells, decreased levels of IL-7 could only be

detected in co-cultures with $CD8^+$ T cells and decreased levels of IL-15 in co-cultures with $CD16^+CD56^+$ NK cells.

IL-8 has been described to be enhanced in the peripheral blood and lymphoid tissue of HIV-1 infected patients, indicating an importance of this cytokine in disease [193]. It is an important pro-inflammatory cytokine with chemoattractant functions and can be secreted by a variety of cells, inducing not only the migration of neutrophils but also causing the respiratory burst [194]. In this study, patients with high pVL (therapy-naïve) show high levels of IL-8 compared to healthy controls. Elevated plasma levels of pro-inflammatory cytokines, such as the here described IL-8 can be detected in untreated, chronic HIV-1 infections and are accompanied by an increase of virus transcription and possibly also the activation of transcription from latently infected cells [195]. Investigating HIV-1 infected patients with low (therapy-experienced) pVL, levels of IL-8 were significantly lower compared to healthy controls. In literature the impact of treatment on immune activation and thereby on cytokine and chemokine release is discussed controversially. While for some cytokines and chemokines a significant reduction of release below levels in healthy controls was described, levels of the same cytokine / chemokine remain above or are equal in patients under treatment compared to healthy controls in other studies including this work [171, 196]. Nevertheless, an overall reduction of the overwhelming immune activation has been shown to be related to decreased pVL achieved by antiretroviral treatment, indicating a correlation between cytokine and chemokine secretion and pVL [171, 197]. Not only IL-8 has been described to be elevated in HIV-1 infected patients, also IL-7 levels have been found to be increased [198]. IL-7 is a cytokine involved in the homeostasis of T cells, playing a role in the development, function, proliferation, and survival of $CD8^+$ T cells [199]. It can be produced not only by dendritic cells, but also by lymphocytes and its disrupted signalling has been shown to result in impaired immunity [200]. In this study, infected patients with low pVL showed lower levels of IL-7 compared to healthy controls. In contrast, patients with high pVL showed high levels of IL-7. IL-15 has been found to be associated with viremia in primary HIV-1 infection, with a rapid elevation in plasma levels [201]. It is a specific maturation factor for NK cells and can function as a NK cell survival factor [202]. In this study, investigating HIV-1 infected patients with low and high pVL, levels of IL-15 were significantly lower in patients with low pVL compared to healthy controls. In contrast, patients with high pVL showed high levels of IL-15.

In conclusion, the results of this study suggest that monitoring levels of IL-7, IL-8 and IL-15 could be beneficial investigating the activation of immune responses with respect to HIV-1 immune escape mutations.

Analyzing the influence of the so far not investigated putative immune escape mutations associated with different HLA alleles could strengthen the role of IL-7, IL-8 and IL-15 as potential biomarkers. Another interesting aspect to proof the role of IL-7, IL-8 and IL-15 as biomarkers would be translating findings back into patients. Plasma samples deriving from patients with relatively high pVL could be analyzed for a decrease in the secretion of IL-7, IL-8 and IL-15 indicating a putative immune escape in the restricting HLA background.

6. Abstract

Understanding host-specific innate and adaptive immune responses in therapy-naïve HIV-1 infected patients is of high importance. In a drug-free environment, the immune system is the most dominant factor shaping the evolution of HIV-1. Mutations can be selected, causing the adaption of the virus to the HLA alleles of the infected individuals, negatively influencing the immunogenicity of epitopes. However, in treatment-experienced patients, the most dominant factors influencing viral evolution are antiretroviral drugs. As a consequence, drug resistance associated mutations (RAMs) within targeted HIV-1 proteins can evolve which can be transmitted (tRAMs) from one individual to another, resulting in the finding of 10 % of persisting tRAMs in therapy-naïve patients. It is assumed, that such a persistence of tRAMs in therapy-naïve patients is influenced by the HLA alleles of the new host and that persisting tRAMs are most likely located within HLA class I restricted epitopes, leading to immune escape.

Interactions of immune system and antiretroviral treatment could especially be important in the treatment of therapy-naïve patients already harbouring tRAMs. The consideration of HLA allele mediated immune selection could exclude antiretroviral drugs promoting a therapy failure by providing a selective pressure for tRAMs conferring not only resistance to the drug but also immune escape. Treatment could be optimized using all available information regarding virus and host to facilitate a long lasting therapy success.

In this work, a statistical analysis was performed using Fishers exact test and correcting for multiple testing, identifying nine significant associations between protease inhibitor (PI), nucleoside reverse transcriptase inhibitor, non-nucleoside reverse transcriptase inhibitor tRAMs, found in a cohort of 139 therapy-naïve HIV-1 infected patients and the patients' HLA alleles.

This statistical analysis was used as the basis to establish a cell culture model to identify a direct impact of tRAMs on host-specific innate and adaptive immune responses in the background of certain HLA types. Immature monocyte-derived dendritic cells (moDCs), the most important antigen presenting cells, were transduced using lentiviral vectors to introduce HLA alleles of interest (here: HLA-A*02:01 and HLA-B*44:03). Subsequently, these moDCs were infected with HIV-1 ADA_V82A and ADA_L210F, respectively while ADA_V82A included the possible immune escape mutant V82A (protease), which is at the same time associated with

PI resistance, ADA_L210F carried the already described immune escape mutation L210F. In order to study the impact on both, the innate as well as the adaptive immune system, infected recombinant moDCs were co-cultured with either $CD16^+CD56^+$ NK cells or $CD8^+$ T cells. For the screening of characteristic cytokines and/or chemokines a human 25-plex luminex assay was used. While the secretion of IL-7 is decreased in co-cultures with $CD8^+$ T cells, levels of IL-15 are comparably low in co-cultures with $CD16^+CD56^+$ NK cells. The secretion of IL-8 is decreased in co-cultures with both, $CD16^+CD56^+$ NK cells and $CD8^+$ T cells, upon encountering the putative immune escape mutation in the background of the restricting HLA allele.

These data identified IL-7, IL-8 and IL-15 as putative biomarkers monitoring immune activation regarding immune escape. However, more research has to be done to strengthen the role of IL-7, IL-8 and IL-15.

7. Zusammenfassung

Bei therapienaiven HIV-1-Patienten ist das Verständnis der wirtsspezifischen angeborenen und adaptiven Immunantwort von großer Bedeutung. Bei diesen Patienten ist das Immunsystem der dominierende Faktor, der durch die Selektion von Mutationen eine Anpassung des Virus an die HLA-Allele des Wirts beeinflusst. Hierbei kann die Immunogenität von Epitopen negativ beeinflusst werden. Bei therapieerfahrenen Patienten hingegen steuern antiretrovirale Wirkstoffe die virale Evolution. In HIV-1 können sich so resistenzassoziierte Mutationen (RAMs) entwickeln und im Zuge einer Transmission weitergegeben werden. Dieses führt dazu, dass in ca. 10 % der therapienaiven Patienten persistierende, übertragene RAMs gefunden werden. Höchstwahrscheinlich wird die Persistenz von übertragenen RAMs durch die HLA-Allele des neuen therapienaiven Wirts beeinflusst. Möglicherweise befinden sich diese übertragenen RAMs innerhalb von HLA Klasse I restringierten Epitopen und ermöglichen einen Immunescape. Wechselwirkung zwischen Immunsystem und antiretroviraler Therapie könnte dadurch, besonders bei der Wahl der Erst-Therapie der therapienaiven Patienten mit übertragenen RAMs, eine wichtige Rolle spielen. Eine Therapie sollte antiretrovirale Wirkstoffe ausschließen, die unter Berücksichtigung der HLA-Allele der verschiedenen Patienten, RAMs selektieren, die gleichzeitig einen Immunescape bewirken.

Mit Hilfe einer statistischen Analyse wurden hier, unter Verwendung des Exakten Fisher-Tests und einer Korrektur für multiple Teste, wurden neun signifikante Assoziationen zwischen übertragenen Protease-Inhibitor- (PI-), Nukleosid-Reverse-Transkriptase-Inhibitor-, Nicht-Nukleosid-Reverse-Transkriptase-Inhibitor-RAMs und den HLA-Allelen von 139 therapienaiven Patienten identifiziert. Die Ergebnisse dieser statistischen Analyse wurde als Grundlage für die Etablierung eines Zellkulturmodels genutzt, mit dem der direkte Einfluss von übertragenen RAMs auf die wirtsspezifische angeborene und adaptive Immunantwort untersucht werden kann. In diesem Zellkulturmodel wurden unreife dendritische Zellen (DC), welche die wichtigsten antigen-präsentierenden Zellen darstellen, mit Hilfe von lentiviralen Vektoren transduziert, um eine Überexpression von bestimmten HLA-Allelen (hier: HLA-A*02:01 und HLA-B*44:03) zu bewirken. Anschließend wurden diese DC mit HIV-1 ADA_V82A und ADA_L210F infiziert. Während ADA_V82A die mögliche Immunescape Mutante enthielt V82A, welche zusätzlich mit einer PI-Resistenz assoziiert ist, trug ADA_L210F die bereits beschriebene Immunescape Mutation:

L210F (RT). Um die Auswirkungen des angeborenen und des adaptiven Immunsystems auf diese infizierten DC zu untersuchen, wurden diese entweder mit $CD16^+CD56^+$ NK-Zellen oder mit $CD8^+$ T-Zellen kokultiviert. Das humane 25-plex Luminex Assay unterstützte das Screening nach charakteristischen Zytokinen und/oder Chemokinen, die in diesen Kokulturen sekretiert wurden. Während sich die verminderte Sekretion von IL-7 in Kokulturen mit $CD8^+$ T-Zellen als charakteristisch herauskristallisierte, wurde eine Reduktion von IL-15 in Kokulturen mit $CD16^+$ $CD56^+$ NK-Zellen beobachtet. In beiden Kokulturen stellte sich IL-8 als mutmaßlicher Marker eines Immunescapes unter Berücksichtigung des entsprechenden HLA-Allels heraus. Zusammenfassend deutet vieles darauf hin, IL-7, IL-8 und IL-15 als mögliche Biomarker zur Überwachung der Immunaktivierung heranzuziehen. Jedoch sollte das Zellkulturmodel genutzt werden, um weitere Immunescape Mutationen zu analysieren, und so die Rolle von IL-7, IL-8 und IL-15 als mögliche Biomarker zu verifizieren.

8. References

1. Barre-Sinoussi F, Chermann JC, Rey F, Nugeyre MT, Chamaret S, Gruest J, Dauguet C, Axler-Blin C, Vezinet-Brun F, Rouzioux C, et al: **Isolation of a T-lymphotropic retrovirus from a patient at risk for acquired immune deficiency syndrome (AIDS).** *Science* 1983, **220:**868-871.
2. Gallo RC, Salahuddin SZ, Popovic M, Shearer GM, Kaplan M, Haynes BF, Palker TJ, Redfield R, Oleske J, Safai B, et al.: **Frequent detection and isolation of cytopathic retroviruses (HTLV-III) from patients with AIDS and at risk for AIDS.** *Science* 1984, **224:**500-503.
3. Frankel AD, Young JA: **HIV-1: fifteen proteins and an RNA.** *Annu Rev Biochem* 1998, **67:**1-25.
4. Gifford R, Tristem M: **The evolution, distribution and diversity of endogenous retroviruses.** *Virus Genes* 2003, **26:**291-315.
5. Louwagie J, McCutchan FE, Peeters M, Brennan TP, Sanders-Buell E, Eddy GA, van der Groen G, Fransen K, Gershy-Damet GM, Deleys R, et al.: **Phylogenetic analysis of gag genes from 70 international HIV-1 isolates provides evidence for multiple genotypes.** *AIDS* 1993, **7:**769-780.
6. Grez M, Dietrich U, Balfe P, von Briesen H, Maniar JK, Mahambre G, Delwart EL, Mullins JI, Rubsamen-Waigmann H: **Genetic analysis of human immunodeficiency virus type 1 and 2 (HIV-1 and HIV-2) mixed infections in India reveals a recent spread of HIV-1 and HIV-2 from a single ancestor for each of these viruses.** *J Virol* 1994, **68:**2161-2168.
7. Gurtler LG, Zekeng L, Tsague JM, van Brunn A, Afane Ze E, Eberle J, Kaptue L: **HIV-1 subtype O: epidemiology, pathogenesis, diagnosis, and perspectives of the evolution of HIV.** *Arch Virol Suppl* 1996, **11:**195-202.
8. Wainberg MA: **HIV-1 subtype distribution and the problem of drug resistance.** *AIDS* 2004, **18 Suppl 3:**S63-68.
9. Stebbing J, Moyle G: **The clades of HIV: their origins and clinical significance.** *AIDS Rev* 2003, **5:**205-213.
10. Gelderblom HR, Hausmann EH, Ozel M, Pauli G, Koch MA: **Fine structure of human immunodeficiency virus (HIV) and immunolocalization of structural proteins.** *Virology* 1987, **156:**171-176.
11. Paillart JC, Skripkin E, Ehresmann B, Ehresmann C, Marquet R: **A loop-loop "kissing" complex is the essential part of the dimer linkage of genomic HIV-1 RNA.** *Proc Natl Acad Sci U S A* 1996, **93:**5572-5577.
12. Welker R, Hohenberg H, Tessmer U, Huckhagel C, Krausslich HG: **Biochemical and structural analysis of isolated mature cores of human immunodeficiency virus type 1.** *J Virol* 2000, **74:**1168-1177.
13. Mulky A, Sarafianos SG, Arnold E, Wu X, Kappes JC: **Subunit-specific analysis of the human immunodeficiency virus type 1 reverse transcriptase in vivo.** *J Virol* 2004, **78:**7089-7096.
14. Hizi A, McGill C, Hughes SH: **Expression of soluble, enzymatically active, human immunodeficiency virus reverse transcriptase in Escherichia coli and analysis of mutants.** *Proc Natl Acad Sci U S A* 1988, **85:**1218-1222.
15. Prasad VR, Goff SP: **Linker insertion mutagenesis of the human immunodeficiency virus reverse transcriptase expressed in bacteria: definition of the minimal polymerase domain.** *Proc Natl Acad Sci U S A* 1989, **86:**3104-3108.
16. von der Helm K: **Retroviral proteases: structure, function and inhibition from a non-anticipated viral enzyme to the target of a most promising HIV therapy.** *Biol Chem* 1996, **377:**765-774.
17. Wlodawer A, Erickson JW: **Structure-based inhibitors of HIV-1 protease.** *Annu Rev Biochem* 1993, **62:**543-585.
18. Vink C, Plasterk RH: **The human immunodeficiency virus integrase protein.** *Trends Genet* 1993, **9:**433-438.
19. Krishnan L, Engelman A: **Retroviral integrase proteins and HIV-1 DNA integration.** *J Biol Chem* 2012, **287:**40858-40866.
20. Gelderblom HR: **Assembly and morphology of HIV: potential effect of structure on viral function.** *AIDS* 1991, **5:**617-637.
21. Dressler S: *HIV/AIDS Taschenlexikon.* Berlin; 2008.
22. **EEB Web Site** [http://www.yale.edu/bio243/HIV/genome.html]

23. Deng H, Liu R, Ellmeier W, Choe S, Unutmaz D, Burkhart M, Di Marzio P, Marmon S, Sutton RE, Hill CM, et al: **Identification of a major co-receptor for primary isolates of HIV-1.** *Nature* 1996, **381:**661-666.
24. Doranz BJ, Rucker J, Yi Y, Smyth RJ, Samson M, Peiper SC, Parmentier M, Collman RG, Doms RW: **A dual-tropic primary HIV-1 isolate that uses fusin and the beta-chemokine receptors CKR-5, CKR-3, and CKR-2b as fusion cofactors.** *Cell* 1996, **85:**1149-1158.
25. Alkhatib G, Combadiere C, Broder CC, Feng Y, Kennedy PE, Murphy PM, Berger EA: **CC CKR5: a RANTES, MIP-1alpha, MIP-1beta receptor as a fusion cofactor for macrophage-tropic HIV-1.** *Science* 1996, **272:**1955-1958.
26. Dejucq N: **HIV-1 replication in CD4+ T cell lines: the effects of adaptation on co-receptor use, tropism, and accessory gene function.** *J Leukoc Biol* 2000, **68:**331-337.
27. Chan DC, Kim PS: **HIV entry and its inhibition.** *Cell* 1998, **93:**681-684.
28. Zheng YH, Lovsin N, Peterlin BM: **Newly identified host factors modulate HIV replication.** *Immunol Lett* 2005, **97:**225-234.
29. Whitcomb JM, Hughes SH: **Retroviral reverse transcription and integration: progress and problems.** *Annu Rev Cell Biol* 1992, **8:**275-306.
30. Pollard VW, Malim MH: **The HIV-1 Rev protein.** *Annu Rev Microbiol* 1998, **52:**491-532.
31. Kaplan AH, Manchester M, Swanstrom R: **The activity of the protease of human immunodeficiency virus type 1 is initiated at the membrane of infected cells before the release of viral proteins and is required for release to occur with maximum efficiency.** *J Virol* 1994, **68:**6782-6786.
32. Weiss RA: **Gulliver's travels in HIVland.** *Nature* 2001, **410:**963-967.
33. Marcos Y, Phelps BR, Bachman G: **Community strategies that improve care and retention along the prevention of mother-to-child transmission of HIV cascade: a review.** *J Int AIDS Soc* 2012, **15 Suppl 2:**17394.
34. Keele BF, Estes JD: **Barriers to mucosal transmission of immunodeficiency viruses.** *Blood* 2011, **118:**839-846.
35. Goniewicz M, Wloszczak-Szubzda A, Niemcewicz M, Witt M, Marciniak-Niemcewicz A, Jarosz MJ: **Injuries caused by sharp instruments among healthcare workers--international and Polish perspectives.** *Ann Agric Environ Med* 2012, **19:**523-527.
36. Martin N, Welsch S, Jolly C, Briggs JA, Vaux D, Sattentau QJ: **Virological synapse-mediated spread of human immunodeficiency virus type 1 between T cells is sensitive to entry inhibition.** *J Virol* 2010, **84:**3516-3527.
37. Koppensteiner H, Banning C, Schneider C, Hohenberg H, Schindler M: **Macrophage internal HIV-1 is protected from neutralizing antibodies.** *J Virol* 2012, **86:**2826-2836.
38. Coleman CM, Gelais CS, Wu L: **Cellular and viral mechanisms of HIV-1 transmission mediated by dendritic cells.** *Adv Exp Med Biol* 2013, **762:**109-130.
39. de Witte L, Nabatov A, Pion M, Fluitsma D, de Jong MA, de Gruijl T, Piguet V, van Kooyk Y, Geijtenbeek TB: **Langerin is a natural barrier to HIV-1 transmission by Langerhans cells.** *Nat Med* 2007, **13:**367-371.
40. Thacker TC, Zhou X, Estes JD, Jiang Y, Keele BF, Elton TS, Burton GF: **Follicular dendritic cells and human immunodeficiency virus type 1 transcription in CD4+ T cells.** *J Virol* 2009, **83:**150-158.
41. Fox CH, Tenner-Racz K, Racz P, Firpo A, Pizzo PA, Fauci AS: **Lymphoid germinal centers are reservoirs of human immunodeficiency virus type 1 RNA.** *J Infect Dis* 1991, **164:**1051-1057.
42. Piatak M, Jr., Saag MS, Yang LC, Clark SJ, Kappes JC, Luk KC, Hahn BH, Shaw GM, Lifson JD: **High levels of HIV-1 in plasma during all stages of infection determined by competitive PCR.** *Science* 1993, **259:**1749-1754.
43. Ogg GS, Jin X, Bonhoeffer S, Dunbar PR, Nowak MA, Monard S, Segal JP, Cao Y, Rowland-Jones SL, Cerundolo V, et al: **Quantitation of HIV-1-specific cytotoxic T lymphocytes and plasma load of viral RNA.** *Science* 1998, **279:**2103-2106.
44. McMichael AJ, Rowland-Jones SL: **Cellular immune responses to HIV.** *Nature* 2001, **410:**980-987.
45. Chun TW, Carruth L, Finzi D, Shen X, DiGiuseppe JA, Taylor H, Hermankova M, Chadwick K, Margolick J, Quinn TC, et al: **Quantification of latent tissue reservoirs and total body viral load in HIV-1 infection.** *Nature* 1997, **387:**183-188.
46. Hecht FM, Wellman R, Busch MP, Pilcher CD, Norris PJ, Margolick JB, Collier AC, Little SJ, Markowitz M, Routy JP, Holte S: **Identifying the early post-HIV antibody seroconversion period.** *J Infect Dis* 2011, **204:**526-533.

47. Ho DD, Neumann AU, Perelson AS, Chen W, Leonard JM, Markowitz M: **Rapid turnover of plasma virions and CD4 lymphocytes in HIV-1 infection.** *Nature* 1995, **373:**123-126.
48. Jaworowski A, Crowe SM: **Does HIV cause depletion of CD4+ T cells in vivo by the induction of apoptosis?** *Immunol Cell Biol* 1999, **77:**90-98.
49. Vergis EN, Mellors JW: **Natural history of HIV-1 infection.** *Infect Dis Clin North Am* 2000, **14:**809-825, v-vi.
50. Munier ML, Kelleher AD: **Acutely dysregulated, chronically disabled by the enemy within: T-cell responses to HIV-1 infection.** *Immunol Cell Biol* 2007, **85:**6-15.
51. Kawai T, Akira S: **Toll-like receptors and their crosstalk with other innate receptors in infection and immunity.** *Immunity* 2011, **34:**637-650.
52. Kawai T, Akira S: **The role of pattern-recognition receptors in innate immunity: update on Toll-like receptors.** *Nat Immunol* 2010, **11:**373-384.
53. O'Connor GM, Holmes A, Mulcahy F, Gardiner CM: **Natural Killer cells from long-term non-progressor HIV patients are characterized by altered phenotype and function.** *Clin Immunol* 2007, **124:**277-283.
54. Vieillard V, Fausther-Bovendo H, Samri A, Debre P: **Specific phenotypic and functional features of natural killer cells from HIV-infected long-term nonprogressors and HIV controllers.** *J Acquir Immune Defic Syndr* 2010, **53:**564-573.
55. Trapp S, Turville SG, Robbiani M: **Slamming the door on unwanted guests: why preemptive strikes at the mucosa may be the best strategy against HIV.** *J Leukoc Biol* 2006, **80:**1076-1083.
56. Degli-Esposti MA, Smyth MJ: **Close encounters of different kinds: dendritic cells and NK cells take centre stage.** *Nat Rev Immunol* 2005, **5:**112-124.
57. Pope M, Haase AT: **Transmission, acute HIV-1 infection and the quest for strategies to prevent infection.** *Nat Med* 2003, **9:**847-852.
58. Teleshova N, Frank I, Pope M: **Immunodeficiency virus exploitation of dendritic cells in the early steps of infection.** *J Leukoc Biol* 2003, **74:**683-690.
59. Silverstein AM, Rose NR: **On the mystique of the immunological self.** *Immunol Rev* 1997, **159:**197-206; discussion 207-118.
60. Carlson JM, Listgarten J, Pfeifer N, Tan V, Kadie C, Walker BD, Ndung'u T, Shapiro R, Frater J, Brumme ZL, et al: **Widespread impact of HLA restriction on immune control and escape pathways of HIV-1.** *J Virol* 2012, **86:**5230-5243.
61. Turner SJ, La Gruta NL, Kedzierska K, Thomas PG, Doherty PC: **Functional implications of T cell receptor diversity.** *Curr Opin Immunol* 2009, **21:**286-290.
62. Carrega P, Ferlazzo G: **Natural killer cell distribution and trafficking in human tissues.** *Front Immunol* 2012, **3:**347.
63. Regner M, Pavlinovic L, Young N, Mullbacher A: **In vivo elimination of MHC-I-deficient lymphocytes by activated natural killer cells is independent of granzymes A and B.** *PLoS One* 2011, **6:**e23252.
64. Tessmer MS, Fatima A, Paget C, Trottein F, Brossay L: **NKT cell immune responses to viral infection.** *Expert Opin Ther Targets* 2009, **13:**153-162.
65. Barreira da Silva R, Munz C: **Natural killer cell activation by dendritic cells: balancing inhibitory and activating signals.** *Cell Mol Life Sci* 2011, **68:**3505-3518.
66. Juno JA, Keynan Y, Fowke KR: **Invariant NKT cells: regulation and function during viral infection.** *PLoS Pathog* 2012, **8:**e1002838.
67. Vivier E, Raulet DH, Moretta A, Caligiuri MA, Zitvogel L, Lanier LL, Yokoyama WM, Ugolini S: **Innate or adaptive immunity? The example of natural killer cells.** *Science* 2011, **331:**44-49.
68. Cohen GB, Gandhi RT, Davis DM, Mandelboim O, Chen BK, Strominger JL, Baltimore D: **The selective downregulation of class I major histocompatibility complex proteins by HIV-1 protects HIV-infected cells from NK cells.** *Immunity* 1999, **10:**661-671.
69. Williams M, Roeth JF, Kasper MR, Filzen TM, Collins KL: **Human immunodeficiency virus type 1 Nef domains required for disruption of major histocompatibility complex class I trafficking are also necessary for coprecipitation of Nef with HLA-A2.** *J Virol* 2005, **79:**632-636.
70. Jaffer U, Wade RG, Gourlay T: **Cytokines in the systemic inflammatory response syndrome: a review.** *HSR Proc Intensive Care Cardiovasc Anesth* 2010, **2:**161-175.
71. Sowrirajan B, Barker E: **The natural killer cell cytotoxic function is modulated by HIV-1 accessory proteins.** *Viruses* 2011, **3:**1091-1111.

72. Varadarajan N, Julg B, Yamanaka YJ, Chen H, Ogunniyi AO, McAndrew E, Porter LC, Piechocka-Trocha A, Hill BJ, Douek DC, et al: **A high-throughput single-cell analysis of human CD8(+) T cell functions reveals discordance for cytokine secretion and cytolysis.** *J Clin Invest* 2011, **121:**4322-4331.
73. Sabado RL, O'Brien M, Subedi A, Qin L, Hu N, Taylor E, Dibben O, Stacey A, Fellay J, Shianna KV, et al: **Evidence of dysregulation of dendritic cells in primary HIV infection.** *Blood* 2010, **116:**3839-3852.
74. Tisoncik JR, Korth MJ, Simmons CP, Farrar J, Martin TR, Katze MG: **Into the eye of the cytokine storm.** *Microbiol Mol Biol Rev* 2012, **76:**16-32.
75. Hamilton JA: **GM-CSF in inflammation and autoimmunity.** *Trends Immunol* 2002, **23:**403-408.
76. Samuel CE: **Antiviral actions of interferons.** *Clin Microbiol Rev* 2001, **14:**778-809, table of contents.
77. Brocker C, Thompson D, Matsumoto A, Nebert DW, Vasiliou V: **Evolutionary divergence and functions of the human interleukin (IL) gene family.** *Hum Genomics* 2010, **5:**30-55.
78. Bradley JR: **TNF-mediated inflammatory disease.** *J Pathol* 2008, **214:**149-160.
79. Kerstetter AE, Padovani-Claudio DA, Bai L, Miller RH: **Inhibition of CXCR2 signaling promotes recovery in models of multiple sclerosis.** *Exp Neurol* 2009, **220:**44-56.
80. Le Y, Zhou Y, Iribarren P, Wang J: **Chemokines and chemokine receptors: their manifold roles in homeostasis and disease.** *Cell Mol Immunol* 2004, **1:**95-104.
81. Menzies-Gow A, Ying S, Sabroe I, Stubbs VL, Soler D, Williams TJ, Kay AB: **Eotaxin (CCL11) and eotaxin-2 (CCL24) induce recruitment of eosinophils, basophils, neutrophils, and macrophages as well as features of early- and late-phase allergic reactions following cutaneous injection in human atopic and nonatopic volunteers.** *J Immunol* 2002, **169:**2712-2718.
82. Villatoro-Hernandez J, Loera-Arias MJ, Gamez-Escobedo A, Franco-Molina M, Gomez-Gutierrez JG, Rodriguez-Rocha H, Gutierrez-Puente Y, Saucedo-Cardenas O, Valdes-Flores J, Montes-de-Oca-Luna R: **Secretion of biologically active interferon-gamma inducible protein-10 (IP-10) by Lactococcus lactis.** *Microb Cell Fact* 2008, **7:**22.
83. Deshmane SL, Kremlev S, Amini S, Sawaya BE: **Monocyte chemoattractant protein-1 (MCP-1): an overview.** *J Interferon Cytokine Res* 2009, **29:**313-326.
84. Fae KC, Palacios SA, Nogueira LG, Oshiro SE, Demarchi LM, Bilate AM, Pomerantzeff PM, Brandao C, Thomaz PG, Dos Reis M, et al: **CXCL9/Mig Mediates T cells Recruitment to Valvular Tissue Lesions of Chronic Rheumatic Heart Disease Patients.** *Inflammation* 2013.
85. Wolpe SD, Cerami A: **Macrophage inflammatory proteins 1 and 2: members of a novel superfamily of cytokines.** *FASEB J* 1989, **3:**2565-2573.
86. Crawford A, Angelosanto JM, Nadwodny KL, Blackburn SD, Wherry EJ: **A role for the chemokine RANTES in regulating CD8 T cell responses during chronic viral infection.** *PLoS Pathog* 2011, **7:**e1002098.
87. Ito T, Connett JM, Kunkel SL, Matsukawa A: **The linkage of innate and adaptive immune response during granulomatous development.** *Front Immunol* 2013, **4:**10.
88. Pufnock JS, Cigal M, Rolczynski LS, Andersen-Nissen E, Wolfl M, McElrath MJ, Greenberg PD: **Priming CD8+ T cells with dendritic cells matured using TLR4 and TLR7/8 ligands together enhances generation of CD8+ T cells retaining CD28.** *Blood* 2011, **117:**6542-6551.
89. Sallusto F, Lanzavecchia A: **The instructive role of dendritic cells on T-cell responses.** *Arthritis Res* 2002, **4 Suppl 3:**S127-132.
90. Bevan MJ: **Helping the CD8(+) T-cell response.** *Nat Rev Immunol* 2004, **4:**595-602.
91. Stephens R, Horton R, Humphray S, Rowen L, Trowsdale J, Beck S: **Gene organisation, sequence variation and isochore structure at the centromeric boundary of the human MHC.** *J Mol Biol* 1999, **291:**789-799.
92. Horton R, Wilming L, Rand V, Lovering RC, Bruford EA, Khodiyar VK, Lush MJ, Povey S, Talbot CC, Jr., Wright MW, et al: **Gene map of the extended human MHC.** *Nat Rev Genet* 2004, **5:**889-899.
93. Robinson J, Mistry K, McWilliam H, Lopez R, Parham P, Marsh SG: **The IMGT/HLA database.** *Nucleic Acids Res* 2011, **39:**D1171-1176.
94. Vyas JM, Van der Veen AG, Ploegh HL: **The known unknowns of antigen processing and presentation.** *Nat Rev Immunol* 2008, **8:**607-618.
95. Hoof I, van Baarle D, Hildebrand WH, Kesmir C: **Proteome sampling by the HLA class I antigen processing pathway.** *PLoS Comput Biol* 2012, **8:**e1002517.

96. Sette A, Sidney J: **Nine major HLA class I supertypes account for the vast preponderance of HLA-A and -B polymorphism.** *Immunogenetics* 1999, **50:**201-212.
97. Lund O, Nielsen M, Kesmir C, Petersen AG, Lundegaard C, Worning P, Sylvester-Hvid C, Lamberth K, Roder G, Justesen S, et al: **Definition of supertypes for HLA molecules using clustering of specificity matrices.** *Immunogenetics* 2004, **55:**797-810.
98. Marsh SG, Albert ED, Bodmer WF, Bontrop RE, Dupont B, Erlich HA, Fernandez-Vina M, Geraghty DE, Holdsworth R, Hurley CK, et al: **Nomenclature for factors of the HLA system, 2010.** *Tissue Antigens* 2010, **75:**291-455.
99. Martinu T, Chen DF, Palmer SM: **Acute rejection and humoral sensitization in lung transplant recipients.** *Proc Am Thorac Soc* 2009, **6:**54-65.
100. Bell MJ, Burrows JM, Brennan R, Miles JJ, Tellam J, McCluskey J, Rossjohn J, Khanna R, Burrows SR: **The peptide length specificity of some HLA class I alleles is very broad and includes peptides of up to 25 amino acids in length.** *Mol Immunol* 2009, **46:**1911-1917.
101. Rock KL, York IA, Saric T, Goldberg AL: **Protein degradation and the generation of MHC class I-presented peptides.** *Adv Immunol* 2002, **80:**1-70.
102. Doms RW, Trono D: **The plasma membrane as a combat zone in the HIV battlefield.** *Genes Dev* 2000, **14:**2677-2688.
103. Ahlenstiel G, Roomp K, Daumer M, Nattermann J, Vogel M, Rockstroh JK, Beerenwinkel N, Kaiser R, Nischalke HD, Sauerbruch T, et al: **Selective pressures of HLA genotypes and antiviral therapy on human immunodeficiency virus type 1 sequence mutation at a population level.** *Clin Vaccine Immunol* 2007, **14:**1266-1273.
104. Keet IP, Tang J, Klein MR, LeBlanc S, Enger C, Rivers C, Apple RJ, Mann D, Goedert JJ, Miedema F, Kaslow RA: **Consistent associations of HLA class I and II and transporter gene products with progression of human immunodeficiency virus type 1 infection in homosexual men.** *J Infect Dis* 1999, **180:**299-309.
105. Saah AJ, Hoover DR, Weng S, Carrington M, Mellors J, Rinaldo CR, Jr., Mann D, Apple R, Phair JP, Detels R, et al: **Association of HLA profiles with early plasma viral load, CD4+ cell count and rate of progression to AIDS following acute HIV-1 infection. Multicenter AIDS Cohort Study.** *AIDS* 1998, **12:**2107-2113.
106. Yewdell JW, Reits E, Neefjes J: **Making sense of mass destruction: quantitating MHC class I antigen presentation.** *Nat Rev Immunol* 2003, **3:**952-961.
107. Zuniga-Pflucker JC: **T-cell development made simple.** *Nat Rev Immunol* 2004, **4:**67-72.
108. Rudd CE, Taylor A, Schneider H: **CD28 and CTLA-4 coreceptor expression and signal transduction.** *Immunol Rev* 2009, **229:**12-26.
109. Bucks CM, Katsikis PD: **New insights into classical costimulation of CD8+ T cell responses.** *Adv Exp Med Biol* 2009, **633:**91-111.
110. Davis MM, Bjorkman PJ: **T-cell antigen receptor genes and T-cell recognition.** *Nature* 1988, **334:**395-402.
111. Milstein O, Hagin D, Lask A, Reich-Zeliger S, Shezen E, Ophir E, Eidelstein Y, Afik R, Antebi YE, Dustin ML, Reisner Y: **CTLs respond with activation and granule secretion when serving as targets for T-cell recognition.** *Blood* 2011, **117:**1042-1052.
112. Liu Y, McNevin JP, Holte S, McElrath MJ, Mullins JI: **Dynamics of viral evolution and CTL responses in HIV-1 infection.** *PLoS One* 2011, **6:**e15639.
113. Seki S, Matano T: **CTL Escape and Viral Fitness in HIV/SIV Infection.** *Front Microbiol* 2011, **2:**267.
114. Vittinghoff E, Scheer S, O'Malley P, Colfax G, Holmberg SD, Buchbinder SP: **Combination antiretroviral therapy and recent declines in AIDS incidence and mortality.** *J Infect Dis* 1999, **179:**717-720.
115. Palella FJ, Jr., Delaney KM, Moorman AC, Loveless MO, Fuhrer J, Satten GA, Aschman DJ, Holmberg SD: **Declining morbidity and mortality among patients with advanced human immunodeficiency virus infection. HIV Outpatient Study Investigators.** *N Engl J Med* 1998, **338:**853-860.
116. Hogg RS, O'Shaughnessy MV, Gataric N, Yip B, Craib K, Schechter MT, Montaner JS: **Decline in deaths from AIDS due to new antiretrovirals.** *Lancet* 1997, **349:**1294.
117. Gandhi RT, Deeks SG: **Plasma HIV-1 RNA levels during antiretroviral therapy: how low is low enough?** *Clin Infect Dis* 2012, **54:**733-735.
118. Barbaro G, Scozzafava A, Mastrolorenzo A, Supuran CT: **Highly active antiretroviral therapy: current state of the art, new agents and their pharmacological interactions useful for improving therapeutic outcome.** *Curr Pharm Des* 2005, **11:**1805-1843.
119. Tang MW, Shafer RW: **HIV-1 antiretroviral resistance: scientific principles and clinical applications.** *Drugs* 2012, **72:**e1-25.

120. Mitsuya H, Weinhold KJ, Furman PA, St Clair MH, Lehrman SN, Gallo RC, Bolognesi D, Barry DW, Broder S: **3'-Azido-3'-deoxythymidine (BW A509U): an antiviral agent that inhibits the infectivity and cytopathic effect of human T-lymphotropic virus type III/lymphadenopathy-associated virus in vitro.** *Proc Natl Acad Sci U S A* 1985, **82:**7096-7100.
121. Esnouf R, Ren J, Ross C, Jones Y, Stammers D, Stuart D: **Mechanism of inhibition of HIV-1 reverse transcriptase by non-nucleoside inhibitors.** *Nat Struct Biol* 1995, **2:**303-308.
122. Debouck C: **The HIV-1 protease as a therapeutic target for AIDS.** *AIDS Res Hum Retroviruses* 1992, **8:**153-164.
123. Mansky LM: **HIV mutagenesis and the evolution of antiretroviral drug resistance.** *Drug Resist Updat* 2002, **5:**219-223.
124. Little SJ, Holte S, Routy JP, Daar ES, Markowitz M, Collier AC, Koup RA, Mellors JW, Connick E, Conway B, et al: **Antiretroviral-drug resistance among patients recently infected with HIV.** *N Engl J Med* 2002, **347:**385-394.
125. Johnson VA, Brun-Vezinet F, Clotet B, Gunthard HF, Kuritzkes DR, Pillay D, Schapiro JM, Richman DD: **Update of the drug resistance mutations in HIV-1: December 2010.** *Top HIV Med* 2010, **18:**156-163.
126. Hirsch MS, Brun-Vezinet F, Clotet B, Conway B, Kuritzkes DR, D'Aquila RT, Demeter LM, Hammer SM, Johnson VA, Loveday C, et al: **Antiretroviral drug resistance testing in adults infected with human immunodeficiency virus type 1: 2003 recommendations of an International AIDS Society-USA Panel.** *Clin Infect Dis* 2003, **37:**113-128.
127. Oette M, Kaiser R, Daumer M, Fatkenheuer G, Rockstroh JK, Knechten H, Mitrenga D, Beerenwinkel N, Sagir A, Pfister H, Haussinger D: **[Epidemiology of primary drug resistance in chronically HIV-infected patients in Nordrhein-Westfalen, Germany, 2001-2005].** *Dtsch Med Wochenschr* 2007, **132:**977-982.
128. Sagir A, Oette M, Kaiser R, Daumer M, Fatkenheuer G, Rockstroh JK, Knechten H, Schmutz G, Hower M, Emmelkamp J, et al: **Trends of prevalence of primary HIV drug resistance in Germany.** *J Antimicrob Chemother* 2007, **60:**843-848.
129. Booth CL, Garcia-Diaz AM, Youle MS, Johnson MA, Phillips A, Geretti AM: **Prevalence and predictors of antiretroviral drug resistance in newly diagnosed HIV-1 infection.** *J Antimicrob Chemother* 2007, **59:**517-524.
130. Allen TM, Altfeld M, Yu XG, O'Sullivan KM, Lichterfeld M, Le Gall S, John M, Mothe BR, Lee PK, Kalife ET, et al: **Selection, transmission, and reversion of an antigen-processing cytotoxic T-lymphocyte escape mutation in human immunodeficiency virus type 1 infection.** *J Virol* 2004, **78:**7069-7078.
131. Allen TM, Yu XG, Kalife ET, Reyor LL, Lichterfeld M, John M, Cheng M, Allgaier RL, Mui S, Frahm N, et al: **De novo generation of escape variant-specific CD8+ T-cell responses following cytotoxic T-lymphocyte escape in chronic human immunodeficiency virus type 1 infection.** *J Virol* 2005, **79:**12952-12960.
132. John M, Mallal S: **CTL responses to HIV and SIV: wrestling with smoke.** *Nat Immunol* 2005, **6:**232-234.
133. Karlsson AC, Deeks SG, Barbour JD, Heiken BD, Younger SR, Hoh R, Lane M, Sallberg M, Ortiz GM, Demarest JF, et al: **Dual pressure from antiretroviral therapy and cell-mediated immune response on the human immunodeficiency virus type 1 protease gene.** *J Virol* 2003, **77:**6743-6752.
134. Mahnke L, Clifford D: **Cytotoxic T cell recognition of an HIV-1 reverse transcriptase variant peptide incorporating the K103N drug resistance mutation.** *AIDS Res Ther* 2006, **3:**21.
135. Mason RD, Bowmer MI, Howley CM, Gallant M, Myers JC, Grant MD: **Antiretroviral drug resistance mutations sustain or enhance CTL recognition of common HIV-1 Pol epitopes.** *J Immunol* 2004, **172:**7212-7219.
136. Moore CB, John M, James IR, Christiansen FT, Witt CS, Mallal SA: **Evidence of HIV-1 adaptation to HLA-restricted immune responses at a population level.** *Science* 2002, **296:**1439-1443.
137. Mueller SM, Schaetz B, Eismann K, Bergmann S, Bauerle M, Schmitt-Haendle M, Walter H, Schmidt B, Korn K, Sticht H, et al: **Dual selection pressure by drugs and HLA class I-restricted immune responses on human immunodeficiency virus type 1 protease.** *J Virol* 2007, **81:**2887-2898.
138. Samri A, Haas G, Duntze J, Bouley JM, Calvez V, Katlama C, Autran B: **Immunogenicity of mutations induced by nucleoside reverse transcriptase inhibitors for human immunodeficiency virus type 1-specific cytotoxic T cells.** *J Virol* 2000, **74:**9306-9312.

139. Schmitt M, Harrer E, Goldwich A, Bauerle M, Graedner I, Kalden JR, Harrer T: **Specific recognition of lamivudine-resistant HIV-1 by cytotoxic T lymphocytes.** *AIDS* 2000, **14:**653-658.
140. Verheyen J, Schweitzer F, Harrer EG, Knops E, Mueller SM, Daumer M, Eismann K, Bergmann S, Spriewald BM, Kaiser R, Harrer T: **Analysis of immune selection as a potential cause for the presence of cleavage site mutation 431V in treatment-naive HIV type-1 isolates.** *Antivir Ther* 2010, **15:**907-912.
141. Brandt SM, Mariani R, Holland AU, Hope TJ, Landau NR: **Association of chemokine-mediated block to HIV entry with coreceptor internalization.** *J Biol Chem* 2002, **277:**17291-17299.
142. Lusso P, Cocchi F, Balotta C, Markham PD, Louie A, Farci P, Pal R, Gallo RC, Reitz MS, Jr.: **Growth of macrophage-tropic and primary human immunodeficiency virus type 1 (HIV-1) isolates in a unique CD4+ T-cell clone (PM1): failure to downregulate CD4 and to interfere with cell-line-tropic HIV-1.** *J Virol* 1995, **69:**3712-3720.
143. Akatsuka Y, Goldberg TA, Kondo E, Martin EG, Obata Y, Morishima Y, Takahashi T, Hansen JA: **Efficient cloning and expression of HLA class I cDNA in human B-lymphoblastoid cell lines.** *Tissue Antigens* 2002, **59:**502-511.
144. Lizee G, Aerts JL, Gonzales MI, Chinnasamy N, Morgan RA, Topalian SL: **Real-time quantitative reverse transcriptase-polymerase chain reaction as a method for determining lentiviral vector titers and measuring transgene expression.** *Hum Gene Ther* 2003, **14:**497-507.
145. Demaison C, Parsley K, Brouns G, Scherr M, Battmer K, Kinnon C, Grez M, Thrasher AJ: **High-level transduction and gene expression in hematopoietic repopulating cells using a human immunodeficiency [correction of imunodeficiency] virus type 1-based lentiviral vector containing an internal spleen focus forming virus promoter.** *Hum Gene Ther* 2002, **13:**803-813.
146. Zufferey R, Nagy D, Mandel RJ, Naldini L, Trono D: **Multiply attenuated lentiviral vector achieves efficient gene delivery in vivo.** *Nat Biotechnol* 1997, **15:**871-875.
147. Naldini L, Blomer U, Gallay P, Ory D, Mulligan R, Gage FH, Verma IM, Trono D: **In vivo gene delivery and stable transduction of nondividing cells by a lentiviral vector.** *Science* 1996, **272:**263-267.
148. Westervelt P, Gendelman HE, Ratner L: **Identification of a determinant within the human immunodeficiency virus 1 surface envelope glycoprotein critical for productive infection of primary monocytes.** *Proc Natl Acad Sci U S A* 1991, **88:**3097-3101.
149. Johnson VA, Calvez V, Gunthard HF, Paredes R, Pillay D, Shafer RW, Wensing AM, Richman DD: **Update of the drug resistance mutations in HIV-1: March 2013.** *Top Antivir Med* 2013, **21:**6-14.
150. Mullis K, Faloona F, Scharf S, Saiki R, Horn G, Erlich H: **Specific enzymatic amplification of DNA in vitro: the polymerase chain reaction.** *Cold Spring Harb Symp Quant Biol* 1986, **51 Pt 1:**263-273.
151. De Vreese K, Barylski R, Pughe F, Blaser M, Evans C, Norton J, Semana G, Holman R, Loiseau P, Masson D, et al: **Performance characteristics of updated INNO-LiPA assays for molecular typing of human leukocyte antigen A (HLA-A), HLA-B, and HLA-DQB1 alleles.** *Clin Diagn Lab Immunol* 2004, **11:**430-432.
152. Carlson JM, Brumme ZL, Rousseau CM, Brumme CJ, Matthews P, Kadie C, Mullins JI, Walker BD, Harrigan PR, Goulder PJ, Heckerman D: **Phylogenetic dependency networks: inferring patterns of CTL escape and codon covariation in HIV-1 Gag.** *PLoS Comput Biol* 2008, **4:**e1000225.
153. Bland JM, Altman DG: **Statistics notes. The odds ratio.** *BMJ* 2000, **320:**1468.
154. Storey JD, Tibshirani R: **Statistical significance for genomewide studies.** *Proc Natl Acad Sci U S A* 2003, **100:**9440-9445.
155. Zen Z, Espinoza Y, Bleu T, Sommer JM, Wright JF: **Infectious titer assay for adeno-associated virus vectors with sensitivity sufficient to detect single infectious events.** *Hum Gene Ther* 2004, **15:**709-715.
156. Mascolini M, Larder BA, Boucher CA, Richman DD, Mellors JW: **Broad advances in understanding HIV resistance to antiretrovirals: report on the XVII International HIV Drug Resistance Workshop.** *Antivir Ther* 2008, **13:**1097-1113.
157. Altman JD, Feinberg MB: **HIV escape: there and back again.** *Nat Med* 2004, **10:**229-230.

158. Allen TM, Altfeld M, Geer SC, Kalife ET, Moore C, O'Sullivan K M, Desouza I, Feeney ME, Eldridge RL, Maier EL, et al: **Selective escape from CD8+ T-cell responses represents a major driving force of human immunodeficiency virus type 1 (HIV-1) sequence diversity and reveals constraints on HIV-1 evolution.** *J Virol* 2005, **79:**13239-13249.
159. Frater AJ, Edwards CT, McCarthy N, Fox J, Brown H, Milicic A, Mackie N, Pillay T, Drijfhout JW, Dustan S, et al: **Passive sexual transmission of human immunodeficiency virus type 1 variants and adaptation in new hosts.** *J Virol* 2006, **80:**7226-7234.
160. Jones NA, Wei X, Flower DR, Wong M, Michor F, Saag MS, Hahn BH, Nowak MA, Shaw GM, Borrow P: **Determinants of human immunodeficiency virus type 1 escape from the primary CD8+ cytotoxic T lymphocyte response.** *J Exp Med* 2004, **200:**1243-1256.
161. Kent SJ, Fernandez CS, Dale CJ, Davenport MP: **Reversion of immune escape HIV variants upon transmission: insights into effective viral immunity.** *Trends Microbiol* 2005, **13:**243-246.
162. Leslie A, Kavanagh D, Honeyborne I, Pfafferott K, Edwards C, Pillay T, Hilton L, Thobakgale C, Ramduth D, Draenert R, et al: **Transmission and accumulation of CTL escape variants drive negative associations between HIV polymorphisms and HLA.** *J Exp Med* 2005, **201:**891-902.
163. Schweitzer F: **Correlations between transmitted HIV drug resistance mutations and the HLA of therapy-naïve HIV-patients**
University of Maastricht, The Netherlands, Institut of Virology, University of Cologne, Germany; 2008.
164. Schweitzer F: *Correlations between HIV drug resistance mutations and the HLA of therapy-naive HIV-patients.* Schriftenreihe Infektiologie; 2013, in press.
165. Chatterjee A, Rathore A, Vidyant S, Kakkar K, Dhole TN: **Chemokines and chemokine receptors in susceptibility to HIV-1 infection and progression to AIDS.** *Dis Markers* 2012, **32:**143-151.
166. Rancez M, Couedel-Courteille A, Cheynier R: **Chemokines at mucosal barriers and their impact on HIV infection.** *Cytokine Growth Factor Rev* 2012, **23:**233-243.
167. Simbiri K, Jha, H., Dzeng R., Massaro-Giordano G., Robertson E. : **Cytokine and Chemokine Expression Profiles in HIV-1 Infected Patients with Ocular Surface Squamous Neoplasia from Botswana.** *Cancer and Clinical Oncology* 2012, **1:**10-24.
168. Byrnes AA, Harris DM, Atabani SF, Sabundayo BP, Langan SJ, Margolick JB, Karp CL: **Immune activation and IL-12 production during acute/early HIV infection in the absence and presence of highly active, antiretroviral therapy.** *J Leukoc Biol* 2008, **84:**1447-1453.
169. Pizzolo G, Vinante F, Sinicco A, Chilosi M, Agostini C, Perini A, Zuppini B, Semenzato G, Battistella L, Foa R: **Increased levels of soluble interleukin-2 receptor in the serum of patients with human immunodeficiency virus infection.** *Diagn Clin Immunol* 1987, **5:**180-183.
170. Radkowski M, Kopicz-Kaminska E, Laskus T, Rogers S, Babiuch L, Slusarczyk J: **[Occurrence of free receptor for interleukin 2 in serum and quantitative determinations of CD25+ in patients infected with HIV].** *Pol Arch Med Wewn* 1994, **91:**201-205.
171. Haissman JM, Vestergaard LS, Sembuche S, Erikstrup C, Mmbando B, Mtullu S, Lemnge MM, Gerstoft J, Ullum H: **Plasma cytokine levels in Tanzanian HIV-1-infected adults and the effect of antiretroviral treatment.** *J Acquir Immune Defic Syndr* 2009, **52:**493-497.
172. Liovat AS, Rey-Cuille MA, Lecuroux C, Jacquelin B, Girault I, Petitjean G, Zitoun Y, Venet A, Barre-Sinoussi F, Lebon P, et al: **Acute plasma biomarkers of T cell activation set-point levels and of disease progression in HIV-1 infection.** *PLoS One* 2012, **7:**e46143.
173. Kamat A, Misra V, Cassol E, Ancuta P, Yan Z, Li C, Morgello S, Gabuzda D: **A plasma biomarker signature of immune activation in HIV patients on antiretroviral therapy.** *PLoS One* 2012, **7:**e30881.
174. Moore C, John, M., James, I., Mallal, S.: **The influence of host HLA on antiretroviral drug resistance mutation in HIV-1.** In *9th Conference on Retrovirus and Opportunistic Infections*. Seattle, USA; 2002.
175. Harrer T. M-SM: **Comparing Statistically Significant Assaciations between RAMs and HLA Alleles of 2 Cohorts (Erlangen and RESINA).** (Schweitzer F ed. Erlangen, Germany; 2010.
176. Moretta A: **Natural killer cells and dendritic cells: rendezvous in abused tissues.** *Nat Rev Immunol* 2002, **2:**957-964.
177. Savina A, Amigorena S: **Phagocytosis and antigen presentation in dendritic cells.** *Immunol Rev* 2007, **219:**143-156.
178. Turville SG, Aravantinou M, Stossel H, Romani N, Robbiani M: **Resolution of de novo HIV production and trafficking in immature dendritic cells.** *Nat Methods* 2008, **5:**75-85.

179. Breckpot K, Dullaers M, Bonehill A, van Meirvenne S, Heirman C, de Greef C, van der Bruggen P, Thielemans K: **Lentivirally transduced dendritic cells as a tool for cancer immunotherapy.** *J Gene Med* 2003, **5:**654-667.
180. Breckpot K, Emeagi P, Dullaers M, Michiels A, Heirman C, Thielemans K: **Activation of immature monocyte-derived dendritic cells after transduction with high doses of lentiviral vectors.** *Hum Gene Ther* 2007, **18:**536-546.
181. Bartholomae CC, Arens A, Balaggan KS, Yanez-Munoz RJ, Montini E, Howe SJ, Paruzynski A, Korn B, Appelt JU, Macneil A, et al: **Lentiviral vector integration profiles differ in rodent postmitotic tissues.** *Mol Ther* 2011, **19:**703-710.
182. Wanisch K, Yanez-Munoz RJ: **Integration-deficient lentiviral vectors: a slow coming of age.** *Mol Ther* 2009, **17:**1316-1332.
183. Cronin J, Zhang XY, Reiser J: **Altering the tropism of lentiviral vectors through pseudotyping.** *Curr Gene Ther* 2005, **5:**387-398.
184. Fauci AS, Mavilio D, Kottilil S: **NK cells in HIV infection: paradigm for protection or targets for ambush.** *Nat Rev Immunol* 2005, **5:**835-843.
185. Alter G, Altfeld M: **NK cells in HIV-1 infection: evidence for their role in the control of HIV-1 infection.** *J Intern Med* 2009, **265:**29-42.
186. Boyton RJ, Altmann DM: **Natural killer cells, killer immunoglobulin-like receptors and human leucocyte antigen class I in disease.** *Clin Exp Immunol* 2007, **149:**1-8.
187. Kumar V, McNerney ME: **A new self: MHC-class-I-independent natural-killer-cell self-tolerance.** *Nat Rev Immunol* 2005, **5:**363-374.
188. Klein MR, van Baalen CA, Holwerda AM, Kerkhof Garde SR, Bende RJ, Keet IP, Eeftinck-Schattenkerk JK, Osterhaus AD, Schuitemaker H, Miedema F: **Kinetics of Gag-specific cytotoxic T lymphocyte responses during the clinical course of HIV-1 infection: a longitudinal analysis of rapid progressors and long-term asymptomatics.** *J Exp Med* 1995, **181:**1365-1372.
189. Curtsinger JM, Johnson CM, Mescher MF: **CD8 T cell clonal expansion and development of effector function require prolonged exposure to antigen, costimulation, and signal 3 cytokine.** *J Immunol* 2003, **171:**5165-5171.
190. Smyth MJ, Cretney E, Kelly JM, Westwood JA, Street SE, Yagita H, Takeda K, van Dommelen SL, Degli-Esposti MA, Hayakawa Y: **Activation of NK cell cytotoxicity.** *Mol Immunol* 2005, **42:**501-510.
191. Janssen EM, Lemmens EE, Gour N, Reboulet RA, Green DR, Schoenberger SP, Pinkoski MJ: **Distinct roles of cytolytic effector molecules for antigen-restricted killing by CTL in vivo.** *Immunol Cell Biol* 2010, **88:**761-765.
192. Alcami A, Koszinowski UH: **Viral mechanisms of immune evasion.** *Trends Microbiol* 2000, **8:**410-418.
193. Rollenhagen C, Asin SN: **IL-8 decreases HIV-1 transcription in peripheral blood lymphocytes and ectocervical tissue explants.** *J Acquir Immune Defic Syndr* 2010, **54:**463-469.
194. Baggiolini M, Clark-Lewis I: **Interleukin-8, a chemotactic and inflammatory cytokine.** *FEBS Lett* 1992, **307:**97-101.
195. Appay V, Sauce D: **Immune activation and inflammation in HIV-1 infection: causes and consequences.** *J Pathol* 2008, **214:**231-241.
196. Keating SM, Golub ET, Nowicki M, Young M, Anastos K, Crystal H, Cohen MH, Zhang J, Greenblatt RM, Desai S, et al: **The effect of HIV infection and HAART on inflammatory biomarkers in a population-based cohort of women.** *AIDS* 2011, **25:**1823-1832.
197. Autran B, Carcelain G, Debre P: **Immune reconstitution after highly active anti-retroviral treatment of HIV infection.** *Adv Exp Med Biol* 2001, **495:**205-212.
198. Llano A, Barretina J, Gutierrez A, Blanco J, Cabrera C, Clotet B, Este JA: **Interleukin-7 in plasma correlates with CD4 T-cell depletion and may be associated with emergence of syncytium-inducing variants in human immunodeficiency virus type 1-positive individuals.** *J Virol* 2001, **75:**10319-10325.
199. Capitini CM, Chisti AA, Mackall CL: **Modulating T-cell homeostasis with IL-7: preclinical and clinical studies.** *J Intern Med* 2009, **266:**141-153.
200. Young CD, Angel JB: **HIV infection of thymocytes inhibits IL-7 activity without altering CD127 expression.** *Retrovirology* 2011, **8:**72.

201. Stacey AR, Norris PJ, Qin L, Haygreen EA, Taylor E, Heitman J, Lebedeva M, DeCamp A, Li D, Grove D, et al: **Induction of a striking systemic cytokine cascade prior to peak viremia in acute human immunodeficiency virus type 1 infection, in contrast to more modest and delayed responses in acute hepatitis B and C virus infections.** *J Virol* 2009, **83:**3719-3733.
202. Verbist KC, Klonowski KD: **Functions of IL-15 in anti-viral immunity: multiplicity and variety.** *Cytokine* 2012, **59:**467-478.

9. Appendix

(A)

```
>IMGTHLA:HLA00005 A*02:01:01:01 1098 bp
        Length = 1098

  Plus Strand HSPs:

 Score = 5454 (824.4 bits), Expect = 9.8e-243, P = 9.8e-243, Group = 1
 Identities = 1094/1098 (99%), Positives = 1094/1098 (99%), Strand = Plus / Plus

Query:   150 ATGGCCGTCATGGCGCCCCGAACCCTCGTCCTGCTACTCTCGGGGGCTCTGGCCCTGACC 209
             ||||||||||||||||||||||||||||||||||||||||||||||||||||||||||||
Sbjct:     1 ATGGCCGTCATGGCGCCCCGAACCCTCGTCCTGCTACTCTCGGGGGCTCTGGCCCTGACC 60

Query:   210 CAGACCTGGGCGGGCTCTCACTCCATGAGGTATTTCTTCACATCCGTGTCCCGGCCCGGC 269
             ||||||||||||||||||||||||||||||||||||||||||||||||||||||||||||
Sbjct:    61 CAGACCTGGGCGGGCTCTCACTCCATGAGGTATTTCTTCACATCCGTGTCCCGGCCCGGC 120

Query:   270 CGCGGGGAGCCCCGCTTCATCGCAGTGGGCTACGTGGACGACACGCAGTTCGTGCGGTTC 329
             ||||||||||||||||||||||||||||||||||||||||||||||||||||||||||||
Sbjct:   121 CGCGGGGAGCCCCGCTTCATCGCAGTGGGCTACGTGGACGACACGCAGTTCGTGCGGTTC 180

Query:   330 GACAGCGACACCGCGAGCCAGAGGATGGAGCCGCGGGCGCCGTGGATAGAGCAGGAGGGT 389
             ||||||||| ||||||||||||||||||||||||||||||||||||||||||||||||||
Sbjct:   181 GACAGCGACGCCGCGAGCCAGAGGATGGAGCCGCGGGCGCCGTGGATAGAGCAGGAGGGT 240

Query:   390 CCGGAGTATTGGGACGGGGAGACACGGAAAGTGAAGGCCCACTCACAGACTCACCGAGTG 449
             ||||||||||||||||||||||||||||||||||||||||||||||||||||||||||||
Sbjct:   241 CCGGAGTATTGGGACGGGGAGACACGGAAAGTGAAGGCCCACTCACAGACTCACCGAGTG 300

Query:   450 GACCTGGGGACCCTGCGCGGCTACTACAACCAGAGCGAGGCCGGTTCTCACACCGTCCAG 509
             ||||||||||||||||||||||||||||||||||||||||||||||||||||||||||||
Sbjct:   301 GACCTGGGGACCCTGCGCGGCTACTACAACCAGAGCGAGGCCGGTTCTCACACCGTCCAG 360

Query:   510 AGGATGTATGGCTGCGACGTGGGGTCGGACTGGCGCTTCCTCCGCGGGTACCACCAGTAC 569
             ||||||||||||||||||||||||||||||||||||||||||||||||||||||||||||
Sbjct:   361 AGGATGTATGGCTGCGACGTGGGGTCGGACTGGCGCTTCCTCCGCGGGTACCACCAGTAC 420

Query:   570 GCCTACGACGGCAAGGATTACATCGCCCTGAAAGAGGACCTGCGCTCTTGGACCGCGGCG 629
             ||||||||||||||||||||||||||||||||||||||||||||||||||||||||||||
Sbjct:   421 GCCTACGACGGCAAGGATTACATCGCCCTGAAAGAGGACCTGCGCTCTTGGACCGCGGCG 480

Query:   630 GACATGGCAGCTCAGACCACCAAGCACAAGTGGGAGGCGGCCCATGTGGCGGAGCAGTTG 689
             ||||||||||||||||||||||||||||||||||||||||||||||||||||||||||||
Sbjct:   481 GACATGGCAGCTCAGACCACCAAGCACAAGTGGGAGGCGGCCCATGTGGCGGAGCAGTTG 540

Query:   690 AGAGCCTACCTGGAGGGCACGTGCGTGGAGTGGCTCCGCAGATACCTGGAGAACGGGAAG 749
             ||||||||||||||||||||||||||||||||||||||||||||||||||||||||||||
Sbjct:   541 AGAGCCTACCTGGAGGGCACGTGCGTGGAGTGGCTCCGCAGATACCTGGAGAACGGGAAG 600

Query:   750 GAGATGCTGCAGCGCACGGACGCCCCCAAAACGCATATGACTCACCACGCTGTCTCTGAC 809
             |||| ||||||||||||||||||||||||||||||||||||||||||||||||||||||
Sbjct:   601 GAGACGCTGCAGCGCACGGACGCCCCCAAAACGCATATGACTCACCACGCTGTCTCTGAC 660

Query:   810 CATGAAGCCACCCTGAGGTGCTGGGCCCTGAGCTCCTACCCTGCGGAGATCACACTGACC 869
             |||||||||||||||||||||||||||||||| ||||||||||||||||||||||||||
Sbjct:   661 CATGAAGCCACCCTGAGGTGCTGGGCCCTGAGCTTCTACCCTGCGGAGATCACACTGACC 720

Query:   870 TGGCAGCGGGATGGGGAGGACCAGACCCAGGACACGGAGCTCGTGGAGACCAGGCCTGCA 929
             ||||||||||||||||||||||||||||||||||||||||||||||||||||||||||||
Sbjct:   721 TGGCAGCGGGATGGGGAGGACCAGACCCAGGACACGGAGCTCGTGGAGACCAGGCCTGCA 780

Query:   930 GGGGATGGAACCTTCCAGAAGTGGGCGGCTGTGGTGGTGCCTTCTGGACAGGAGCAGAGA 989
             ||||||||||||||||||||||||||||||||||||||||||||||||||||||||||||
Sbjct:   781 GGGGATGGAACCTTCCAGAAGTGGGCGGCTGTGGTGGTGCCTTCTGGACAGGAGCAGAGA 840

Query:   990 TACACCTGCCATGTGCAGCATGAGGGTTTGCCCAAGCCCCTCACCCTGAGATGGGAGCCG 1049
             ||||||||||||||||||||||||||||||||||||||||||||||||||||||||||||
Sbjct:   841 TACACCTGCCATGTGCAGCATGAGGGTTTGCCCAAGCCCCTCACCCTGAGATGGGAGCCG 900

Query:  1050 TCTTCCCAGCCCACCATCCCCATCGTGGGCATCATTGCTGGCCTGGTTCTCTTTGGAGCT 1109
             ||||||||||||||||||||||||||||||||||||||||||||||||||||||||||||
Sbjct:   901 TCTTCCCAGCCCACCATCCCCATCGTGGGCATCATTGCTGGCCTGGTTCTCTTTGGAGCT 960
```

```
Query:  1110 GTGATCACTGGAGCTGTGGTCGCTGCTGTGATGTGGTGGAGGAAGAGCTCAGATAGAAAA 1169
             |||||||||||||||||||||||||||||||||| ||||||||||||||||||||||||
Sbjct:   961 GTGATCACTGGAGCTGTGGTCGCTGCTGTGATGTGGAGGAGGAAGAGCTCAGATAGAAAA 1020

Query:  1170 GGAGGGAGCTACTCTCAGGCTGCAAGCAGTGACAGTGCCCAGGGCTCTGATGTGTCTCTC 1229
             ||||||||||||||||||||||||||||||||||||||||||||||||||||||||||||
Sbjct:  1021 GGAGGGAGCTACTCTCAGGCTGCAAGCAGTGACAGTGCCCAGGGCTCTGATGTGTCTCTC 1080

Query:  1230 ACAGCTTGTAAAGTGTGA 1247
             ||||||||||||||||||
Sbjct:  1081 ACAGCTTGTAAAGTGTGA 1098
```

(B)

```
>IMGTHLA:HLA00319 B*44:03:01 1089 bp
        Length = 1089

  Plus Strand HSPs:

 Score = 5430 (820.8 bits), Expect = 1.2e-241, P = 1.2e-241, Group = 1
 Identities = 1086/1086 (100%), Positives = 1086/1086 (100%), Strand = Plus / Plus

Query:    62 ATGCGGGTCACGGCGCCCCGAACCCTCCTCCTGCTGCTCTGGGGGGCAGTGGCCCTGACC 121
             ||||||||||||||||||||||||||||||||||||||||||||||||||||||||||||
Sbjct:     1 ATGCGGGTCACGGCGCCCCGAACCCTCCTCCTGCTGCTCTGGGGGGCAGTGGCCCTGACC 60

Query:   122 GAGACCTGGGCCGGCTCCCACTCCATGAGGTATTTCTACACCGCCATGTCCCGGCCCGGC 181
             ||||||||||||||||||||||||||||||||||||||||||||||||||||||||||||
Sbjct:    61 GAGACCTGGGCCGGCTCCCACTCCATGAGGTATTTCTACACCGCCATGTCCCGGCCCGGC 120

Query:   182 CGCGGGGAGCCCCGCTTCATCACCGTGGGCTACGTGGACGACACGCTGTTCGTGAGGTTC 241
             ||||||||||||||||||||||||||||||||||||||||||||||||||||||||||||
Sbjct:   121 CGCGGGGAGCCCCGCTTCATCACCGTGGGCTACGTGGACGACACGCTGTTCGTGAGGTTC 180

Query:   242 GACAGCGACGCCACGAGTCCGAGGAAGGAGCCGCGGGCGCCATGGATAGAGCAGGAGGGG 301
             ||||||||||||||||||||||||||||||||||||||||||||||||||||||||||||
Sbjct:   181 GACAGCGACGCCACGAGTCCGAGGAAGGAGCCGCGGGCGCCATGGATAGAGCAGGAGGGG 240

Query:   302 CCGGAGTATTGGGACCGGGAGACACAGATCTCCAAGACCAACACACAGACTTACCGAGAG 361
             ||||||||||||||||||||||||||||||||||||||||||||||||||||||||||||
Sbjct:   241 CCGGAGTATTGGGACCGGGAGACACAGATCTCCAAGACCAACACACAGACTTACCGAGAG 300

Query:   362 AACCTGCGCACCGCGCTCCGCTACTACAACCAGAGCGAGGCCGGGTCTCACATCATCCAG 421
             ||||||||||||||||||||||||||||||||||||||||||||||||||||||||||||
Sbjct:   301 AACCTGCGCACCGCGCTCCGCTACTACAACCAGAGCGAGGCCGGGTCTCACATCATCCAG 360

Query:   422 AGGATGTACGGCTGCGACGTGGGGCCGGACGGGCGCCTCCTCCGCGGGTATGACCAGGAC 481
             ||||||||||||||||||||||||||||||||||||||||||||||||||||||||||||
Sbjct:   361 AGGATGTACGGCTGCGACGTGGGGCCGGACGGGCGCCTCCTCCGCGGGTATGACCAGGAC 420

Query:   482 GCCTACGACGGCAAGGATTACATCGCCCTGAACGAGGACCTGAGCTCCTGGACCGCGGCG 541
             ||||||||||||||||||||||||||||||||||||||||||||||||||||||||||||
Sbjct:   421 GCCTACGACGGCAAGGATTACATCGCCCTGAACGAGGACCTGAGCTCCTGGACCGCGGCG 480

Query:   542 GACACCGCGGCTCAGATCACCCAGCGCAAGTGGGAGGCGGCCCGTGTGGCGGAGCAGCTG 601
             ||||||||||||||||||||||||||||||||||||||||||||||||||||||||||||
Sbjct:   481 GACACCGCGGCTCAGATCACCCAGCGCAAGTGGGAGGCGGCCCGTGTGGCGGAGCAGCTG 540

Query:   602 AGAGCCTACCTGGAGGGCCTGTGCGTGGAGTCGCTCCGCAGATACCTGGAGAACGGGAAG 661
             ||||||||||||||||||||||||||||||||||||||||||||||||||||||||||||
Sbjct:   541 AGAGCCTACCTGGAGGGCCTGTGCGTGGAGTCGCTCCGCAGATACCTGGAGAACGGGAAG 600

Query:   662 GAGACGCTGCAGCGCGCGGACCCCCCAAAGACACATGTGACCCACCACCCCATCTCTGAC 721
             ||||||||||||||||||||||||||||||||||||||||||||||||||||||||||||
Sbjct:   601 GAGACGCTGCAGCGCGCGGACCCCCCAAAGACACATGTGACCCACCACCCCATCTCTGAC 660

Query:   722 CATGAGGTCACCCTGAGGTGCTGGGCCCTGGGCTTCTACCCTGCGGAGATCACACTGACC 781
             ||||||||||||||||||||||||||||||||||||||||||||||||||||||||||||
Sbjct:   661 CATGAGGTCACCCTGAGGTGCTGGGCCCTGGGCTTCTACCCTGCGGAGATCACACTGACC 720

Query:   782 TGGCAGCGGGATGGCGAGGACCAAACTCAGGACACCGAGCTTGTGGAGACCAGACCAGCA 841
             ||||||||||||||||||||||||||||||||||||||||||||||||||||||||||||
Sbjct:   721 TGGCAGCGGGATGGCGAGGACCAAACTCAGGACACCGAGCTTGTGGAGACCAGACCAGCA 780

Query:   842 GGAGATAGAACCTTCCAGAAGTGGGCAGCTGTGGTGGTGCCTTCTGGAGAAGAGCAGAGA 901
             ||||||||||||||||||||||||||||||||||||||||||||||||||||||||||||
Sbjct:   781 GGAGATAGAACCTTCCAGAAGTGGGCAGCTGTGGTGGTGCCTTCTGGAGAAGAGCAGAGA 840
```

```
Query:   902 TACACATGCCATGTACAGCATGAGGGGCTGCCGAAGCCCCTCACCCTGAGATGGGAGCCG 961
             ||||||||||||||||||||||||||||||||||||||||||||||||||||||||||||
Sbjct:   841 TACACATGCCATGTACAGCATGAGGGGCTGCCGAAGCCCCTCACCCTGAGATGGGAGCCG 900

Query:   962 TCTTCCCAGTCCACCGTCCCCATCGTGGGCATTGTTGCTGGCCTGGCTGTCCTAGCAGTT 1021
             ||||||||||||||||||||||||||||||||||||||||||||||||||||||||||||
Sbjct:   901 TCTTCCCAGTCCACCGTCCCCATCGTGGGCATTGTTGCTGGCCTGGCTGTCCTAGCAGTT 960

Query:  1022 GTGGTCATCGGAGCTGTGGTCGCTGCTGTGATGTGTAGGAGGAAGAGCTCAGGTGGAAAA 1081
             ||||||||||||||||||||||||||||||||||||||||||||||||||||||||||||
Sbjct:   961 GTGGTCATCGGAGCTGTGGTCGCTGCTGTGATGTGTAGGAGGAAGAGCTCAGGTGGAAAA 1020

Query:  1082 GGAGGGAGCTACTCTCAGGCTGCGTGCAGCGACAGTGCCCAGGGCTCTGATGTGTCTCTC 1141
             ||||||||||||||||||||||||||||||||||||||||||||||||||||||||||||
Sbjct:  1021 GGAGGGAGCTACTCTCAGGCTGCGTGCAGCGACAGTGCCCAGGGCTCTGATGTGTCTCTC 1080

Query:  1142 ACAGCT 1147
             ||||||
Sbjct:  1081 ACAGCT 1086
```

Figure 13.1 Sequence alignment of (A) HLA-A*02:01 ORF and (B) HLA-B*44:03 ORF with reference strains.

Table 13.1 Albumin and WPRE concentrations and calculated normalized WPRE expression

LV_HLA-A*02	Albumin concentration	DNA WPRE concentration	Normalized WPRE expression
neg. control	19.6	28.9	1.47
1	14100	12500	0.89
2	20850	7730	0.37
3	20800	11200	0.54
LV_HLA-B*44			
1	13000	8790	0.68
2	27450	10900	0.40
3	13550	7650	0.56
LV_HLA-GFP			
1	13450	7260	0.54
2	17800	8700	0.49
3	23900	8420	0.35

Table 13.2 β-actin and WPRE concentrations and calculated normalized WPRE expression

LV_HLA-A*02	β-actin concentration	RNA WPRE concentration	Normalized WPRE expression
neg. control	19.3	28.9	1.50
1	68500	22400	0.33
2	41350	13400	0.32
3	21300	7600	0.36
LV_HLA-B*44			
1	25900	260000	10.04
2	49050	414000	8.44
3	31100	362000	11.64
LV_HLA-GFP			
1	42450	455000	10.72
2	30300	331000	10.92
3	52000	543000	10.44

(A)

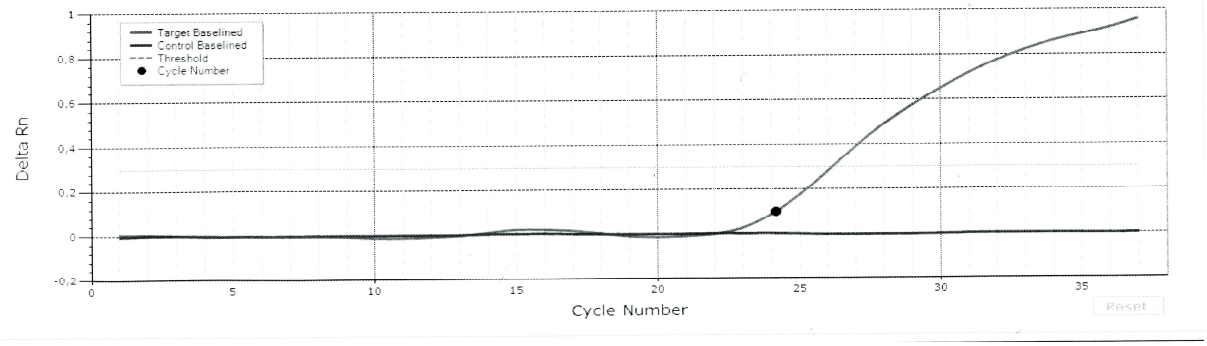
Target Baselined
Control Baselined
Threshold
Cycle Number
Delta Rn
Cycle Number
Reset

(B)

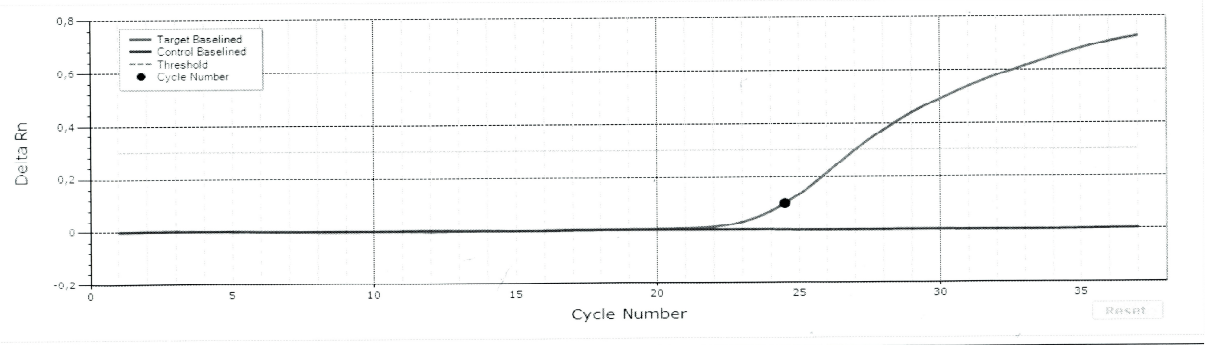
Target Baselined
Control Baselined
Threshold
Cycle Number
Delta Rn
Cycle Number
Reset

(C)

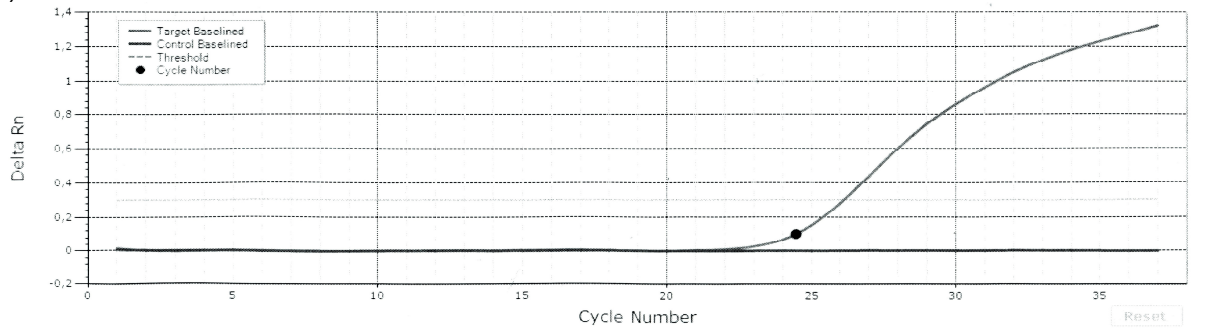
Target Baselined
Control Baselined
Threshold
Cycle Number
Delta Rn
Cycle Number
Reset

(D)

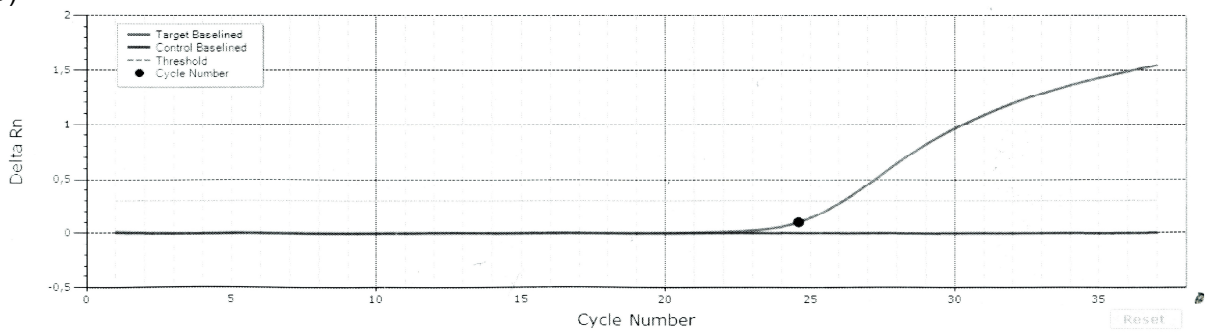
Target Baselined
Control Baselined
Threshold
Cycle Number
Delta Rn
Cycle Number
Reset

(E)

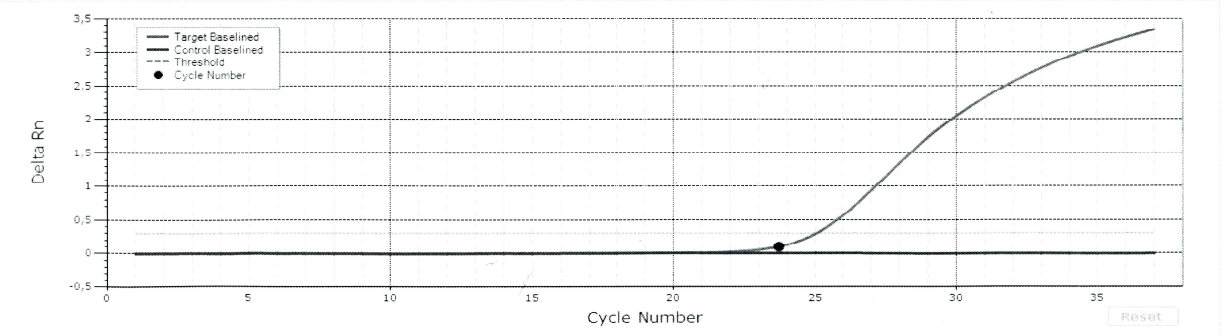

(F)

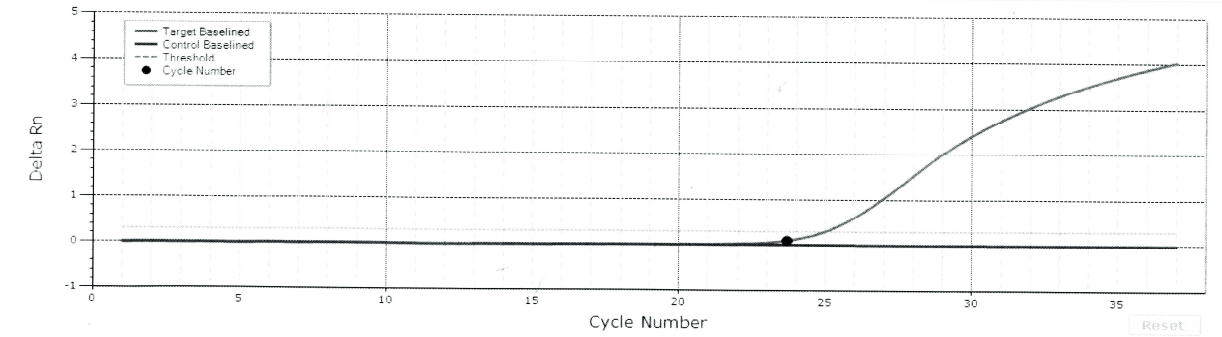

Figure 13.2 Real-time PCR amplification curves of an assay, targeting the integrase region of the polymerase gene, used to verify the successful infection of moDCs, deriving from different donors with HIV-1 ADA_V82A or ADA_L210F. (A) healthy donor 2 infected with ADA_V82A. (B) healthy donor 2 infected with ADA_L210F. (C) healthy donor 3 infected with ADA_V82A. (D) healthy donor 3 infected with ADA_L210F. (E) healthy donor 4 infected with ADA_V82A. (F) healthy donor 4 infected with ADA_L210F.

10. Abbreviations

°C	degree celsius
%	percent
µ	micro
µL	micro liter
µg	microgram
µm	micrometer
aa	amino acids
AA	acrylamid
Ab	antibody
AEC	3-amino-9-ethylcarbazole
Ag	antigen
AIDS	acquired immunodeficiency syndrome
Amp^R	ampicillin resistance gene
APC	antigen presenting cell
APC	allophycocyanin
APS	ammonium persulfate
Arevir	Analysis of HIV resistance mutations
ATCC	American Type Culture Collection
bp	base pair
BSA	bovine serum albumin
CA	capsid protein
CCLR	cell culture lysis reagent
CCR5	C-C chemokine receptor type 5
CCl2 / 3 / 4 / 5 / 11	C-C chemokine ligand 2 / 3 / 4 / 5 / 11
CD4 / 8 / 16 / 56	cluster of differentiation 4 / 8 / 16 / 56
cDNA	complementary DNA
CMV	cytomegalovirus
CO_2	carbon dioxide
cp	crossing point
CPE	cytopathic effect
cPPT	central polypurine tract
CTL	cytotoxic T cell
CXCL9 / 10	C-X-C chemokine ligand 9 / 10
DC	dendritic cell
ddNTP	dideoxynuceotide
DMSO	dimethyl sulfoxide
DNA	deoxyribonucleic acid
dNTP	deoxynucleotide
D-PBS	Dulbecco's Phosphate-buffered saline

DTT	dithiothreitol
E.coli	Escherichia coli
EDTA	ethylenediaminetetraacetic acid
eGFP	enhanced green fluorescent protein
ELISPOT	enzyme linked immuno spot
env	envelope
ER	endoplasmatic reticulum
FACS	fluorescence-activated cell sorting
FBS	fetal bovine serum
FDR	false discovery rate
FITC	fluorescein isothiocyanate
g	g-force
g	gram
gag	group-specific antigen
GM-CSF	granulocyte macrophage colony-stimulating factor
gp 41 / 120	glycoprotein 41 / 120
H_2O	water
H_2O_2	hydrogen peroxide
HAART	highly active antiretroviral therapy
HCl	hydrogen chloride
HF	high fidelity
His	histidin
HIV-1	human immunodeficiency virus type 1
HLA	human leukocyte antigen
IFN-α / -β / -γ	interferon alpha / beta / gamma
Ig	immunoglobulin
IL-1β / -1RA / -2 / -2R / -12 / -15 / -18	interleukin-1β / -1RA / -2 / -2R / -12 / -15 / -18
IN	integrase
IP-10	IFN-γ induced protein 10
Kan^R	kanamycin resistance gene
kb	kilo bases
kDa	kilo dalton
L	liter
LC	langerhans cell
LPS	lipopoysaccharide
LTR	long terminal repeats
LV	lentiviral vector
MΦ	macrophage
MA	matrix protein
MCP-1	monocyte chemotactic protein-1

MFI	mean fluorescence intensity
$MgCl_2$	magnesium chloride
$MgSO_4$	magnesium sulfate
MIG	monocyte interferon gamma inducing factor
min	Minute
MIP	MΦ inflammatory protein
mL	milliliter
mm	millimeter
mM	millimolar
moDC	monocyte-derived DC
MOI	multiplicity of infection
mRNA	messenger RNA
NaCl	sodium chloride
NaN_3	sodium azide
NC	nucleocapsid protein
nef	negative factor
NK cell	natural killer cell
nm	nanometer
NNRTI	non-nucleoside reverse-transcriptase inhibitor
NRTI	nucleoside / nucleotide reverse transcriptase inhibitor
OD	optical density
OR	odds ratio
ORF	open reading frame
p6 / 24 / 51 / 66	protein
PAMP	pathogen-associated molecular pattern
PBMC	peripheral blood mononuclear cells
PCR	polymerase chain reaction
PE	phycoerythrin
PEG	polythylene glycol
PerCP	peridin chlorophyll A protein
PFA	paraformaldehyde
pH	hydrogen ion concentration
PI	protease inhibitor
PR	protease
RAM	Resistance associated mutation
RANTES	regulated upon activation normal T cell expressed and presumably secreted
RESINA	resistance in treatment-naïve HIV-1 infected patients
rev	regulator of expression of virion proteins

RNA	ribonucleic acid
RRE	rev response element
RT	reverse transcriptase
S2 / 3	safety level 2 / 3
SAP	shrimp alkaline phosphatase
SDM	site-directed mutagenesis
sec	second
SFFV	spleen focus-forming virus
SIN	
SIV	simian immunodeficiency virus
ss	single-stranded
SV40	simian virus 40
TAE	tris-acetate-EDTA-buffer
tat	trans-activator of transcription
$TCID_{50}$	tissue culture infectious dose 50
TEMED	tetramethylethylenediamine
TLR	toll-like receptor
TNF-α	tumor necrosis factor α
tRAM	transmitted RAM
TSB	transformation and storage-buffer
TU	transducing unit
U	unit
URF	unique recombinant forms
UV	ultraviolet
v	volume
V	volt
vif	viral infectivity factor
vpr	viral protein r
vpu	viral protein unique
VSVg	vesicular stomatitis virus G glycoprotein
w	weight
WPRE	woodchuck hepatitis virus posttranscriptional regulatory element

IUB-Code for amino acids

A: Adenine	U: Uracil	S: G or C	D: A, G or T
C: Cytosine	K: G or T	W: A or T	H: A, C or T
G: Guanine	M: A or C	Y: C or T	V: A, C or G
T: Thymine	R: A or G	B: C, G or T	N: A, C, G or T

International abbreviations for amino acids

Alanine	ala	A	Leucine	leu	L
Arginine	arg	R	Lysine	lys	K
Aspartic acid	asp	D	Methionine	met	M
Asparagine	asn	N	Phenylalanine	phe	F
Cysteine	cys	C	Proline	pro	P
Glutamic acid	glu	E	Serine	ser	S
Glutamine	gln	Q	Threonine	thr	T
Glycine	gly	G	Tryptophan	trp	W
Histidine	his	H	Tyrosine	tyr	Y
Isoleucine	ile	I	Valine	val	V

10. Danksagung

Das Gelingen dieser Arbeit beruht nicht auf dem Werk einer einzelnen Person, sondern eine Vielzahl von Personen hat das Gelingen positiv beeinflusst. Deshalb möchte ich mich an dieser Stelle bei allen Personen bedanken, die mich fachlich sowie menschlich unterstützt haben.

An erster Stelle möchte ich mich bei Herr Dr. Rolf Kaiser und Frau Dr. Susanna Trapp bedanken. Herr Dr. Rolf Kaiser hat mich all die Jahre immer wieder herzlich empfangen und mir die Möglichkeit gegeben, nicht nur meine eigenen Ideen zu verwirklichen, sondern auch die Ergebnisse bei verschiedensten Möglichkeiten selber zu präsentieren, wie zum Beispiel auf schneebedeckten Bergen mit der Aussicht auf reifbedeckte Bäume. Bei Frau Dr. Susanna Trapp bedanke ich mich für den unermüdlichen Einsatz, egal ob fachliche Diskussionen, „einfach nur mal reden“ oder die hundertste verrückte Idee, wie man um 1 Uhr nachts den Graphen vielleicht doch noch anders darstellen könnte, nicht zu vergessen, die „all-inclusive“ Versorgung.

Prof. Dr. Herbert Pfister danke ich für die konstruktiven Hinweise und Diskussionen, die zum Gelingen dieser Arbeit beigetragen haben.

Bei Herr Prof. Dr. Walter Doerfler, Herr Prof. Dr. Kay Hofmann, Herr Prof. Dr. Siegfried Roth und Herr Dr. Matthias Cramer bedanke ich mich für die Bereitschaft, die vorliegende Arbeit vor der Mathematisch-Naturwissenschaftlichen Fakultät der Universität zu Köln zu vertreten.

Ich bedanke mich bei allen aktuellen und ehemalige Mitgliedern der Arbeitsgruppe Kaiser, die mich sowohl praktisch als auch theoretisch und mit Literweise Kaffee bei dieser Arbeit unterstützt haben: Claudia, Dörte, Ellie, Eugen, Eva, Laura, Maria, Mel, MTW, Nadine, Susi, Saleta und Steffi. An dieser Stelle einen besonderen Dank an MTW, die mich an der wunderbaren Welt, der Diagnostik-Geräte hat teilhaben lassen und immer helfend zur Seite stand. Dem Science Club danke ich für seine großartige Hilfe, auch wenn es einmal heiß her ging, hatte man sich ja hinterher doch wieder lieb.

Mein Dank gilt natürlich auch allen anderen Mitarbeitern des Instituts für Virologie für die herzliche und heitere Atmosphäre. Speziell bei den Damen der Diagnostik danke ich für Ihre Hilfsbereitschaft bei der Untersuchung meine Proben.

Meinen lieben Blutspendern, Birgit, Kathleen, Rolf, Mama und Clemens danke ich, ohne euch wäre diese Arbeit nicht möglich gewesen. Im Zuge dessen bedanke ich mich auch bei Herr Prof. Dr. Oldenburg und seinen Damen aus der Blutspendezentrale Uniklinik Bonn, sowie Dr. Bjoern Jensen und seinen Kollegen von der Uniklinik Düsseldorf, für die Entnahme des Blutes.

Prof. Dr. Thomas Harrer danke ich für die hilfreichen Diskussionen und Sandra Müller-Schmucker zusätzlich für die Übersetzung aus dem „fränkischen“.

Bei Susi, Dave, Mellie, Maria und Kathleen, den fleißigen Korrekturlesern, bedanke ich mich herzlich.

Nico Pfeifer danke ich für die unermüdlichen Versuche, mich der Statistik näher zu bringen und seinem Einsatz die ein oder andere statistische Analyse durchzuführen.

Bernhard Thiele, Martin Däumer, Alex Thielen, sowie den Mädels aus Kaiserslautern danke ich für die Unterstützung bei der HLA Typisierung und in eigentlich allen Dingen bezüglich des großen Themas: HLA am Telefon oder bei einem Plausch auf der Hütte. Speziell danke ich Martin Däumer, der vor vielen Jahren einmal den Anstoß für diese Arbeit gegeben hat.

Meinen Freunden danke ich, die mir in allen Lebenslagen zur Seite standen, mich aber auch vor die Tür gelockt und für Abwechslung gesorgt haben. Oder einfach zwischendurch nachgehorcht haben, ob ich noch lebe: Danke Corinna, Kathleen, Rene und Simone.

Zu guter Letzt danke ich Familie Hartnack, dem Peter, der Bine, meiner Oma und meiner Mama für den unerschütterlichen Glauben in mich. Und was ich noch zu aller, aller Letzt hinzufügen möchte: Danke, danke, danke, danke, danke, Mama!

11. Erklärung

Ich versichere, dass ich die von mir vorgelegte Dissertation selbständig angefertigt, die benutzten Quellen und Hilfsmittel vollständig angegeben und die Stellen der Arbeit – einschließlich Tabellen, Karten und Abbildungen –, die anderen Werken im Wortlaut oder dem Sinn nach entnommen sind, in jedem Einzelfall als Entlehnung kenntlich gemacht habe; dass diese Dissertation noch keiner anderen Fakultät oder Universität zur Prüfung vorgelegen hat; dass sie – abgesehen von unten angegebenen Teilpublikationen – noch nicht veröffentlicht worden ist, sowie, dass ich eine solche Veröffentlichung vor Abschluss des Promotionsverfahrens nicht vornehmen werde.
Die Bestimmungen der Promotionsordnung sind mir bekannt. Die von mir vorgelegte Dissertation ist von Herrn Dr. rer. nat. Rolf Kaiser und Frau Dr. rer. nat. Susanna Trapp betreut worden. Herr Prof. Dr. Walter Doerfler vertrat die vorliegende Arbeit vor der Mathematisch-Naturwissenschaftlichen Fakultät der Universität zu Köln.

Teile der vorliegenden Dissertation wurden unter folgendem Titel veröffentlicht oder zur Veröffentlichung eingereicht:

Mascolini M, Larder BA, Boucher CA, Richman DD, Mellors JW: **Broad advances in understanding HIV resistance to antiretrovirals: report on the XVII International HIV Drug Resistance Workshop.** *Antivir Ther* 2008, **13:**1097-1113.

Schweitzer F: **Correlations between transmitted HIV drug resistance mutations and the HLA of therapy-naive HIV-patients**. *Schriftenreihe Infektiologie* 2013 in press, Band **17**

Köln, _____ (Finja Schweitzer)

12. Lebenslauf

Persönliche Daten:

Name:	Finja Schweitzer
Adresse:	Cranachstr. 31, 50733 Köln
Geburtsdatum:	09. März 1983
Geburtsort:	Langenfeld
Staatsangehörigkeit:	deutsch
Familienstand:	ledig

Schulausbildung:

1989 – 1993	Don Bosco Grundschule, Haan
1993 – 1999	Städtisches Gymnasium, Haan
1999 – 2000	Mountain Crest High School, Hyrum, UT, USA
2000 – 2001	Städtisches Gymnasium, Haan
2001 – 2003	Ernst-Moritz-Arndt Gymnasium, Remscheid Abschluss: Allgemeine Hochschulreife

Studium:

10/2003 – 08/2006	Fachhochschule Bonn-Rhein-Sieg Abschluss: Bachelor of Science
08/2005 – 12/2005	Katholische Universität zu Valparaiso, Chile
09/2006 – 06/2008	Universität zu Maastricht, Niederlande Abschluss: Master of Science

Köln, _____ (Finja Schweitzer)